A Cellular automaton model for crowd movement and egress simulation

Article · July 2003

Source: OAI

1 author:

Hubert Klüpfel
University of Cologne
82 PUBLICATIONS **2,678** CITATIONS

SEE PROFILE

A Cellular Automaton Model for Crowd Movement and Egress Simulation

Von der Fakultät 4 – Naturwissenschaften

der

Universität Duisburg–Essen

Standort Duisburg

zur Erlangung des akademischen Grades eines

Doktors der Naturwissenschaften

genehmigte Dissertation

von

Hubert Ludwig Klüpfel

aus

Würzburg

Referent:	Prof. Dr. Michael Schreckenberg
Koreferent:	Prof. Dr. Dietrich Wolf
Tag der mündlichen Prüfung:	28. Juli 2003

Abstract

The movement of crowds is a field of research that attracts increasing interest. This is due to three major reasons: pattern formation and self-organization processes that occur in crowd dynamics, the advancement of simulation techniques and hardware that enable fast and realistic simulations, and finally the growing area of potential applications (planning of pedestrian facilities, crowd management, or evacuation analysis). The field is spanning the borders of various disciplines: physiology, psychology, sociology, civil engineering, mathematics, physics, etc. It depends on the point of view which aspects are given the main focus. One approach is to reduce complexity to fundamental principles that make a mathematical (quantitative) formulation possible and at the same time are sufficiently complex to reproduce the major phenomena that can be observed in reality.

The major aim of this dissertation is to define and validate a model for the simulation of evacuation processes and their analysis. To this end the analogy between non-equilibrium many particle systems and crowds is used. However, it will also become clear that this analogy is not sufficient for complex scenarios and realistic egress simulations and additional, 'non-physical', parameters and principles must be introduced. Even though the investigation is motivated by the applications, the dynamics of crowd movement and model properties are scrutinized. This also includes a thorough review of the data available in the literature, the calibration of the model parameters and the comparison of simulated and empirical flow-density relations.

The core of any evacuation simulation is a set of rules or equations for the movement of people. This is connected to the representation of space, population, and behavior. These topics will be investigated generally (micro- vs. macroscopic, discrete vs. continuous) and especially with regard to a specific two-dimensional cellular automaton model, where the movement dynamics is based on discrete space and time. This allows an efficient implementation and therefore large scale simulations. The route-choice is done via the orientation along a discrete vector field which can in principal be derived from a discrete potential. It is therefore not explicitly simulated but taken into account in a pre-determined way, i.e., the coupling to the vector field is static (constant coupling parameter). In addition to the model characteristics, extensions like competition, multiple and dynamically varying orientation potentials or coupling parameters, or individual egress routes are discussed.

In order to validate the simulation results and the application to full-scale problems, simulations for realistic scenarios are performed and compared to data from evacuation trials. Design variants, aspects of crowd management, or operational measures to optimize evacuation performance are also mentioned. However, they are the task of experts (architects, psychologists, safety engineers) who might use simulations as a design and evaluation tool. Therefore, these results are rather case studies supplementing the major topics of the model characteristics and implementation.

Zusammenfassung

Die Bewegung von Menschenmengen ist ein Forschungsgebiet das zunehmend an Aufmerksamkeit gewinnt. Dafür gibt es im wesentlichen drei Gründe: die Ausbildung von Mustern und Selbstorganisationsphänomene, der Fortschritt im Bereich der Simulationstechnik, die schnelle und realitätsnahe Simulationen ermöglicht und schließlich die wachsende Zahl möglicher Anwendungen (die Planung von Fußgängeranlagen, die Steuerung von Personenströmen oder die Evakuierungsanlyse). Das Gebiet überspannt verschiedene Disziplinen: Physiologie, Psychologie, Soziologie, Ingenieurwissenschaften, Mathematik, Physik, etc. Es hängt vom Blickpunkt ab, welche Aspekte dabei im Mittelpunkt stehen. Ein Ansatz ist, die Komplexität dadurch zu reduzieren, dass man sie auf grundlegende Prinzipien zurück führt. Dadurch wird eine mathematische (quantitative) Formulierung möglich und gleichzeitig können die wichtigsten Phänomene, die in der Realität beobachtet werden, reproduziert werden.

Das Hauptziel dieser Dissertation ist die Formulierung und Validierung eines Modells für die Simulation und Analyse von Evakuierungsvorgängen. Zu diesem Zweck wird die Analogie zwischen physikalischen Vielteilchen-Systemen und Menschenmengen benutzt. Es wird jedoch auch deutlich werden, dass diese Analogie nicht ausreicht, um komplexe Szenarien zu erfassen und realistische Entfluchtungs-Simulationen durchzuführen. Dazu müssen zusätzliche 'nicht-physikalische' Parameter eingeführt werden. Auch wenn die Untersuchungen durch die Anwendung motiviert sind, so stehen doch die Dynamik der Bewegung von Menschenmengen und die charakteristischen Modell-Eigenschaften im Mittelpunkt. Das umfasst auch eine Übersicht der einschlägigen Literatur zur Kalibrierung der Modell-Parameter und den Vergleich von Simulationsergebnissen mit empirischen Fluss-Dichte-Relationen.

Den Kern einer Evakuierungssimulation stellt ein Satz von Regeln oder Gleichungen für die Bewegung der Menschen dar. Verbunden damit ist die Art und Weise, wie Raum, Personen und Verhalten repräsentiert werden. Diese Punkte werden sowohl allgemein (mikroskopisch gegenüber makroskopisch, diskret gegenüber kontinuierlich) als auch spezifisch mit Bezug zu einem zweidimensionalen Zellularautomaten-Modell untersucht. Im zweiten Fall sind die Bewegungsgesetze in diskreter Zeit formuliert. Dadurch ergibt sich auch eine Diskretisierung des Raumes. Gleichzeitig werden eine effiziente Implementierung und die Simulation großer Personenzahlen ermöglicht. Die Routenwahl wird auf die Orientierung entlang eines diskreten Vektorfeldes zurückgeführt, das grundsätzlich von einem diskreten Potential abgeleitet werden kann. Die Routenwahl ist daher nicht im Modell enthalten sondern wird von außen vorgegeben, d.h. das Vektorfeld ist statisch. Neben den Modelleigenschaften werden auch mögliche Erweiterungen für Konkurrenzverhalten, mehrere oder sich ändernde Orientierungs-Potentiale oder individuelle Fluchtwege diskutiert.

Um die Simulationsergebnisse zu überprüfen (Validierung) und die Anwendbarkeit zu testen, wird die Simulation auch auf umfangreiche Probleme und realistische Szenarien angewandt. Das erlaubt einen Vergleich mit em-

pirischen Daten. Entwurfsvarianten, Aspekte der Steuerung von Menschenmengen oder andere Maßnahmen werden ebenfalls erwähnt, wo sich ein Bezug ergibt. Allerdings sind das Aufgaben für Experten (Architekten, Psychologen, Sicherheits-Ingenieure), die solche Simulationen als Werkzeuge zum Entwurf und zur Auswertung benutzen. Daher sind diese Ergebnisse als Fallstudien zu sehen, die die Anwendbarkeit der Simulation belegen.

Contents

Chapter 1

Introduction

This chapter gives an overview of the topics dealt with in this dissertation. It describes the intention, scope, and limitations of simulation models for evacuation analysis and roughly outlines the content of the succeeding chapters.

Contents

1.1 Why Simulating Crowd Motion and Evacuation Processes?

The field of pedestrian movement has received growing interest over the last decades. This is due to several reasons:

1. Growing mobility: Even if walking is not the most important form of locomotion when the distance covered is concerned it is necessary for every other form of traveling (e.g., walking to the bus, the car, or to the airport terminal) and it is probably the most time-intensive form of mobility if waiting and queuing are taken into account. Simulations can help to increase the level of comfort and decrease waiting times by assessing alternative layouts or procedures.

2. Large facilities, like theme parks and shopping centers, are usually populated by a large number of persons. In densely packed crowds high 'pressure' can occur and pose a threat on peoples health [Smith and Dickie, 1993]. This requires detailed planning of the "walkways" and crowd management to avoid such dangerous situations.

3. Events like rock concerts or sport matches often attract a huge number of persons. To manage this situation a profound knowledge of the laws of crowd motion is necessary. Scientific research is one tool to gain this knowledge which can be used to 'channel' flows (make them more homogeneous), increase capacity by decreasing orientation problems or holding back persons to avoid peak flows in critical areas.

4. In case of an emergency buildings or passenger vessels have to be evacuated within a short time span under stress conditions. Simulations help to improve the building or vessel layout and to optimize the evacuation performance.

5. The requirements to the safety of passenger vessels are increasing. And there is a tendency to increase the number of persons carried in airplanes (Airbus A 380) or on ships (large passenger ships with more than 5000 persons on board are currently planned).

6. Numerous phenomena can be observed in crowd motion: shock waves, oscillation at bottlenecks, lane-formation, etc. Can they be explained by simple rules and assumptions? To identify those basic principles increases the understanding of crowd dynamics.

7. Finally, crowd motion is an important topic in the investigation of group dynamics. And it is connected to several other fields, like social psychology, traffic engineering and safety science. Deepening this connection might lead to fruitful results and new insights on a level beyond the limitations of the single disciplines.

For all these reasons, a thorough investigation of the laws of crowd motion and the influences on it, e.g., the geometrical layout, the environment, or the procedure, especially in case of an evacuation is required.[1]

As stated before, the potential applications of a theory for crowd movement are quite numerous. At the same time, there are many fundamental questions concerning the application of such a theory, especially when it comes to the assumptions that have to be made and the implementation into a specific model:

- How can cognitive aspects be modeled? Can psychological and social aspects under certain circumstances be represented by fairly easy assumptions?

- What are the differences between continuous and discrete models?

- How do model characteristics influence macroscopic quantities like the flow of persons or the egress time from a room?

- How can the model be validated for the application to evacuation simulations?

There are of course many more questions. Some of them will be addressed in the remaining chapters. Others – like the simulation of decision making by using artificial intelligence – are beyond the scope of this thesis, however.

Considering the requirements stated in table 1.1 computer simulations are the tool of choice for investigating crowd movement and especially assessing evacuation processes. As will be argued in the following chapters, they are able to cover the relevant influences in a uniform and comprehensive way, provide useful information about the dynamics and time evolution, and can be build up from intuitive and comprehensible basic assumptions and rules. Of course, the range covered and influences explicitly taken into account in a model for crowd movement have to be restricted. From a practical as well as a theoretical point of view, a model should be as simple as possible. Of course, the question remains, what as simple as possible means, e.g., whether or not cognition must be explicitly

[1]The relevance of the topic for society and technology is reflected by its coverage in newspapers as well as magazines [GEO, 2001, NZZ Folio, 2002, Spektrum der Wissenschaft, 2001, Spiegel, 2001, SZ, 2001].

Table 1.1. Requirements for a theory of crowd motion and its application to the assessment of evacuation processes. These requirements are very general. If interpreted in a broad sense they describe a desired optimal standard. A specific model might nevertheless focus on certain aspects of such a theory and therefore be based on simplifying assumptions.

Feature	Explanation
comprehensive	covering all essential aspects
dynamic	describing the time evolution
detailed	representing population and space individually, resp. fine grained
comprehensible	based on assumptions and rules as simple as possible
flexible	covering a wide range of layouts and scenarios

modeled. This topic will be discussed in the following chapters and arguments presented for the hypothesis that under certain circumstances (i.e., mainly when route choice is pre-determined) it is justified, to use a 'physical' model for crowd motion.

Taking into account the application to real world structures and processes, another requirement is flexibility, especially concerning the application to various phenomena and settings or environments. The potential areas of application are again numerous: buildings, urban systems like pedestrian crossings, shopping malls, theme parks, airports, railway and subway stations, ships, aircraft, buses, trains, etc. Most of them have already been covered by simulations and references to the literature are given in chapter 4.

In summary, the aims of this thesis are the following:

1. Compilation of the basic principles, the aim, and the scope of computer simulations for evacuation processes (remaining part of this chapter);

2. Developing a consistent theory for crowd movement (chapter 2) and its formulation in a form suitable for an algorithmic representation (chapter 3);

3. Implementing this model into a simulation and applying it to realistic egress and evacuation scenarios – for buildings (chapter 4) as well as for ships (chapter 5);

4. Using empirical data (a literature review is given in section 2.5) and experiments (own experiments are presented in section 2.7) to calibrate the model parameters in chapter 3, assess the scope of its application, and validate the simulation results (chapters 4 and 5).

1.2 Models for Social Systems

A crowd is a group of interacting individuals and therefore a social system. Crowd movement can be described on different levels according to the cognitive and social processes involved.

1. Physical/Physiological

2. Psychological

3. Social

Behavior is related to the psychological and social level. However, it can also be taken into account implicitly (cf. fig. 1.1). Therefore, a 'physical' model is able to cover

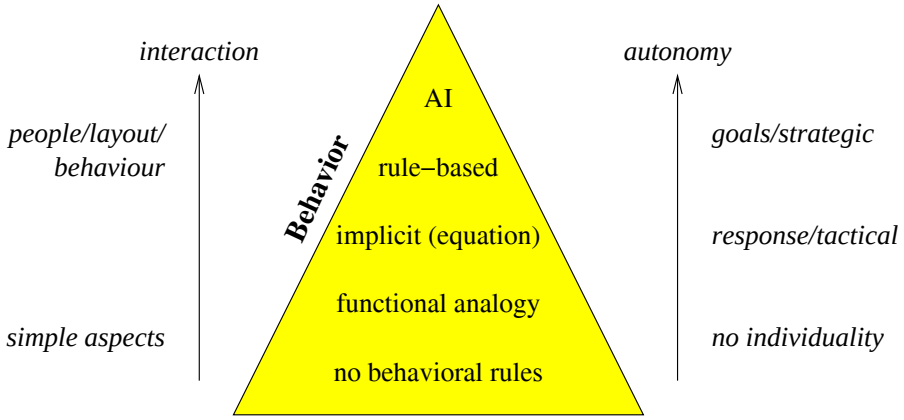

Fig. 1.1. The representation of behavior can range from its neglecting to artificial intelligence (AI), which aims at even modeling the decision making process [cf. ISO, 1999]. However, the more complex approaches are not completely different from the basic ones but include additional features. Therefore, the autonomy and interaction increase towards the top but are not completely absent and completely present in one case or the other. These qualities are rather a question of interpretation than of direct representation in a set of rules.

the essential aspects of crowd movement in an egress situation when route-choice is predetermined. Traditionally, physics has dealt with matter and the rules governing it, e.g., particles and fields (or forces). In order to master the complexity emerging from rather simple principles, many concepts and methods have been developed. Those tools are not only useful to tackle the problems they have originally been developed for but can fruitfully be extended to other areas.

The motion of a crowd can always be modeled 'physically' by a description of the trajectories of all individuals. Therefore it can be viewed as a many particle system governed by appropriate rules or 'forces'. This does not imply that those forces can be represented in the same way as, e.g., gravitational or electro-magnetic forces. However, they share common features with them that allow to employ some of the concepts used there. What remains necessary, of course, is input from empirical psychology about the decisions of people, e.g., whether or not they follow the provided escape routes.

Another aspect that is often mentioned in connection with evacuation is that of panic. However, Sime [1990] argues that the concept is misguiding and that the behavior of people can usually be explained rationally.[2] It seems to be irrational due to the lack of information and the pressure people face in a dangerous situation. Harbst and Madsen [1996] argue along the same lines. Panic is mentioned usually in the context of masses.[3] These mass phenomena (like de-individuation) do not necessarily play an important role in evacuation processes, though. To assess the topic more thoroughly, a distinction has to be made between groups and collectives [Brown, 1986, Forsyth, 1999]

[2]This is in a sense similar to deterministic chaos, where the indeterminism is not inherent but due to the lack of information (incomplete knowledge of the initial conditions).

[3]Le Bon [1895] claimed that masses behave completely different from individuals, e.g., they are less rational and are transformed into another state of mind. Freud [1924] followed his argumentation. However, the concept of de-individuation via a mass soul was vehemently criticized later [Hofstätter, 1990].

Table 1.2. Characteristics of collectives or crowds [from Forsyth, 1999, abridged].

Quality	Description
Size and proximity	large (more than 20 members)
Joint action	"common or concerted" forms of behavior
Ephemeral	sometimes (but not always) form and disband rapidly
Unplanned	form spontaneously in response to a situation or event
Unconventional	exist outside of traditional forms of social structures

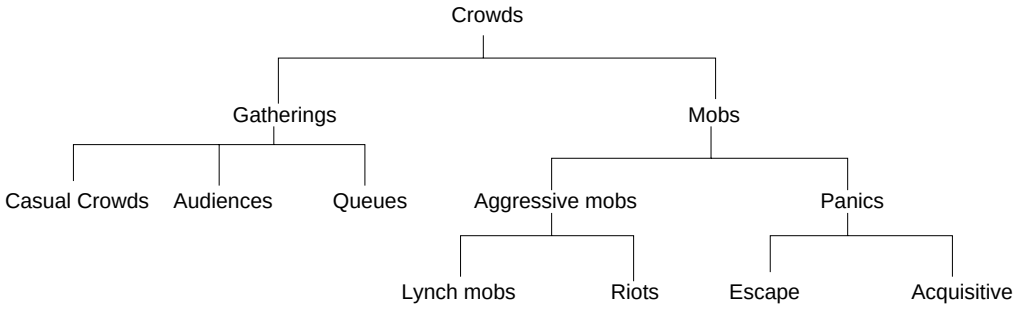

Fig. 1.2. Classification of crowds: [Forsyth, 1999]. Crowds are large groups that occupy a single location and share a common focus.

(cf. fig 1.2). The distinction between groups, masses and collectives is the following: Any gathering of two or more persons is a group, a large group is called a mass. And if they *occupy a single location and share a common focus*, they form a crowd (cf. fig. 1.2). The term collective is used more or less as a synonym for crowd. Many collectives spring up spontaneously, exist only briefly, and then fade away as members go their separate ways. Further investigations concerning the topic of crowd behavior in the context of evacuation can be found in [Canter, 1990, Schreckenberg and Sharma, 2002, Smith and Dickie, 1993].

These general considerations can be further specified when restricting the intented scope of a model. The application of the theories discussed and the model presented here are evacuation processes.

1.3 Evacuation Assessment and how to Improve

When considering evacuation processes, the movement of a crowd becomes simpler and is therefore easier to model. This is mainly due to the fact, that the destinations and goals of the individuals are determined. Furthermore, the egress routes are known. With respect to models for evacuation processes, two main aims can be identified: simulation and optimization. There is an obvious difference between both: Optimization techniques provide a well-defined quantity, e.g. the value of a function, that can be minimized. Thus, one obtains (within the restrictions of the boundary conditions) an optimal solution. This is not the case for a simulation: Here, the situation is modeled and a prediction about the outcome under certain initial conditions is made. What will be presented here is simulation. It might be used – by using some additional measure – for optimization.

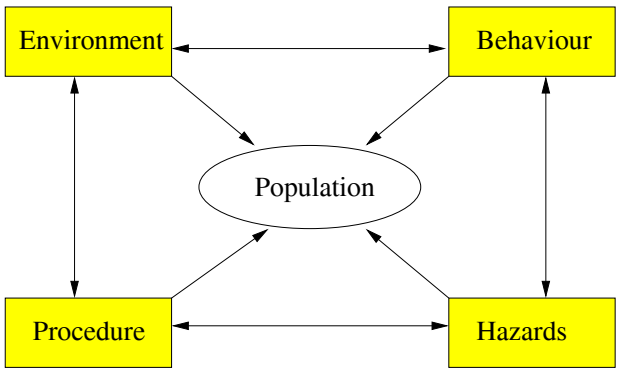

Fig. 1.3. Influences on an evacuation: The rectangles represent the parameters influencing the population. The movement is described basically by the variables of the individual evacuees which form the population [cf. Gwynne et al., 1999]. The several influences can be treated separately and therefore provide a natural division of the model into sub-models.

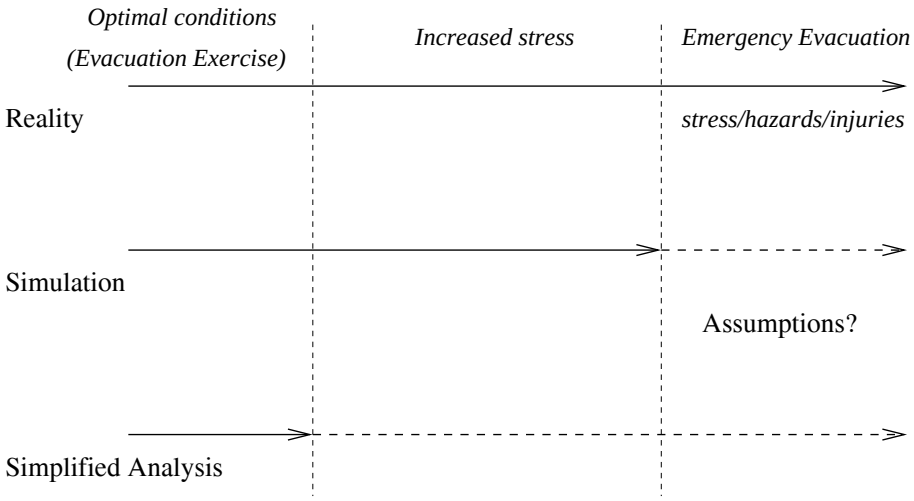

Fig. 1.4. A simplified analysis can basically cover the same range as an evacuation exercise. Aggravating circumstances like hazards can be included via extrapolation of the obtained results. A simulation, however, allows to include those influences via the adaption of the parameters, i.e., the extrapolation is made on the input and not on the output.

However, this will result in an iterative process, where not the optimal solution but one that is close enough to the desired output, is aimed at. The reason is, that there is usually no function for the quantity to optimize. It has therefore to be borne in mind that a simulation by itself is not an optimization tool. It is a description of a system covering the relevant dynamical aspects.

The different influences for the simulation of an evacuation or egress are summarized in figure 1.3. In order to improve, one has to state what should be changed, what to optimize, and how an improvement can be reached. The overall evacuation or egress time is one quantity in this context. Others are the length of queues, the densities occurring,

etc. Chapter 4 contains further remarks concerning the assessment of evacuation routes (configuration) and procedures (see fig. 1.3). The environment and the population can usually not be changed and are determined by the situation. Therefore, the major aim of evacuation simulations is to quantify the influence of the layout and the procedure and investigate potential improvements. Changes in the population or the environment are not of immediate concern. Some general aspects of emergency planning can be found in a brochure issued by the Health and Safety Executive [1999] of the UK.

To be able to use simulation results for assessment and improvement of layouts and evacuation procedures they must at least comprise the sequence of the evacuation, the overall evacuation time and especially information about bottlenecks and retardation. Second, the whole evacuation process has to be taken into account spatially, e.g., a complete building or vessel, as well as temporarily, i.e., from the alarm or abandon ship signal until the last person has reached a place of safe refuge.

1.4 The Perspective of Physics

It should have become clear by now that the movement of crowds is influenced by many factors and its description can easily become very complex because of the many interacting individuals. Nevertheless, from the 'physical' point of view it can be regarded as an interacting many 'particle' system. And there are similarities and analogies to processes far from equilibrium. However, the nature of the interaction between the pedestrians and their driving force are not known in detail. And the system is open with respect to the kinetic energy (i.e., persons might stop abruptly) and the number of pedestrians might not be conserved[4].

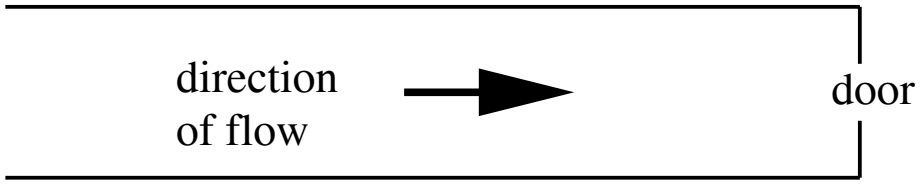

Fig. 1.5. Schematic view of a mockup used for crowd flow experiments as described by Müller [1999]. The corridor width and the door width were variable and the experiments were compared to others performed using smaller mockups and metal balls representing the persons. The initial density was 6 persons/m^2 and pulsed outflow as well as the formation of arches in front of the door were observed.

It can therefore be viewed as sort of an 'exotic fluid' and there are analogies to the flow of granular material, especially at high densities, when the 'pressure' from behind keeps the flow going. And in fact experiments using inclined mockups of rooms and sections of buildings (consisting of several rooms connected by corridors) filled with metal balls have been carried out [Müller, 1999]. In order to compare the results to the movement of real crowds another mockup (cf. fig. 1.5) was used. The major conclusion is that there are no differences for the flow characteristics between balls and persons. This justifies a 'physical' approach as a starting point for simple geometries and the outflow problem.

[4]This is not understood in the sense of persons being created or annihilated, of course, but leaving the system.

For complex geometries, however, building down-sized mockups becomes tedious. Therefore, computer simulations are a more appropriate tool. In the following chapters, general properties of crowd movement will be investigated, different modeling approaches compared to each other, and a specific discrete (cellular automaton) model will be analyzed and applied to the simulation of evacuation processes.

Chapter 2

Modeling Pedestrian and Crowd Dynamics – Methodology

This chapter contains basic remarks on how to model pedestrian movement. It therefore deals with the methodology rather than a specific model in detail. The problem setting, as introduced in the previous chapter, is the investigation, description, and prediction of crowd motion and the aspects of evacuation processes related to it. To this end a theory (a set of assumptions and statements) is developed. Different model classes that comply with the theory will be introduced and briefly described. This is the first step providing the basis for empirical studies, model development, and finally the implementation in a simulation.

Contents

2.1 General Concepts

Firstly, the task of formulating a theory and subsequently a model for crowd movement and behavior is approached systematically. A correct interpretation of a theory is called a model, where interpretation is understood as the reduction of choices or degrees of freedom by specifying one of several alternatives without loosing consistency (cf. fig. 2.1). Examples for such reductions are the representation of space as a discrete grid or the exclusion of direct verbal communication between individuals. This is possible, as long

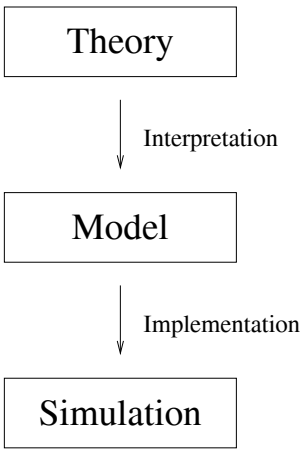

Fig. 2.1. The interpretation of a theory provides a model which can be implemented in a simulation. In physics this connection between model and theory is usually taken for granted. However, one could also call a set of consistent models a theory.

as those aspects comply with the scope and aim of the underlying theory. By implementing a model one obtains a simulation program (in short simulation) which is a valid representation of the model and therefore of the subject matter of the theory. In the case of crowd motion, a theory contains assumptions about the reaction of pedestrians to their environment, orientation and route-choice, physiological constraints, etc. Even if those assumptions have been stated, there are different ways of representing them.

As could already be seen from fig. 1.1 analogies to physical systems can provide a starting point for investigating crowd movement. Moreover, they might provide insight into the basic properties of the models. A crowd of pedestrians might be viewed as a driven many particle system with dissipation. It is a system far from equilibrium, though. There are therefore similarities as well as differences between pedestrian motion and non-equilibrium many-particle systems: the concepts used to treat the physical systems can usually not straightforwardly be applied, since the representation of, e.g., the route choice via external fields becomes very tedious and the dissipation (which is typical for non-equilibrium systems) adds further difficulties. However, from a technical point of view continuous models for crowd motion are – with restrictions – similar to molecular dynamics (MD). MD simulations are based on the numerical solution of the Newtonian equations for many interacting particles. And the *social force model*, which is briefly described in section 2.3.1 employs exactly this correspondence.

In general, models can be characterized according to *scale*, *resolution*, and *fidelity* [Nagel, 1996]. A high fidelity model is one with many parameters that directly takes into account all the different influences (e.g., parameters like age, height, weight, mobility impairment, etc. in the case of pedestrians), resolution is the level of detail regarding the representation of space, and finally, scale is the size of the problem with respect to time, space, etc. The scale of a pedestrian simulation depends on the application of course. For football stadia or theme parks, a model that 'scales' linearly (with respect to computation time and memory requirement) with the number of persons or the size of the layout is desirable. To some extent high resolution low fidelity simulations can do as well as low resolution high fidelity ones, i.e., resolution can make up for fidelity [Nagel, 1996].

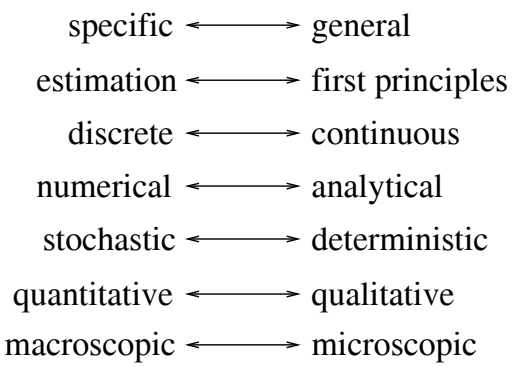

Fig. 2.2. Modeling criteria that can be used for classifying different theories and models [from Gershenfeld, 1999]. The major choices for models and simulations of crowd movement are discrete vs. continuous and stochastic vs. deterministic.

Additional modeling criteria are illustrated in fig. 2.2. A high resolution (microscopic) model is usually also based on first principles and intented to be of general use. It can then be treated only numerically, though. Furthermore, in order to be able to make predictions and assess evacuation processes, quantitative results are required. Finally, since there will remain influences on human behavior that cannot be completely quantified, the outcome of an evacuation as well as crowd movement in general are to some extent uncertain. This is reflected by a stochastic model. Whether a discrete or continuous model is more appropriate cannot be directly answered from a theoretical point of view. The differences between discrete and continuous become important for simulations of real world problems (i.e., complete buildings or ships), especially concerning the scalability (which is not a model characteristic but one of the implementation).

With respect to resolution, models for pedestrian motion can be classified into two major categories: microscopic and macroscopic. Macroscopic models cannot represent a general theory of crowd motion and are restricted to specific applications. Their advantage is that they usually can be treated analytically. An example for a macroscopic model is given by Pauls [1995].

Examples for different microscopic models are given in table 2.1. Microscopic models (for pedestrian motion) can be roughly defined according to the following criteria: They are based on

- a detailed representation of space,
- the representation of individual persons,
- a uniform movement algorithm, and
- the consideration of personal abilities and characteristics.

The third and fourth criterion follow from the first and second, which are the proper characteristics. The connection between the geometry and the population for microscopic models is made via the rules (or equations) of motion (see fig. 2.3). This is different from macroscopic, hydrodynamic, or regression models, where this connection is made via a parameter in the respective flow equation.

According to the criteria just introduced (cf. figure 2.2) the model that will be presented in chapter 3 is microscopic, based on first principles, numerical, stochastic, and quantitative.

2.2 Movement Dynamics

The movement of pedestrians can be represented by their trajectories. The number of pedestrians be N. If the coordinates of the N pedestrians are given by vectors $\vec{r_i} \in \mathbb{D}^2$ ($\mathbb{D} = \mathbb{R}$ for spatially continuous and $\mathbb{D} = \mathbb{N}$ for discrete models) the new positions $\vec{r_i}'$ are given by $\vec{r_i} + \vec{v_i}$, where $\vec{v} \in \mathbb{D}^2$ is the velocity at time t and Δt denotes the time-step in the discrete case:

$$\vec{r_i}' = \vec{r_i}(t + dt), \text{ in a continuous model, and} \tag{2.1}$$

$$\vec{r_i}' = \vec{r_i}(t + \Delta t), \text{ in a discrete model.} \tag{2.2}$$

This means that the discrete space is represented by a two-dimensional lattice and the lattice sites can be identified by two numbers. Although this notation is intuitive for a square lattice, the lattice type is not restricted and could also be hexagonal or triangular.

The problem of determining the velocities can be subdivided into three steps: Route choice, orientation, and interaction. Route choice requires the autonomy to set strategic goals. Modeling this decision making process from first principles is outside the scope of the approach presented here. Rather, the routes are assumed to be pre-determined and therefore implicitly contained in the rules or equations of movement (cf. fig. 1.1). Then, the route choice can be represented by a vector field $\vec{V} \in \mathbb{D}^2$ and $\vec{v_i} = \vec{V}(\vec{r_i})$. This leads to the analogy to physical systems: orientation is the coupling to a vector field.

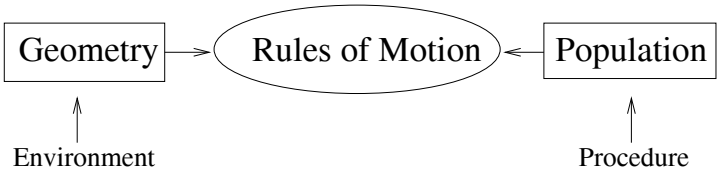

Fig. 2.3. The connection between geometry and population is made via rules of motion, i.e., they determine the movement with respect to the layout.

2.3 Representation of Space: Discrete vs. Continuous

With respect to the representation of space in a microscopic model, there are two basic approaches (see fig. 2.2): discrete or continuous. If space is represented in a discrete fashion, usually a regular lattice is used. This notion is quite familiar in statistical mechanics and is often used for modeling systems with restricted degrees of freedom such as solids (lattice gas, Ising-model, percolation models). In reality, the degrees of freedom for pedestrian movement are not restricted in this way, though. Whether to use a discrete or continuous representation of space is closely connected to the implementation (similar to models for road traffic). A strong argument in favor of discrete models is that they are simple and can be used for large scale simulations. Additionally, for pedestrian motion and behavior there is a finite reaction time, which introduces a time scale. If the

Table 2.1. Examples for microscopic models, classified with respect to the dynamics of pedestrian motion. Δt is the time step, a is the length of a quadratic cell, hence $\rho_{\max} = 1/a^2$ for a square grid. If the cell length a is not specified, $\rho_{\max}$ cannot be compared to empirical data (denoted by n.a. for not applicable in the third column).

	type	characteristics	$\rho_{\max}$	$v_{\max}$
1	lattice gas	biased random walk	n.a.	1 cell/Δt
	[Muramatsu et al., 1999]			
2	CA	collision avoidance	n.a.	1 cell/Δt
	[Fukui and Ishibashi, 1999]			
3	CA	uni- and bidirectional	$4.8\,\mathrm{P/m^2}$	1.8 m/s (5%), 1.3 m/s (90%), 0.85 m/s (5%)
	[Blue and Adler, 1999]			
4	continuous	extremal principle	$5\,\mathrm{P/m^2}$	$1.5\,\mathrm{m/s}$ ($0.5\,\mathrm{m^2/s^2}$)
	[Hoogendoorn and Bovy, 2001, Hoogendoorn et al., 2002]			
5	continuous	social force		$1.34\,\mathrm{m/s} \pm 0.26\,\mathrm{m/s}$
	[Helbing, 1995]			

time is chosen to be discrete in the model, too, this naturally (but not necessarily) leads to a discrete representation of space. Firstly, the continuous approach will be outlined, and then the main aspects concerning the discrete or grid-based models are introduced. One special class of the discrete models are the so called Cellular Automata (CA) models. Their properties will be discussed in depth (together with a specific model for pedestrian dynamics in egress simulations) in chapter 3.

2.3.1 Continuous Models

Even though the major topic of this work are two-dimensional CA models, reference will be made at various places to continuous models for pedestrian dynamics. Due to this and the importance of continuous models as the alternative approach towards representing space, this section describes the *social force model* and some of its properties in some detail [Helbing et al., 2002, Helbing and Molnar, 1995]. Further models belonging to this class are those of Hoogendoorn [2000], Hoogendoorn and Bovy [2001], Hoogendoorn et al. [2002] and (for the case of evacuation simulation) Thompson et al. [1996]. The former provides a generalization of the social force model where the way finding is based on an extremal principle, whereas the latter is a full scale implementation covering also complex geometries like floor-plans of large office buildings or passenger vessels.

The social force model is based on continuous space and time:

$$\frac{d\vec{x}_i(t)}{dt} = \vec{v}_i(t)\,, \tag{2.3}$$

where $\vec{x}_i$ denotes the position and $\vec{v}_i$ the velocity of pedestrian i. The pedestrians are represented as disks with radii r_i. The sum of forces pedestrian i is subject to is called $\vec{f}_i(t)$, m_i is the mass of pedestrian i, and $\vec{\xi}_i(t)$ are individual fluctuations. The equation of motion is then given by:

$$m_i \frac{d\vec{v}_i}{dt} = \vec{f}_i(t) + \vec{\xi}_i(t)\,. \tag{2.4}$$

Then the task is to determine $\vec{f}_i(t)$ and $\vec{\xi}_i(t)$. The resulting system of partial differential equations can be solved numerically (e.g, by applying methods of Molecular Dynamics

Simulations[1]). The force terms are [Helbing et al., 2002]:

$$\vec{f}_i(t) = m_i \frac{v_i^0(t)\vec{e}_i^{\,0}(t) - \vec{v}_i(t)}{\tau_i} + \sum_{j(\neq i)} [\vec{f}_{ij}^{\,\mathrm{soc}}(t) + \vec{f}_{ij}^{\,\mathrm{phys}}(t) + \vec{f}_{ij}^{\,\mathrm{att}}(t)] + \sum_b \vec{f}_{ib}(t) + \sum_k \vec{f}_{ik}^{\,\mathrm{att}}(t)\,, \quad (2.5)$$

where the first term describes the adaption to the desired velocity and direction (which is the internal driving force) within a relaxation time, the first sum repulsive social forces, physical forces ('body force' and sliding friction), and attractive forces between pedestrians, the second sum the repulsion from the boundary, and finally, the last term attraction to landmarks. If the term containing the desired velocity $v_i^0(t)\vec{e}_i^{\,0}(t)$ was absent, then the movement would be accelerated. Therefore, the first term represents a dissipative force. The relaxation time τ can be compared with the reaction time Δt in a discrete model (eq. 2.2). The social force between individuals as well as the repulsion from walls is assumed to decrease exponentially with the distance and the 'physical' force ensures that persons do not penetrate each other (an equivalent term is present in the wall or boundary term $\vec{f}_{ib}$):

$$\vec{f}_{ij}^{\,\mathrm{soc}} = \{A_i \exp[(r_{ij} - d_{ij})/B_i]\}\,\vec{n}_{ij}\,, \quad (2.6)$$

$$\vec{f}_{ij}^{\,\mathrm{phys}}(t) = k\Theta(r_{ij} - d_{ij})\vec{n}_{ij} - \kappa\Theta(r_{ij} - d_{ij})\Delta v_{ij}^t \vec{t}_{ij}\,, \quad (2.7)$$

$$\vec{f}_{ij}^{\,\mathrm{att}}(t) = -C_{ij}\vec{n}_{ij}\,, \quad (2.8)$$

$$\vec{f}_{ib}(t) = \{A_i \exp[(r_i - d_{ib})/B_i]\}\,\vec{n}_{ib} + k\Theta(r_i - d_{ib})\vec{n}_{ib} - \kappa\Theta(r_{ij} - d_{ij})\Delta v_i^t \vec{t}_{ib}\,. \quad (2.9)$$

$\Theta(x)$ is x for $x \geq 0$, zero otherwise (Heaviside-function), i.e., the corresponding terms are only relevant, if the pedestrians touch each other ($d_{ij} < r_{ij}$). $\vec{n}_{ij}$ is the normal vector pointing from i to j, $\vec{t}_{ij}$ the tangential vector perpendicular to it, and $\Delta v_{ij}^t = (\vec{v}_j - \vec{v}_i)\cdot\vec{t}_{ij}$ the tangential component of the velocity difference. The distance between pedestrian i and j (i.e., the centers of the disks) is denoted d_{ij}.

The parameters are the interaction strength A_i, its range B_i, and $r_{ij} = r_i + r_j$ is the sum of the radii. $d_{ij}(t) = \|\vec{x}_i(t) - \vec{x}_j(t)\|$ is the distance between the centers of i and j. For so called 'panic' situations the fluctuations are set to

$$\xi_i = (1 - n_i)\xi_0 + n_i\,\xi_{\max}\,, \quad (2.10)$$

where n_i with $0 \leq n_i \leq 1$ is the nervousness of pedestrian i, ξ_0 the normal and $\xi_{\max}$ the maximum fluctuation strength. Additionally, the social interaction f_{ij}^{soc} is reduced to a hard-core potential (i.e., $\kappa \gg A_i, B_i$) and for many purposes the attraction strength C_{ij} is set to zero. In normal situations, there might be no fluctuations. The numerical values for the parameters in different situations can be found in [Helbing et al., 2000].

In order to be able to assess the influence of the different contributions, in the following typical values are assigned to the parameters: $\tau_i = 0.5$ s, $A_i = 2 \cdot 10^3$ N, $B_i = 0.08$ m, $v_i^0 = 1.0$ ms^{-1} for normal situations, $k = 1.2 \cdot 10^5$ kg s^{-2}, and $\kappa = 2.4 \cdot 10^5$ kg m^{-1}s^{-1}. Additionally, the masses are $m_i = 80$ kg and the radii of the pedestrians are set to $2r_i \in [0.5\text{ m}, 0.7\text{ m}]$ in order to avoid exactly symmetrical configurations. For distances $(d_{ij} - r_{ij})$ larger than $5\,B$ and $v \approx 1$m/s, the first term in eq. 2.5 is about 160 N, whereas

[1]Information about MD techniques (containing algorithms) can be found in, e.g., [Rapaport, 1995].

the sum of the remaining terms is about 13.5 N. This might be used to simplify the implementation by neglecting interaction ranges $> 5\,B = 0.4\,\mathrm{m}$.

Lane formation can be observed in this model even for isotropic interaction forces, oscillation at bottlenecks and clogging can be simulated. One problem that is harder to tackle in this model than in discrete models are complex geometries. Since there are N^2 interaction terms, one either has to evaluate them explicitly or to check, whether some of them can be neglected. For complicated structures (like shopping centers or large passenger ships), this is a major challenge. The same holds for the interactions of the pedestrians with the walls, i.e., assuring that walls are not penetrated.[2] Similarly, it has to be checked whether the forces are screened by walls, i.e., two pedestrians do not repel (or attract, if A_i is negative) each other if there is a wall between them.

2.3.2 Discrete (Grid-based) Models

Especially for the reasons stated above, discrete models are appealing for simulations of large complex structures. Another factor is simulation speed, since cellular automata are per construction well suited for efficient implementation. The Nagel-Schreckenberg model [Nagel and Schreckenberg, 1992] is a very well understood model for the simulation of road traffic and can therefore provide insights into some aspects of models for crowd movement. Due to its simplicity, it provides a good starting point for relating fundamental properties of the model to its characteristics.[3] For the sake of completeness, the definition of the Nagel-Schreckenberg (NaSch) model is included here. The rule set (parallel update) for $t \to t + \Delta t$ is:

1. Accelerate: $v_i^t \to \min(v_{\max}, v_i^t + 1)$,
2. Mind the gap: $v_i^t \to \min(v_i^t, g_i^t)$,
3. Braking noise: $v_i^t \to \max(0, v_i^t - 1)$ with probability p_{dec} ($p_{\mathrm{dec}} \in [0, 1]$), and
4. Move: $x_i^{t+1} = x_i^t + v_i^t$.

Please note that i denotes cars not cells. Lengths and velocities are measured in units of the cell size a and $a/\Delta t$, respectively, with Δt being the time-step. Parallel update means that all cars move synchronously. Therefore, each step (1, 2, and 3) is carried out for all cars first before going to the next step, i.e., the velocities are determined for all cars, before the cars move. This can be implemented (and is equivalent to) a sequential update (of cars) in the direction of movement.[4] This leads effectively to a car blocking all the cells of its trajectory within the update step Δt.[5]

The parameters in this case are the cell size a, the maximum velocity $v_{\max}$, and the deceleration probability (braking noise) p_{dec}. v_i denotes the actual velocity of car i and g_i the distance to its predecessor in cells (see fig. 2.4). If Δt is set to 1 s, the maximal velocity $v_{\max} = 5$ corresponds to $37.5\,\mathrm{m/s} = 135\,\mathrm{km/h}$ and the acceleration is $7.5\,\mathrm{m/s^2}$.

[2] A typical plan of a large building may contain more than 10,000 line elements. If there are 10,000 persons in a simulation then this means 10^8 checks every time-step, if no further simplifications are utilized.

[3] Nagel [1996] provides a framework for road traffic in the language of particle hopping models.

[4] For periodic boundary conditions it has to be checked whether a car crosses the boundary. In this case, it must be ensured that it does not drive onto a cell that has been left by another car in the same update step.

[5] This equivalence will become useful when generalizing the model to 2D.

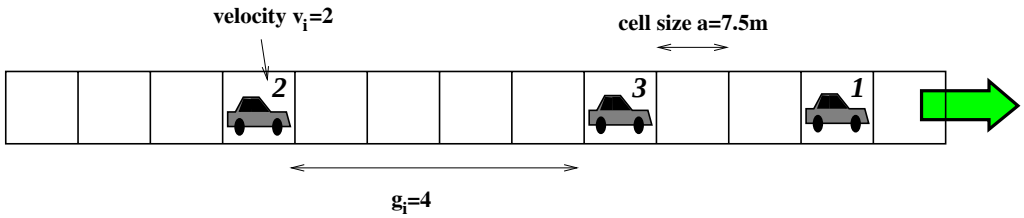

Fig. 2.4. Definitions and notations in the Nagel-Schreckenberg model. The numbers in the cells give the current velocity, g_i denotes the gap between car i and its predecessor. The cell size in the standard model is 7.5 m which leads for $\Delta t = 1\,\mathrm{s}$ to a maximum velocity of 135 km/h and an acceleration of $7.5\,\mathrm{m/s^2}$.

The results obtained for the NaSch model concerning the influence of $v_{\max}$ and fundamental flow-density-relations are important for understanding the generalization to two dimensions, where similar decisions concerning the cell size, the type of the update, and $v_{\max}$ have to be made. Exact results can be obtained for the case $v_{\max} = 1$, where the NaSch model is equivalent to the asymmetric simple exclusion process [Rajewsky et al., 1998]. In this case, the backward sequential update (against the direction of motion) produces the highest flow[6], which is given by

$$J_{\leftarrow}(\rho, p) = p\rho\frac{1-\rho}{1-p\rho}\,. \tag{2.11}$$

p is the hopping probability[7] and J grows with p. If p is set to 1, then $J = \rho$, i.e., all cars always move. The density for which the flow takes its maximum is shifted to the right when p is increased. This is different for the parallel update:

$$J_{||}(\rho, p) = \frac{1}{2}\left(1 - \sqrt{1 - 4p\rho(1-\rho)}\right)\,. \tag{2.12}$$

In this case, the maximum of J is always at $\rho = 1/2$.[8] Those results will be useful when comparing the different updates for the 2D model in the next chapter.

The limit of high acceleration in the NaSch-model is similar to the case of pedestrians: the acceleration when walking is instant. Rule 1 is then replaced by $v_i^t = v_{\max}$. In the case of $v_{\max} = 1$ this is of course trivial.

For road traffic, the distance between cars is determined by the time gap, i.e., $g_i \sim v_i$. This is necessary, since deceleration from $v_{\max}$ to 0 takes time, i.e., cars must obey a 'safety distance' proportional to the speed. Therefore, the trajectory of a car is effectively blocked, i.e., cannot be accessed by another car. This is automatically taken into account by the parallel update. This behavior is not the case for pedestrians: Stopping is possible instantly and therefore a pedestrian does not necessarily have to keep a distance to his predecessor. Whether this requires to introduce a different type of update for the 2D case will be discussed in the next section.

Therefore, the update type deserves special consideration. As before, the simpler 1D case provides a good starting point. Figure 3.17 shows a comparison of the parallel update and a so called shuffled update for the NaSch model. In the shuffled update, the sequence of the cars moving is random. However, each car is allowed to move only once

[6] In this case, updating cells or cars is equivalent.

[7] corresponding to $1 - p_{\mathrm{dec}}$ in the NaSch–model

[8] The case of different p for each particle has been investigated by Evans [1997].

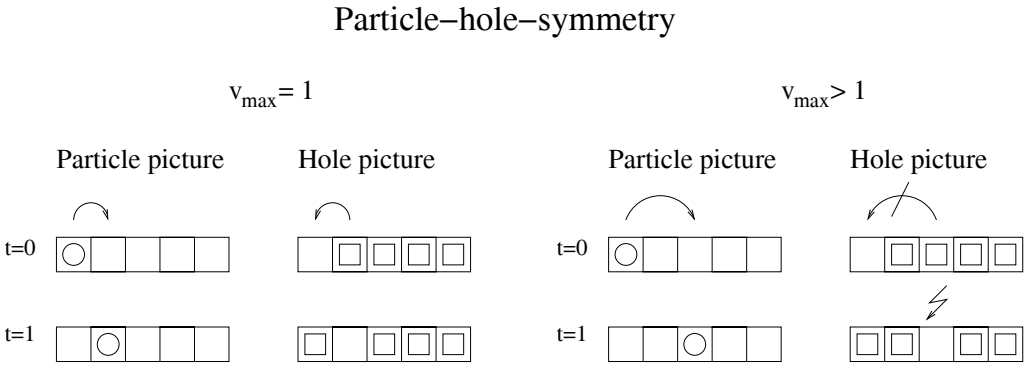

Fig. 2.5. Particle-hole symmetry holds for $v_{\max} = 1$ but does not for $v_{\max} > 1$. Left: the dynamics remains the same, if holes move instead of particles in the opposite direction but according to the same rules. Right: For $v_{\max} > 1$ this does not hold, since the one but leftmost hole would have to move together with the leftmost one, which is not allowed for a parallel update. The particle-hole symmetry leads to a symmetry in the fundamental diagram as can be seen from eq. 2.15 and is shown in fig. 3.17.

in a time-step. Since in this case the particle hole symmetry is broken, the fundamental diagram – other than for the parallel update – is not symmetric with respect to $\rho = 1/2$ for $v_{\max} = 1$. Particle hole symmetry means that switching particles with holes and changing the direction of motion without changing the rules otherwise does not change the time evolution of the system (see fig. 2.5). The importance of the symmetry lies in the fact that it enforces the fundamental diagram (flow vs. density relation) to be symmetric around $\rho = 1/2$. This can be seen from the following equations:

$$\rho_{\text{particles}} = 1 - \rho_{\text{holes}} , \tag{2.13}$$

$$j_{\text{particles},\uparrow}(\rho) = j_{\text{holes},\downarrow}(1 - \rho). \tag{2.14}$$

$j_\uparrow$ denotes the flow in the direction of motion (of the particles) and $j_\downarrow$ against the direction of motion (for the parallel update). For $\rho_{\text{particles}} = 1/2+x$, $\rho_{\text{holes}} = 1/2-x$, and therefore

$$j_{\text{particles},\uparrow}(1/2 - x) = j_{\text{particles},\uparrow}(1/2 + x). \tag{2.15}$$

Please note that particle hole symmetry does never hold for an interaction range larger than 1 cell, i.e., neither for $v_{\max} > 1$ (cf. fig. 2.5) nor for particle sizes A larger than the cell size a as shown in fig. 2.6. This can be summarized:

$$\text{Particle hole symmetry } \Leftrightarrow v_{\max} = A = 1. \tag{2.16}$$

This statement is not contradicted by the choice $v_{\max} = v_{\min} = A = n$, with n arbitrary, e.g., $n = 3$, since this can easily be rescaled to $v_{\max} = A = 1$.

The NaSch model is covering in its basic form only single-lane traffic either with periodic or open boundary conditions. This is not sufficient for simulating real traffic scenarios. The model can be improved or extended in various ways:

1. multiple lanes [Nagel et al., 1998],
2. smaller cells [Knospe et al., 2000],

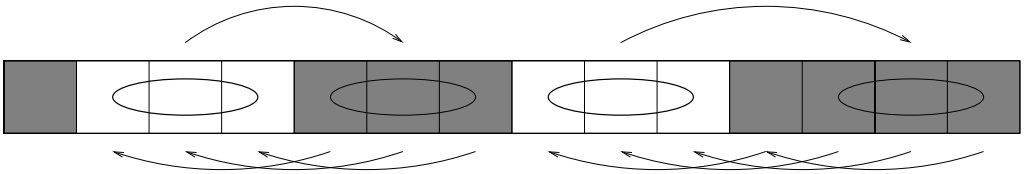

Fig. 2.6. The particle hole symmetry is broken in the 1D case (i.e., NaSch model) for interaction ranges larger than a ($A > a$). The arrows above the grid indicate the motion of the particles, the ones below the grid the motion of the holes (see also fig. 2.5). Since the movement of one particle corresponds to the movement of three holes, there is no symmetry between particles and holes.

3. anticipation of preceeding car's movement, and braking lights [Knospe, 2002],
4. on– and off–ramps [Diedrich et al., 2000],
5. sinks and sources (varying number of cars) [Kaumann et al., 2000], and
6. different sizes for cars and trucks.

Decreasing the cell size makes it possible to distinguish between trucks and cars (adapting the speed limits $v_{\max}$ accordingly) and to accelerate more smoothly. The distinction between anticipation and braking lights is basically that the former takes into account the velocity of and the gap to the preceeding car, the latter its deceleration.

The next chapter deals in detail with a specific CA model for pedestrian motion. Here, an overview over some related models is given. Starting from the 1D model, a generalization to 2D models that might be applicable for pedestrian movement is via forming a corridor as a multi-lane structure. This makes it necessary to define lane-changing rules. An overview for road traffic can be found in [Chowdhury et al., 1997, Nagel et al., 1998, Rickert et al., 1996]. However, in this case, there is only one direction of movement. A first step towards generalization is the introduction of two possible walking directions. Blue and Adler [1999] have proposed such a model, which they call *bi-directional*. This was then extended to a four-directional (in the sense of possible walking directions) one [Blue and Adler, 2000] which simulates pedestrian crossings. The idea is highlighted in fig. 2.7. Since there is hard core exclusion, deadlock situations might occur, in which blocks are formed and not resolved. Therefore, a switching process was introduced: two opponents might change their positions if they occupy cells next to each other and have opposite walking direction.

However, this approach is limited to geometries, where the walking direction does not change. Therefore, it is not possible to simulate situations where movement is not from left to right but, e.g., towards an exit. To do this, the walking direction has to be determined taking into account external information like signage. Just recently Burstedde et al. [2001] have proposed a 2D CA model with different kinds of floor fields: a static (S) and a dynamic (D) one. The static floor field is a scalar field representing the distance to either the exit or the destination cells measured by a Manhattan metric, i.e., the number of steps across edges between this cell and the exit.[9]

A more extensive description of this model can be found in [Burstedde, 2001]. One of the interesting results of this approach is its ability to reproduce lane formation without

[9] An extended Manhattan metric (where steps across edges and corners are possible) is illustrated in fig. 3.12.

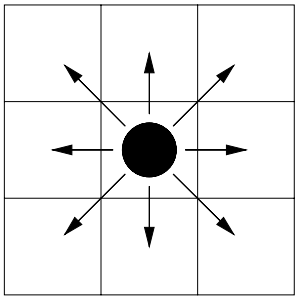

$M_{-1,-1}$	$M_{-1,0}$	$M_{-1,1}$
$M_{0,-1}$	$M_{0,0}$	$M_{0,1}$
$M_{1,-1}$	$M_{1,0}$	$M_{1,1}$

Fig. 2.7. The preferred walking directions can be expressed via a 3×3 matrix. The entries might be interpreted as probabilities, such that $\sum_{i=-1,j=-1}^{i=1,j=1} M_{ij} = 1$. For uni-directional flow (road traffic) $M_{0,1} = 1$ and all particles move in the same direction. For bi-directional flow, there are two different species with uni-directional matrices M^1 and M^2 and for four directional flow, four different ones.

explicitly taking into account the interaction between persons. Therefore, lane formation can be found also in (spatially) discrete models. The static field S enables route choice, whereas D is modified by the pedestrians and introduces long range interactions.

The transition probability is obtained by combining those different influences:

$$p_{ij} = N \cdot \exp\left[k_s \left(S_{ij} - S_{00}\right) + k_d \left(D_{ij} - D_{00}\right)\right] \cdot (1 - n_{ij}). \tag{2.17}$$

k_s and k_d are parameters determining the interaction of the pedestrians with the fields S and D, N is a normalization constant to ensure that $\sum_{i=-1}^{i=1} \sum_{j=-1}^{j=1} p_{ij} = 1$. The ij do not denote cells but neighborhood relations (cf. fig. 2.7), i.e., $i, j \in \{-1, 0, 1\}$ and (00) is the current cell. The occupation number n_{ij} is 0, if the cell j is empty, 1 otherwise, and $n_{00} \equiv 0$. Therefore, n_{ij} can be used to represent walls and other obstacles. This means that the transition probabilities are determined by considering only accessible cells. Otherwise it would be necessary to set $S_j = -\infty$ for wall cells in order to have the same effect in eq. 2.17 with n_{ij} representing only the occupation by pedestrians. The update is done synchronously (parallel update), i.e., all pedestrians move at the same time. For $k_d = 0$ (no interaction, except the hard core exclusion) the coupling constant k_s can be compared to the probability $P(v_x \leq 0)$ which is in a sense the equivalent of p_{dec} in the NaSch-model.[10]. For four possible destination cells this is given by:

$$p_{ij} \sim \exp[k_s \cdot (S_{ij} - S_{00})], \tag{2.18}$$

and the transition probabilities for movement along a corridor can be written in matrix form as

$$P = N \cdot \begin{pmatrix} 0 & 1 & 0 \\ e^{-k_s} & 1 & e^{k_s} \\ 0 & 1 & 0 \end{pmatrix}. \tag{2.19}$$

This yields

$$P(v_x \leq 0)_{k_s} = 1 - \frac{e^{k_s}}{3 + e^{k_s} + e^{-k_s}}. \tag{2.20}$$

[10] p_{dec} denotes the probability for deceleration (stopping in the $v_{\max} = 1$–case). Pedestrians can stop immediately, therefore, p_{dec} is – other than for cars – the probability for stopping and not for reducing the speed by 1. However, for $v_{\max} = 1$ there is of course no difference between both.

Table 2.2. Different influences and their representation

Different influences and their representation in the agent framework. Agents are representing a person in a simulation model and their abilities are represented on different levels.

agent's skills	description	example
operational	physical (mainly reaction)	avoiding obstacles
tactical	decisions (short ranged)	following signage
strategic	goals (long ranged)	moving towards exit

This illustrates that the connection made in eq. 2.20 between k_s and a deceleration probability p_{dec} like the one used in the NaSch model is rather an estimate for interpreting k_s, since k_s does not only determine the probability for deceleration but also for stepping to the side. Furthermore there are negative velocities. Nevertheless, eq. 2.20 allows to connect it with the probability $P(v_{\max} \leq 0)$. This is different from the model investigated in the next chapter, where there are two separate probabilities p_{dec} and p_{sway} for stopping and stepping to the side.

2.4 Population and Behavior

2.4.1 The Agent Framework

Similar to the case of space, there are two basic possibilities for representing the population (cf. fig. 2.2): on the one hand macroscopic models, utilizing aggregated variables and describing the flow of persons as a hydrodynamic system. On the other hand microscopic models, describing the individual movement and behavior (comparable to thermodynamics vs. statistical mechanics). Usually, either space and population are microscopic (detailed geometry and individual persons) or neither.

A general framework for representing a population of individuals are multi-agent-systems. The concept has recently been used to visualize pedestrian activity [Dijkstra et al., 2000] and to investigate the behavior of road users [Wahle, 2002]. An overview over recent developments in the field can be found in [Moss, 2001].

The abilities of an agent can be divided into three different levels:

1. Skill-based – operational level
   (automatic reaction),
2. Rule-based – tactical level
   (stereotypic reaction)
3. Knowledge-based – strategic level
   (cognition, problem-solving, decision making).

Classical Cellular Automata (a definition is given in section 3.1) can be interpreted as multi-agent systems where only the tactical and operational level are present. Examples for tasks and the level they correspond to are shown in table 2.2.

2.4.2 Social Aspects: Competition

Concerning the population one of the major questions is whether social influences can be quantified and reproduced by a simulation. For one aspect of social behavior, namely

competition vs. cooperation, it will be shown in section 3.7.2 that this is possible. Experimental results [Muir, 1996] show that the motivation level has a significant influence on the egress time from a narrow body aircraft (the empirical results are also described in section 3.7.2).

The question arises, how the motivation level can be modeled. Two approaches, with the second being a generalization of the first, can be utilized to cover the influence of the different behavior:

1. Competition is represented via friction in combination with a more assertive behavior (increased walking speeds).

2. There is a pay-off for winning the competition and a penalty for loosing it.

The first approach does penalize everyone for competition. However, since the behavior is more assertive, it might still lead to a more efficient egress (i.e., smaller time). Therefore, there are two opposite contributions: the gain for being more assertive and the loss due to the competition. The latter depends on the exit width, since the number of conflicts decreases with the exit width. The corresponding simulation results are shown in section 3.7.2.

The second approach is not based on increasing the assertiveness of the whole population. However, it can not as easily be incorporated in a simple model without introducing further model features. On the other hand, in such an extension, individuals could increase their pay-off (i.e., decrease their egress time) by behaving more clever. The 'currency' used in this context could be speed, for example. This concept is not further investigated here, since it would lead to a level of complexity beyond the scope of a first principles model.

There are of course further social influences that are important in the case of an emergency. The formation of groups is one prominent example [Kugihara, 2002]. However, these rather complex social processes are (at least for the time being) hard to express in mathematical terms and therefore beyond the scope of this work.

2.5 Empirical Data: Literature Review

This section gives an overview over the empirical and experimental data available in the literature. A major distinction can be made between empirical observations and experimental investigations. The former contain observations of daily walking patterns or crowd behavior, whereas the latter aim at a controlled laboratory environment, where the influence of one controlled variable on preferably one other variable is investigated. The second criterion for classification is into normal or emergency situations. The different sources for data about crowd motion are illustrated in fig. 2.8.

The connection between reality (observations and experiments) and a microscopic theory is threefold:

1. Calibration (Parameter Settings)
   Rule-set and functions, e.g., the maximum individual walking speed as a function of the age, etc. ($v^i_{\max} = f(\text{age}, ...)$);

2. Validation of the model
   Fundamental relations like the one between flow and density ($j(\rho)$);

3. Validation of simulation results
   Full-scale tests, e.g., evacuation drills.

In general the description of the experimental setting contains population, geometrical layout, hazards, stress factors, information available to the participants, and the sequence of the events. For empirical data the description of those factors is often less detailed. The main sources for empirical data are summarized in table 2.3.

Table 2.3. Summary of the empirical data found in the literature. The results are described in more detail in the text. FWHM is short for Full width at half maximum (θ). If no explicit formula or type of distribution is given θ is used to characterize the width of the distribution (for the probability density it holds $f(\mu \pm \theta) = 1/2\, f(\mu)$). Additional reviews for the walking speed on stairs can be found in [Frantzich, 1996] and for the flow on stairs and surface level in [Graat et al., 1999].

Environment	Type of data	Main result
Walkways	frequency distr.	$\mu = 1.34\,\mathrm{m/s}$, $\sigma = 0.26\,\mathrm{m/s}$ [Weidmann, 1992]
Urban	frequency distr.	$\mu = 1.19\,\mathrm{m/s}$, FWHM=$0.21\,m/s$ [Fruin, 1971]
Campus	frequency distr.	$\mu = 1.53\,\mathrm{m/s}$ [Henderson, 1971]
Zebra crossing	frequency distr.	$\mu = 1.44\,\mathrm{m/s}$ [Henderson, 1971]
Walkways	flow vs. density	$\rho_{\max} = 5.4\,\mathrm{P/m^2}$ [Weidmann, 1992]
Urban	speed vs. density	$j(\rho),\ \rho \sim 1\,\mathrm{P/m^2}$ [Fruin, 1971]
Commuters	walking speed	v(age) [Ando et al., 1988]
School yard	walking speed	sexual differences [Henderson, 1972]
Aircraft mockup	egress time	critical exit width [Muir, 1996]
Ships	behavior	panic is very rare [Harbst and Madsen, 1996]
Stair Mockup	upstairs/downstairs	$d_{\mathrm{gap}} \geq 0.25\,\mathrm{m}$, $v_\uparrow$, $v_\downarrow$ [Frantzich, 1996]
Overviews		
Walkways/Urban	[Fruin, 1971, Transportation Research Board, 1994, Weidmann, 1992]	
Buildings	[Pauls, 1995, Predtetschenski and Milinski, 1971]	

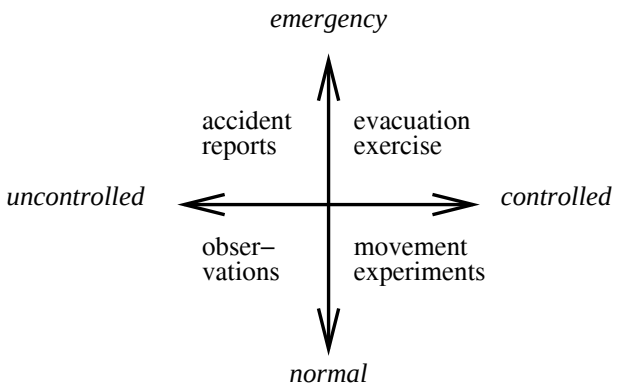

Fig. 2.8. Empirical data (including experiments) can be roughly classified according to controlled/uncontrolled and emergency/normal situations. Of course, there are other important criteria, like validity, reliability and objectivity. This becomes especially important for the uncontrolled situations, where those criteria are harder to ensure due to the lack of an operational definition of the situation.

The empirical observations on pedestrian movement patterns in non emergency situations can be classified into four major categories:

- Oscillations at bottlenecks, resp. pulsed outflow at doors [Helbing, 2001, Müller, 1999],
- Lane formation [Yamori, 2001],
- Round-about traffic [AlGadhi et al., 2002] and the formation of stable walking patterns,
- Jam waves for high densities around $8\,\mathrm{P/m^2}$ [Pauls, 1995] and density fluctuations.

It is difficult to perform experiments on crowd motion, which is mainly due to the fact that reliability requires a statistical analysis and therefore a high number of repetitions. Either one has to restrict oneself to small numbers of participants, which then is rather an experiment on single pedestrians and physiology. Even in this case, the effort can be immense [Bles et al., 2002]. Or one has to accept the fact that the situation is not controlled (in the sense of varying parameters or control variables and observing the controlled variables) and the evaluation is restricted to observation.

2.5.1 Data on Walking Speed Distributions

Frequency Distribution

Walking speed, like any other physiological quantity, can best be described as a statistical distribution. Whether an analytical expression is used to fit the data is mainly a question of practicality, as long as there is no theoretical foundation in favor of it. Weidmann [1992] has evaluated about 150 references. His report contains information about the dependency of walking speed on physiology, height of the persons, space requirement, level of service, etc. The results are usually obtained by averaging over all the different values

given in the literature. Fundamental diagrams $j(\rho)$ (ρ is the density and j the specific flow) are given for movement on surface level and stairs. By summing up the different distributions found in the literature, a walking speed of 1.34m/s ± 0.26m/s (mean value ± standard deviation) for flat terrain results. This gives the frequencies of the walking speed in an average population. They are assumed to be normally distributed.

Henderson [1971] derives distribution types for pedestrians from Maxwell Boltzmann theory. For the speeds in the case of no directed movement ($v = |\vec{v}|$) the probability density is given by:

$$f(v) = \frac{1}{\sqrt{2\pi}v'^3} \cdot v^2 \cdot e^{-v^2/v'^2}, \tag{2.21}$$

where v' is the velocity for which f has its maximum.[11] The parameter v' was obtained for children on a playground to be 0.67 m/s (walk mode) and 1.9 m/s (run mode). In this case, there is no directed movement, i.e., $\langle v_x \rangle = \langle v_y \rangle = 0$.

In the case of directed movement the distribution for the velocities (x-component) is Gaussian:

$$f(v_x) = \frac{1}{\sqrt{2\pi}\sigma} \cdot \exp\left[-\frac{1}{2}\left(\frac{v_x - \mu}{\sigma}\right)^2\right] \tag{2.22}$$

with $\mu = \langle v_x \rangle$ being the velocity of the flow. The parameters obtained for students walking on the campus are $\mu = 1.44\,\mathrm{m/s}$ and $\sigma = 0.228\,\mathrm{m/s}$. For a zebra crossing, the values are $\mu = 1.53\,\mathrm{m/s}$ and $\sigma = 0.201\,\mathrm{m/s}$. Other authors have suggested skewed Gaussian distributions [Werenskiold, 1998]. However, the analytical form is not specified and therefore ambiguities remain. In addition to the asymmetry, the probability density would have to be known to compare this suggestion with the previous formulae.

A further study we performed to check the assumptions concerning the distribution of walking speeds is presented in section 2.6 below.

Flow Density Relation

A second important fundamental relation is the one between the density and the flow. The shape of the fundamental diagram given by Weidmann [1992] for uni-directional pedestrian movement on walkways is shown in fig. 2.9. The analytical expression for the specific flow obtained via fitting to empirical data is given by:

$$v(\rho) = v_{\mathrm{free}}\left[1 - e^{-\gamma\cdot(\frac{1}{\rho} - \frac{1}{\rho_{\max}})}\right], \tag{2.23}$$

$$j_{\mathrm{spec}}(\rho) = v(\rho)\cdot\rho = 1.34\cdot\rho\left[1 - e^{-\gamma\cdot(\frac{1}{\rho} - \frac{1}{\rho_{\max}})}\right], \tag{2.24}$$

where the fit-parameter γ is calculated to be 1.913. Finally from eqs. 2.24 and 2.23 a flow-speed relation can be obtained

$$j_{\mathrm{spec}}(v(\rho)) = \frac{v(\rho)}{\frac{1}{\rho_{\max}} - \frac{\ln(1-\frac{v(\rho)}{v_{\mathrm{free}}})}{\gamma}}\,. \tag{2.25}$$

Additional flow density relations can be found in [Pauls, 1995, Transportation Research Board, 1994]. Predtetschenski and Milinski [1971] carried out extensive experiments on flow of persons for different geometries. The so called 'macroscopic' models

[11] $v' : \langle v \rangle : \sqrt{\langle v^2 \rangle} = 1 : \frac{2}{\sqrt{\pi}} : \sqrt{\frac{3}{2}}$.

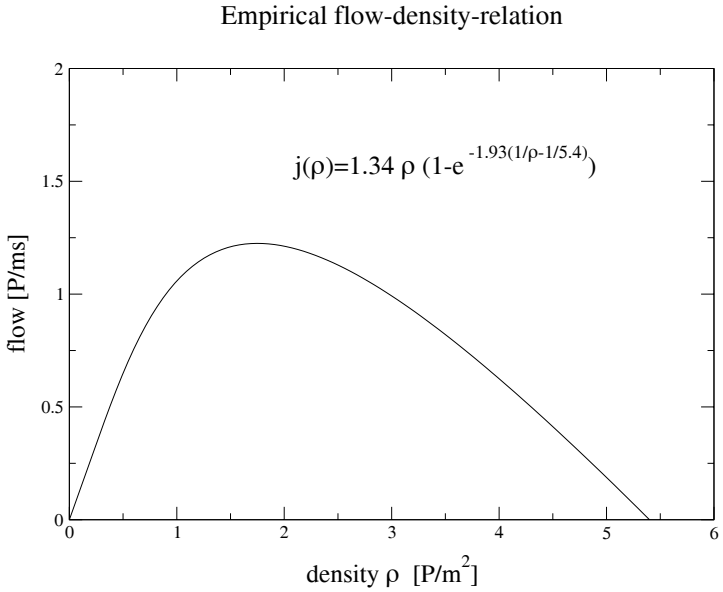

Fig. 2.9. Flow density relation for pedestrian movement. The analytical expression is shown at the top of the figure. The curve is a fit to empirical data [Weidmann, 1992].

employ those fundamental properties – mainly the relation of density to flow and walking speed – to calculate egress times.

Empirical observations on the influence of the width (e.g., of a corridor) on the specific flow could not be found in the literature. The specific flow $j_{\text{spec}} = j/W = \rho \cdot v$ is obtained from the overall flow by dividing it by the width W ($j = \rho \cdot v \cdot W$). This assumes that the specific flow does not depend on the width.

2.5.2 Movement on Stairs and Through Doors

Experiments carried out in Sweden [Frantzich, 1996] addressed the walking speed on stairs up and down. Especially the case of spiral staircases was examined, which had not been done to a larger extent before. Whereas in the earlier studies of Predtetschenski and Milinski [1971] and Fruin [1971] the main results were flow-density relations obtained from observations, in this case flow-distance relations were measured under controlled laboratory conditions. The participants were students of age 20-30. The distance to the person ahead (gap) can be transformed into a local density via

$$\rho_{\text{local}} = \frac{1}{d_{\text{gap}}}\,, \tag{2.26}$$

where d_{gap} includes the 'size' of a pedestrian in walking direction, i.e., for a distance of around 0.25 m (the minimal distance that occurred during the experiments) there was body contact. This gap of 0.25 m corresponds (if the minimal stair width is assumed to be 60 cm) to a maximum density of $\rho_{\text{local}}^{\max} = 6.7\,\text{m}^{-2}$.

The walking speed did not show a dependence on the inter-person distance for distances in the range between 0.5 and 2.5 m for a narrow stair and walking downstairs (0.72 ± 0.29 m/s). Basically the same result was obtained for wider stairs (0.69 ± 0.15 m/s)

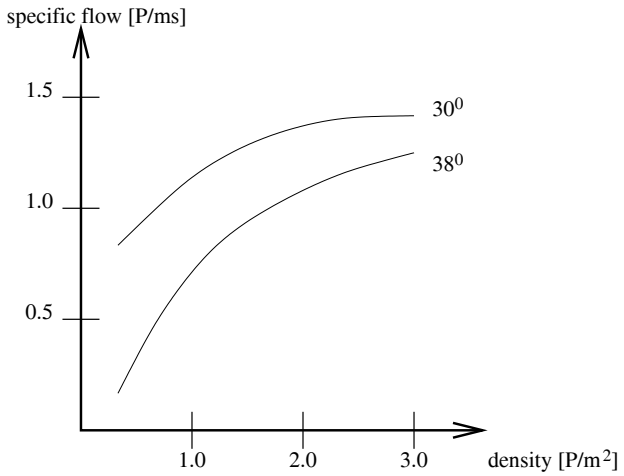

Fig. 2.10. Flow density relation for pedestrian movement on stairs. The dependence on the slope is most prominent for low densities, where steeper stairs perform worst. The experiments have been carried out in a Dutch football stadium. Additionally, the influence of the motivational level on the flow has been investigated [Graat et al., 1999].

and up stair direction ($0.51 \pm 0.10\,\mathrm{m/s}$ for a narrow and $0.56 \pm 0.14\,\mathrm{m/s}$ for a wider stair). The minimum interpersonal distance was measured to be around 0.25 m for both upstairs and downstairs. This range of distances can be transformed into densities between 0.4 and $2\,\mathrm{m}^{-2}$ via eq. 2.26. Therefore, the results are in a sense contradictory to the assumption of a flow density relation for stairs similar to the one in fig. 2.9 and the speed density relation (horizontal component of $\vec{v}$) for movement on stairs [Weidmann, 1992]:

$$v_{\mathrm{horizontal}} = c \cdot [1 - e^{-\gamma(1/\rho - 1/\rho_{\mathrm{max}})}], \tag{2.27}$$

with $c = 0.61$ and $\gamma = -3.7$ for up and $c = 0.69$ and $\gamma = -3.8$ for downstairs.

However, the movement on stairs could be fundamentally different from plain areas. Especially sort of 'synchronization' effects can be observed in railway and subway stations when dense crowds move up or down to a platform with considerable walking speed. The separation of the area into steps might support such an effect.

Furthermore, the report of Frantzich [1996] contains useful remarks about the video analyzing technique (using the software package Persias) as well as the experimental setup.

Movement through doors has mainly been investigated with respect to the capacity of the door, i.e., based on the concept of a specific flow. It is for example common, to assume a maximum specific flow in egress calculations of $1.33\,\mathrm{P/ms}$ [Health and Safety Executive, 1996]. The underlying assumption is a smooth functional relation between the width and the flow, i.e., there are no special widths where there is a jump in the capacity of the door. However, this assumption is limited to a certain range of widths as can be seen from the fact that a bottleneck smaller than the body size can no longer be passed.[12]

[12] Pauls [1995] suggests a value of $1.0\,\mathrm{P/s}$ for a door of width 910 mm and moderate flow conditions.

The flow of persons with respect to the stair angle of the tribune in a football stadium was investigated by [Graat et al., 1999]. Figure 2.10 shows that the specific flow increases more strongly with the density for steep stairs (38°) than for those with a normal angle (30°).

Even though most of these results will not be implemented in the simulations (cf. chapter 4) it is important to know the different influences and to be able to estimate the error that results when they are neglected. A straightforward approach to include these special aspects could be via multiplying the walking speeds with an appropriate reduction factor. This will be done for the maximum individual walking speed $v^i_{\max}$ on stairs (cf. section 4.1.1). This allows to use one parameter for the walking speed. Otherwise, a separate parameter for walking speed on stairs would have to be introduced.

2.5.3 Egress and Evacuation Scenarios

Evacuation exercises have been carried out for different vessels and buildings:

- Aircraft [Jungermann and Göhlert, 2000, Muir, 1996, Owen et al., 1998],
- Land based passenger vessels: trains [Galea and Galparsoro, 1994],
- Passenger Ships [Harbst and Madsen, 1996, Marine Safety Agency, 1997, Wood, 1997],
- Residential, Office, and Public Buildings [Proulx, 1995, Weckman et al., 1999].

The results vary greatly depending on the occupants and the type of the building. One major influence is whether the occupants are familiar with the surrounding or not, i.e., office and residential buildings on the one and public buildings on the other hand. It has been reported for nursing homes and residential buildings that it took up to 30 minutes for some occupants to respond to the alarm and they basically had to be forced by fire fighters to leave the building [Proulx, 1995]. Such a case is not within the scope of a simulation. One could, however, adapt the reaction time distribution for the simulation accordingly, if the necessary data is provided (cf. eq. 4.1).

A long response time is connected to the decision making process. Figure 2.11 shows different possible strategies in an emergency situation. Since the scope of this work is not the decision making but the movement dynamics, it is put into the model as an assumption that the persons are able and decide to egress.

Another topic in this context is the one of panic. Canter [1990] basically discards it and argues that behavior that seems to be strange from the outside is understandable by the restricted amount of information available to those who are actually in an emergency situation. Also Proulx [1995] did not find any hints for flight panic in her investigations. It was rather observed that people become lethargic when facing immense danger. Therefore, the major consequences for representing these special scenarios are higher fluctuations for the parameter values (like walking speed or reaction time) seem to be higher under those unusual and unfamiliar circumstances.

An overview over accidents for buildings (including football stadiums and the like) can be found in [Helbing et al., 2002]. Remarks on safety management for football stadiums and large events in general are contained in [Health and Safety Executive, 1996, 1999].

Route Choice in an Evacuation Exercise

Abe [1986] has investigated the route choice behavior in a mimicked emergency situation. The fire alarm was triggered and artificial smoke occurred. People were asked what the

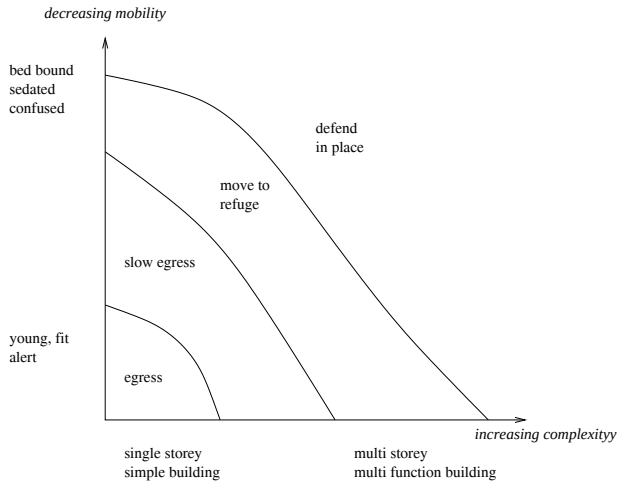

Fig. 2.11. Egress vs refuge in building evacuation: The more complex a building is and the less the mobility the more difficult is the egress from a building. This leads to a distinction between four different strategies: egress, slow egress, move to refuge, and defend in place [Abrahams, 1994].

major motivation for choosing the exit in a large supermarket was. The answers were given with the following frequencies:

1. Following exit signs, announcements via the public address system, or from the staff (53.3%).
2. Choosing the nearest exit (24.7%).
3. Escaping from fire and smoke, taking the direction away from it (12%).
4. Following other persons (6.7%).
5. Using the familiar door (1.7%).
6. A window near to the door, it's bright there (1.0%).
7. The door wasn't crowded (0.7%).
8. Others.

It is remarkable that the familiarity with the exit did not play a very important role concerning the exit choice. A similar observation has been made in an evacuation exercise we carried out in a movie theater that will be presented together with a comparison to simulation results in section 4.3.2.

2.6 Velocity Distribution and Dependance on Group Size

In 2000 the world exhibition (Expo) took place in Hannover. At this event we observed pedestrian movement at different scenes. The most useful one was a pedestrian bridge,

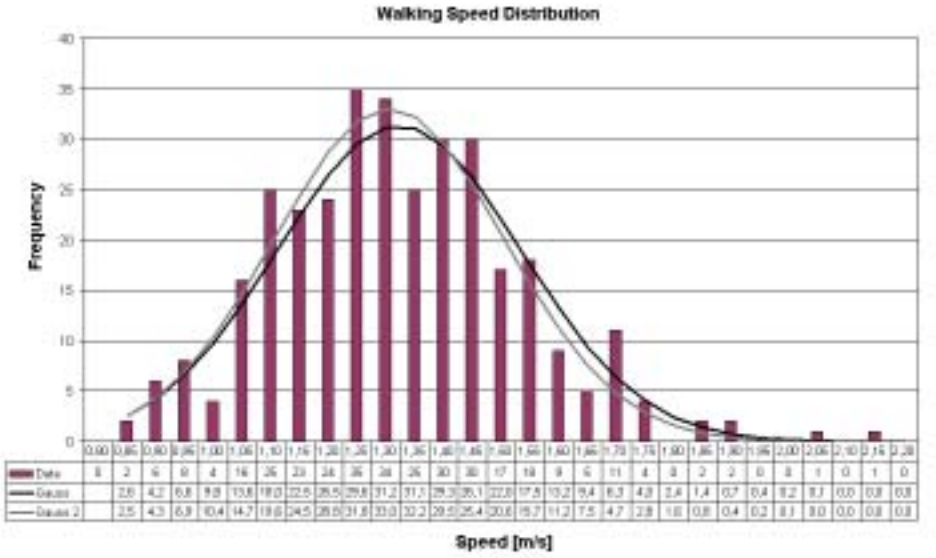

Fig. 2.12. Shown is the walking speed distribution for the pedestrian bridge at the World Exhibition (Expo) 2000 in Hannover. The length that was walked by the pedestrians was 15.5 m. A Gaussian distribution is fitted to the results with μ and σ obtained either from the sample or using adapted values where the medians of the fitted and empirical curves are closer to each other. The data is shown in the table below the horizontal axis. Groups are represented by one data point (cf. table 2.4).

where the frequency distribution of the walking speeds and its relation to the group size was measured. The measurement of the walking speed on the pedestrian bridge comprised 700 persons. There was no slope on the bridge. The measurement area was a square of $7 \times 7\,\mathrm{m}^2$. The width of the bridge was 14 m altogether, i.e., twice the length of this square. The length of the bridge was much larger than its width. The speed of the pedestrians was obtained by $v_i = l/\Delta t_i$, where Δt_i is the time for walking from one edge of the square to the other in the longitudinal direction (across the bridge). Due to the low densities there was no obstruction by other pedestrians, i.e., the walking speeds were that of free flow.

A normal distribution has been fit to the data using the mean and standard deviation of the empirical distribution as well as adapted values. The data and the fitted curves are shown in fig. 2.12. The mean value obtained was $\mu = \langle v_x \rangle = 1.30\,\mathrm{m/s}$ and the standard deviation $\sigma = 0.21\,\mathrm{m/s}$. The third moment of the distribution $E(x^3 - \langle x^3 \rangle)$ is $0.41\,(\mathrm{m/s})^3$. This shows that the distribution is not symmetric but slightly skewed towards the origin. The parameters for the second fit-curve shown in fig. 2.12 are $\mu = 1.28\,\mathrm{m/s}$ and $\sigma = 0.2\,\mathrm{m/s}$.

A second aspect of this investigation is the dependence of the walking speed on the group size. Several persons were identified as a group if the distance between at least two of them was not larger than about 1 m, they walked at the same speed, and in the same 'formation', i.e., they actually formed a social group.

Table 2.4 shows the decrease of the walking speed with increasing group size. It is interesting to note that groups larger than 6 persons were not observed. Of course the

Table 2.4. Walking speed vs. group size for the pedestrian bridge. The speed is obtained by dividing the distance of 7 m by the travel time, i.e., $\langle v_x \rangle$, if the 'direction' of the bridge is denoted x.

Group size	Number of groups	Mean Velocity
1	95	1.38
2	149	1.28
3	59	1.24
4	17	1.24
5	10	1.22
6	2	1.10
	700	1.30

statistics for the larger groups are less reliable since they rarely occurred.

Nevertheless, this information could be useful when integrating the influence of group size into the model. This could – as a first approximation – be done by reducing the walking speed according to the group size. Of course, this would also require knowledge about the division of the population into groups and the distribution of group sizes.

Chapter 3

A Two-dimensional Cellular Automaton Model for Crowd Motion

This section introduces a specific microscopic model for pedestrian and crowd motion. This is embedded in the context of microscopic models, i.e., its properties and features are investigated and compared to those of other similar models that have been described in the previous section.

Contents

3.1 Description of the Model

3.1.1 Assumptions the Model is Based on

Before describing the model, the assumptions made about the movement and behavior of crowds are stated and explained. This is important for understanding the scope and

limitations of the model: it is intented to cover the movement of crowds of humans within complex geometries based on signage but excluding special behavioral characteristics like the formation of groups or the decision whether or not to follow the exit signs. Furthermore, it is intented to simulate evacuation processes. In this context, route-choice is not a topic: the routes are assumed to be pre-determined in the sense that all persons follow the given routes, i.e., the direct way to the exit.[1] Of course, fire and other hazards are important in evacuations. However, they are not included in the model due to its focus on the movement. If fire would be included, then the model would become by far more complex, since the effects of toxic gases on the movement ability would also have to be taken into account.[2]

In summary, the basic assumptions are the following:

1. The dynamics can be represented by a cellular automaton, e.g., a spatially and temporally discrete model. This is based on the assumption that there is a finite reaction time and that in crowded areas the space is used efficiently to avoid blockage.[3]

2. Orientation is based on exit signs. Deviations from the shortest route to the exit (resp. destination) are unusual and can be covered by fluctuations of the direction. Route-choice is pre-determined.

3. Irrational behavior is rare. Therefore, deviations from an efficient movement can be taken into account by fluctuations of the walking speed.

4. Persons are not strongly competitive, i.e., do not hurt each other. However, everyone tries to optimize his walking time.

5. Individual differences can be represented by parameters determining the movement behavior, mainly walking speed and orientation capability.

6. These differences and therefore the parameters can be represented by statistical distributions.

These assumptions are justified by the fact that the cognitive processes underlying decision making are far from being understood [Gigerenzer et al., 1999]. So called "simple heuristics" are often superior to modeling the situation in detail. Therefore it is at this stage of development sufficient to take cognitive abilities for granted and not to model them. Instead, the results of those processes are directly incorporated in the simulation, e.g., the perception and processing of an exit sign (cf. fig. 3.2) is transformed into an information about the best walking direction incorporated in the cell.

3.1.2 Movement Algorithm

For the reasons stated above (the assumptions about crowd movement), cellular automata, which are based on discrete space and time, are sufficient as a model for this theory of crowd movement. The formal definition given below is not necessary for the

[1] The direct way must not necessarily be the shortest one in terms of the given exit directions.

[2] The influence of combustion products on humans is rather complex and requires to calculate effective doses for various gases like NO_x, CO, etc. The corresponding *Fractional Effective Dose (FED)*–model is described in [Purser, 1995].

[3] This is implicitly taken into account in CA, since, e.g., for a corridor, the area is separated into 'lanes' (cf. fig. 3.1).

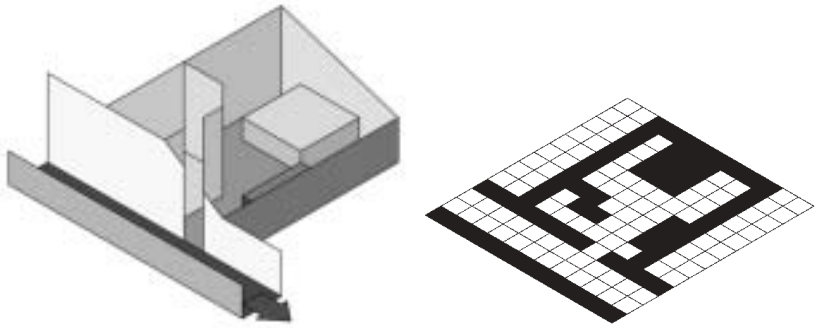

Fig. 3.1. Transformation of a room into a grid of cells. Walls and other fixed obstacles are black, the white cells can be occupied by a pedestrian.

definition of the model. This can also be done in less formal terms. Nevertheless, it is useful for assessing the model and provides a stringent notation. Cellular automata in general provide a framework for discrete models with locally homogeneous interactions. They are characterized by the fundamental properties [Weimar, 1998] shown in table 3.1: $(\mathcal{L}, S, \mathcal{N}, f)$, as defined there, is then called a cellular automaton. A configuration $C_t : \mathcal{L} \to S$ is a function that associates a state with each cell of the lattice. The update function f changes a configuration C_t into a new configuration C_{t+1}:

$$C_{t+1}(r) = f(\{C_t(i) \mid i \in \mathcal{N}(r)\}) \tag{3.1}$$

where $\mathcal{N}(r)$ is the set of neighbors of cell r, $\mathcal{N}(r) = \{i \in \mathcal{L} \mid r - i \in \mathcal{N}\}$. This definition assumes that f is deterministic, however, which is not the case here (cf. fig. 3.3). The notation is illustrated by the following example: the maximal velocity is $v_{\max}$, the rectangular lattice is $x_{\max} \times y_{\max}$ cells large, the cells are ordered consecutively from top left to bottom right, and diagonal motion is possible. The neighborhood $\mathcal{N}$ is then $\{r - v_{\max} \cdot (1 + x_{\max}), r - v_{\max} \cdot (1 + x_{\max}) + 1, \ldots, r + v_{\max} \cdot (1 + x_{\max})\}$, the square around r of size $(2v_{\max} + 1)^2$. Equation 3.1 contains the local influence of the neighborhood $\mathcal{N}(r)$ on the time evolution of the state of cell r, i.e., there are no direct long range interactions. Furthermore, the rules are homogeneous, since the domain of f is $\mathcal{N}(r)$. Narendra and Thathachar [1989] additionally define an input vector $\vec{\alpha}$ and an output vector $\vec{\beta}$; then f takes $\vec{\alpha}$ as an additional argument: $f : \vec{S} \times \vec{\alpha} \to \vec{S}$ and $\vec{\beta}$ is obtained via the output function g, $\vec{\beta}(t) = g(\vec{S}(t))$. $\vec{\alpha}$ could then contain the directional information, i.e., the 'exit signs'. However, in our case it is sufficient to put this into S. Similarly, one can do without $\vec{\beta}$. S therefore consists of the geometrical information (including signage) and the index ('name') and the parameters of a pedestrian:

$$S = (o, w, n, P(n), V) \tag{3.2}$$

o and w are the occupation numbers of a cell, resp. , determine whether it is a wall or other obstacle (like furniture) or not. They can either be zero or one, i.e. a cell can be occupied by at most one pedestrian. n is the index of the pedestrian occupying the cell (if it is empty, then, e.g., $n = -1$), $P(n)$ the set of parameters describing pedestrian n, and finally V the direction, which can be interpreted as sort of a 'gradient'. For the description of the model it is sufficient that the direction towards the exit, i.e., the neighboring cell that is closest to the exit, or more generally, the movement direction, is

Table 3.1. Definition of a cellular automaton. The assumption of a regular lattice and a uniform neighborhood is in accordance with geometries like those in figs. 3.1 and 3.2, since the set of states S also contains information about whether a cell is accessible or not (i.e., a wall cell, w in table 3.2).

Definition	**Description**
$\mathcal{L}$	consists of a regular discrete lattice of cells
$t \to t+1$	evolution takes place in discrete time steps
S	set of 'finite' states
$f : S^n \to S$	each cell evolves according to the same rule (transition function) which depends only on the state of the cell, and a finite number of neighboring cells
$\mathcal{N} : \forall\, c \in \mathcal{N}, \forall\, r \in \mathcal{L} :\ r + c \in \mathcal{L}$	the neighborhood relation is local and uniform

Table 3.2. Assumptions for the model and the empirical correlate. The symbols are explained in the text. The parameters can vary and the values given are typical ones.

empirical	**model**
orientation at exit signs	$V(r) \sim d(r, r_{\text{exit}})$
$\rho_{\max} = 6.25\text{P/m}^2$	$a = 0.4\,\text{m}$
$v_{\max}^{\text{emp}} \approx 2\,\text{m/s} \wedge \Delta t \approx 1\,\text{s}$	$v_{\max}^{\text{mod}} = 5$
stopping due to orientation	$p_{\text{dec}} = 0 \ldots 0.1$
deviations from the optimal direction	$p_{\text{sway}} = 0 \ldots 0.03$
walls are 'black' cells	$w = 1$
hard core exclusion	$o \in \{0, 1\}$

given by V[4]. For more complex geometries, V can be assigned to $\mathcal{L}$ based on the signage. The topic of orientation via a vector or scalar field[5] will be discussed further in section 3.7.3.

Of course, it would be rather tedious to define the transition function explicitly. A more efficient approach is to state the effective rules, i.e., provide a set of rules that changes the states of the cells and could in principle be formulated in terms of the previous definitions. It would be possible to specify f explicitly, as can be seen from the fact that in eq. 3.1 all information about the state of the complete neighborhood is passed to f. From that, the desired destination cell of all the pedestrians in the neighborhood $\mathcal{N}$ can be determined, checked, whether one wants to access the cell to be updated, and if yes, move him to this cell, i.e., replace the state of the cell (that means o, n, $P(n)$) by the state of the cell the pedestrian originates from. Of course, all this has only to be done, if o and w are zero, otherwise, nothing has to be done. Since V contains only the route choice information it is kept fixed all the time.

There are three basic quantities in this CA model: the cell length a (in m/cell), the

[4]For a hallway with movement in positive x-direction: $V(r) = +1\,\forall\, r \in \mathcal{L}$.

[5]A mapping $V : \mathcal{L} \to \mathbb{N}$ will be called a scalar and $V : \mathcal{L} \to \mathbb{N}^2$ a vector field in this context.

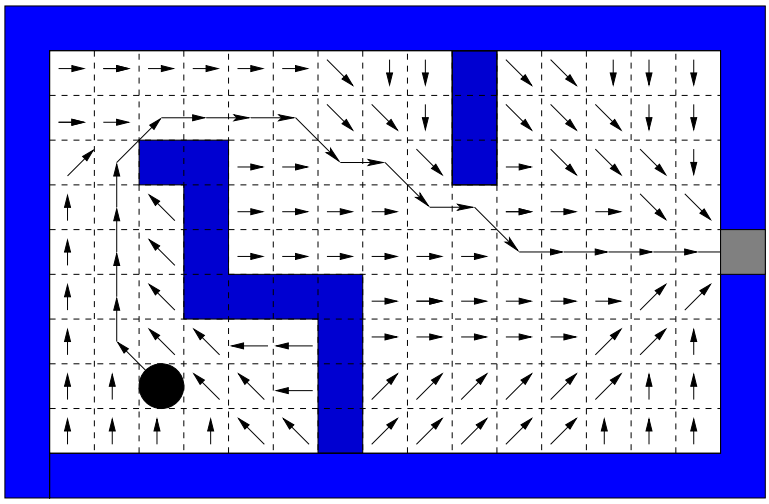

Fig. 3.2. A sample case for illustration of orientation and way-finding. The starting position is marked by the circle, the final position by the filled square. The arrows represent $V(r)$.

maximum velocity $v_{\max}$ (in cells per time-step) and Δt (in seconds per time-step). The size of the quadratic cells is then a^2 (in m^2/cell).[6] a can be directly calibrated by using the highest possible density observed $\rho_{\max}^{\mathrm{emp}}$: The cell size is chosen such that $\frac{1}{a^2} \approx \rho_{\max}^{\mathrm{emp}}$, which is around 6 persons/m^2 [DiNenno, 1995, Transportation Research Board, 1994, Weidmann, 1992] and therefore the cell length is set to $a = 0.4\,\mathrm{m}$. The time scale (reaction time) and the maximum velocity are then connected via:

$$v_{\max}^{\mathrm{emp}} = \frac{a \cdot v_{\max}}{\Delta t}. \tag{3.3}$$

One of those can be freely chosen. However, if Δt is interpreted as the reaction time $t_{\mathrm{react}}^{\mathrm{emp}}$, $v_{\max}$ is determined by measuring this time. In analogy to the Nagel-Schreckenberg model and to results from psychological tests, the reaction time (in the sense of the time it takes to make a decision) is set to 1 s [Roth, 2002]. The maximum velocity is usually set to 2 to 5 cells/Δt (varying among the individuals of a population) for the simulations presented in chapters 4 and 5. This corresponds to a free walking speed of 0.8 to 2 m/s.

The choice $v_{\max} = 1$ is not made for two reasons: (1) For the Nagel-Schreckenberg model $v_{\max} = 1$ leads to a symmetric (around $\rho = 1/2$) fundamental diagram.[7] This result can be (with slight deviations due to the broken particle hole symmetry) be generalized to 2D, as will be shown below in section 3.2. The empirical fundamental diagram (for road traffic, as well as for crowd motion) shows a different shape with a maximum at $\rho < 1/2\,\rho_{\max}$; (2) It does not allow to assign different maximum walking speeds $v_{\max}^i$, which is unfortunate concerning the representation of a realistic population. In other words, if one is interested in representing realistic population characteristics, a distribution of individual maximum walking speeds is appropriate. This second aspect could also be reached, however, by assigning different individual dawdling probabilities p_{dec}^i.

[6] Two of these quantities, namely a and Δt, do not occur explicitly in the model definition. They are necessary for connecting simulation results to empirical data, e.g., via eq. 3.3.

[7] The graphical representation of the function $j(\rho)$ is called fundamental diagram.

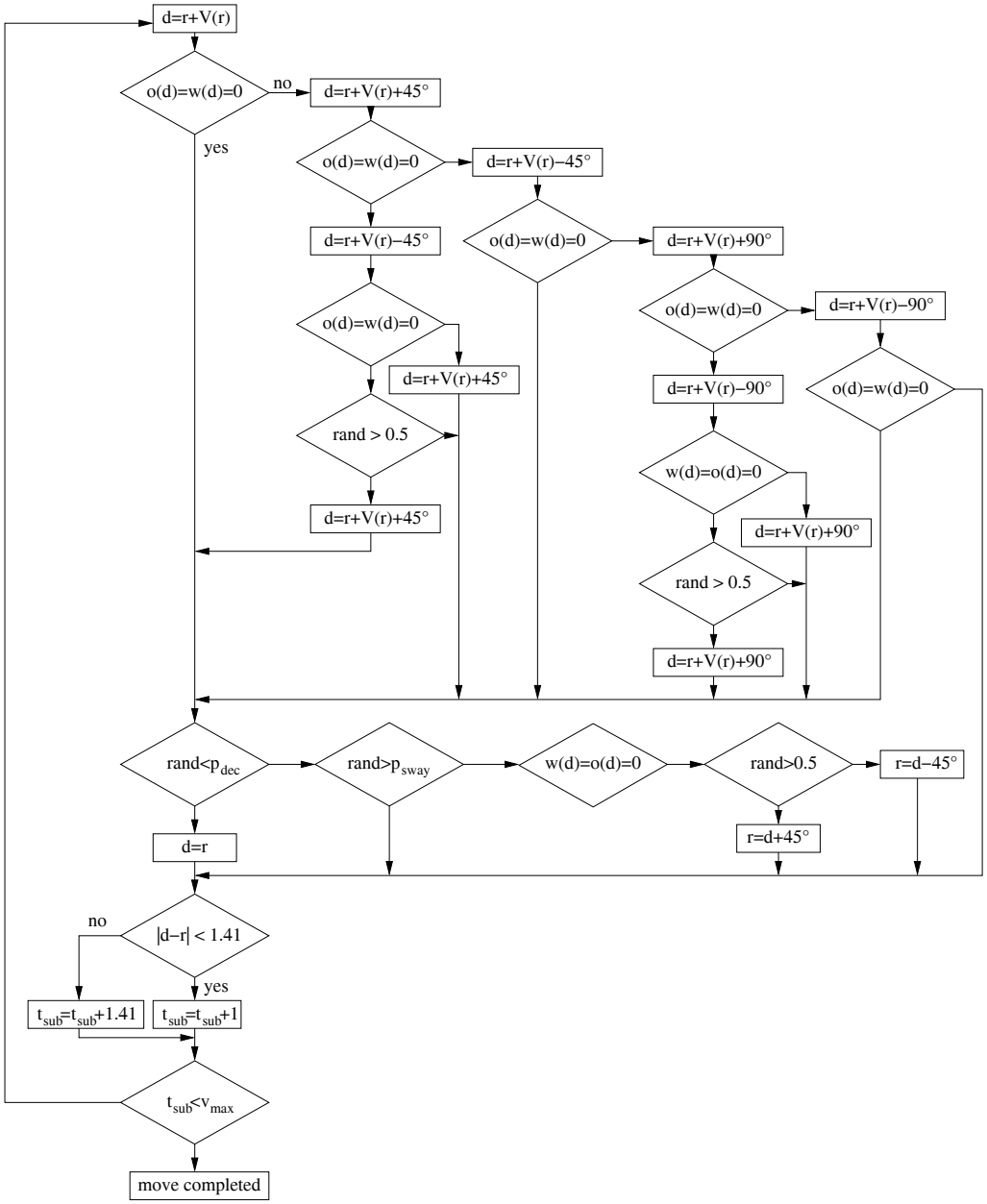

Fig. 3.3. The movement algorithm for a single pedestrian. It consists of a part concerning the determination of the direction and a part including stopping (p_{dec}) and swaying (p_{sway}). The random numbers *rand* are uniformly distributed in the interval [0,1), 45° and 90° denote deviations from the direction given by $V(r)$ (cf. figs. 3.4 and 3.2), i.e., the deviations to the left/right are chosen with probability 0.5, if the direct destination is occupied, resp. in the case of swaying. The sequence of the steps is indicated by the arrows. Rhombs indicate tests and the bottom branch is for *yes* and the right/left one for *no*. The check $|d-r| < \sqrt{2}$ gives true, if the movement is across an edge ($|d-r| = 1$) or no movement ($|d-r| = 0$) and no, if it is across a corner ($|d-r| = \sqrt{2}$). t_{sub} counts the number of moves within one time-step ($\Delta t = 1\,\mathrm{s}$).

Furthermore, the smaller $v_{\max}$ is, the smaller is the reaction time, e.g., for $a = 0.4\,\mathrm{m/cell}$ and $v_{\max} = 1$ the time scale (identified with the reaction time) would be $\approx 0.3\,\mathrm{s}$ under the assumption that $v_{\max}^{\mathrm{empir}} \approx 1.33\,\mathrm{m/s}$. If this reaction time is identified with the tactical level (decision time, cf. table 2.2) then it might be too short. However, 'sub-conscious' processes, which are on the operational level, might take less than 1 s. For $v_{\max} = 1$, a distinction between operational and tactical level is not necessary, since a pedestrian performs only one step per Δt anyway. For $v_{\max} > 1$, however, a pedestrian performs several steps (operations) during Δt. The latter is then the tactical level, since decisions are only made once (within the tactical step Δt).

In addition to the three basic parameters $v_{\max}$, a, and Δt, there are quantities concerning the orientation, which is based on a direction assigned to each cell. Fluctuations in the orientation are governed by two parameters p_{dec} and p_{sway}, which give the probabilities for stopping and for deviating from the given direction. The latter takes into account two influences in case of simulations for ship evacuation, which is one of the major intented applications (cf. chapter 5): (1) the motion of the ship, (2) intoxication of passengers. The calibration of the two parameters p_{dec} and p_{sway} is of course difficult. Therefore, they are usually set to small values, i.e., p_{dec} between 0 and 0.1 and p_{sway} between 0 and 0.03 (uniformly distributed) for the simulations in chapters 4 and 5. Empirical data about the movement on-board ships and the dependence of the walking speed on the dynamics of the ship are shown in chapter 5. The characteristic quantities of the CA model are summarized in table 3.2.

The move of one pedestrian is carried out in the following sequence (r denotes the current cell):

1. Trying to access the desired cell d ($d = r + V(r)$).
2. If this is not possible, try to go to one of the two neighbors of d (cf. fig. 3.4, 45°–direction, with respect to the desired direction).
3. If this is also not possible, try to go to one of the two '90°'–neighbors.
4. If none of those five cells (d and the cells in 45°– and 90°–direction) are accessible, then stop.
5. Stop with probability p_{dec}.
6. Sway (45° in relation to the direction chosen in steps 1 to 3) with probability $p_{\mathrm{sway}} \cdot (1 - o_d - w_d)$, where o_d is the occupation and w_d is the wall number of the new destination cell.
7. Move.

The fact that diagonal movement (across the corner instead of across the edge) corresponds to a longer distance is taken into account by a factor $\sqrt{2} \approx 1.41$ (cf. the movement algorithm in fig. 3.3). For example, for $v_{\max} = 5$, a pedestrian is allowed to do either 5 horizontal or vertical steps or 4 diagonal steps.[8]

The movement algorithm for a single pedestrian is illustrated in fig. 3.3. The cells a pedestrian passes during one time step are blocked, i.e., considered occupied by this pedestrian and $o(r) = 1$ for r belonging to his path. In the case of free flow, the length of the path is $v_{\max} + 1$.[9] At the beginning of the next move (cf. fig. 3.8), $o(r)$ for the cells

[8] Horizontal and vertical means across the edge and diagonal across the corner of a cell.

[9] In free flow, a pedestrian is not forced to stop before having covered the distance $a \cdot v_{\max}$.

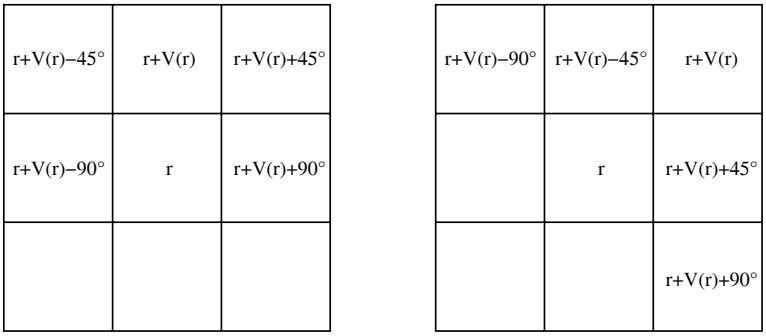

Fig. 3.4. This figure illustrates the notation used for the directions in the movement algorithm (fig. 3.3). There are eight accessible neighbor cells, the top (top right) cell is identified with the desired destination cell, and the cells that are denoted $r + V(r) \pm 45°$ and $r + V(r) \pm 90°$ in fig. 3.3 are as shown here.

r of the path (except of the current cell, i.e., position) are set to 0. Since a pedestrian blocks his path, another pedestrian can not cross directly behind him. The influence of distance keeping between pedestrians is discussed further in section 3.2 below. A time-step Δt in which all N pedestrians have moved is therefore identified with 1s in reality (cf. table 3.2).

The order in which the pedestrians move is shuffled at the beginning of each time-step. This type of update is called shuffled (sequential) update here.[10] Therefore, the problem that two or more pedestrians want to access the same cell (conflict) is avoided. However, if occupied cells are potential destination cells then conflicts might still arise. Since the number of conflict parties increases with $v_{\max}$ (basically proportional to $v_{\max}^2$) the conflict resolution would complicate and slow down the simulation tremendously.[11]

3.1.3 Fundamental Diagram of the Model

Comparison of models and simulation results can be done in two ways: qualitatively and quantitatively. The first is descriptive and based on observed phenomena, the latter on quantitative empirical data or measurements. The specific flow is one of the best investigated empirical quantities [Weidmann, 1992, and references therein]. Opposite to macroscopic models, which are based on empirically determined flow-density-relations, microscopic models allow to determine the flow-density relation from more fundamental rules or principles by carrying out a simulation. In the case of 1D CA for road traffic, the flow per lane is sufficient. However, in the case of pedestrian motion the specific flow is the appropriate measure ($j(\rho)/w$, where w is the width). For a hallway in horizontal direction and uni-directional flow $\langle v_x \rangle$ is measured. Alternatively, one could also measure those persons that walk solely in x–direction. The global specific flow is then obtained via

$$j_{\text{spec},x} = \rho \cdot \langle v_x \rangle \ . \tag{3.4}$$

[10] The mathematical definition of a cellular automaton requires a parallel update. Therefore, the model does not fulfill this definition in the strict sense.

[11] However, for a uniform conflict solution, i.e., all conflict parties have the same chance to win, there is a way of avoiding this technical problem which works also for $v_{\max} > 1$ as will be shown in section 3.6 below.

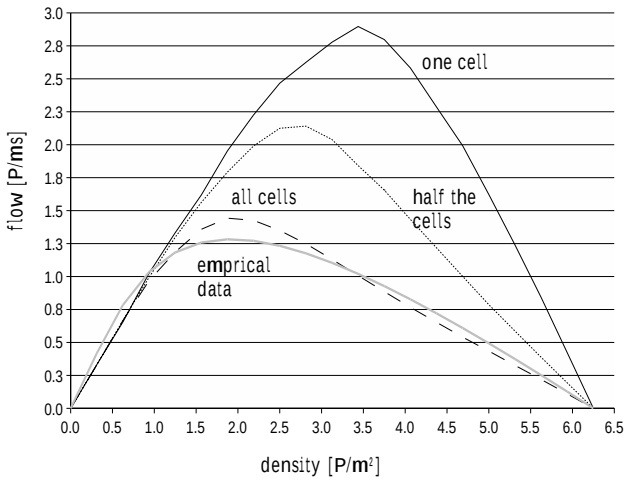

Fig. 3.5. $j(\rho)/w$ (specific flow) for different number of cells blocked by a moving pedestrian. The geometry is a hallway of length 200 cells and width 20 cells.

Since there is a relaxation time in the measurement and the flow is averaged over a few thousand time steps, the global flow is a valid measure for comparison with the empirical data, even though in this case, usually a local flow is measured: $j = \frac{\sum_{i=1}^{N} v_x^i}{N} \cdot \rho$.

Simulation results for $j_{\text{spec}}(\rho)$ are shown in fig. 3.5 for a hallway of length (x-direction) 200 cells (80 m) and width 20 cells (8 m) and periodic boundary conditions in the x-direction. The maximum velocity was set to 2 to 4 cells and $p_{\text{dec}} = 0 \ldots 0.3$, both uniformly distributed among the population (p_{sway}=0). Additionally to the version where a pedestrian blocks all cells of his path for a time Δt, $\langle v_x \rangle$ was measured for only one cell (the final position) and half of the cells blocked, i.e., in the last case, moving pedestrians can cross directly in front of each other. The empirical curve is taken from [Weidmann, 1992]. There, the maximum density is $\rho_{\max} = 5.4\,\text{P/m}^2$. This curve was adapted to $\rho_{\max} = 6.25\,\text{P/m}^2$.

The standard parameter settings with $v_{\max} = 2 \ldots 4$ and $o(r) = 1$ for the complete path provide results that agree well with the empirical curve. It has to be kept in mind that the data was obtained for walkways and therefore in egress situations higher walking speeds might be appropriate. Evacuation exercises, which will be presented in chapter 4 can be used to obtain information on that. The fundamental diagram can be used to calibrate the free walking speed via

$$\lim_{\rho \to 0} \left(\frac{\partial}{\partial \rho} \frac{j(\rho)}{w} \right) = v_{\text{free}} \,. \tag{3.5}$$

The deviation for small densities between the empirical data and the simulation in fig. 3.5 is therefore due to the different free walking speeds v_{free} (1.34 m/s vs. 1.2 m/s).[12]

Figure 3.6 shows a snapshot of that hallway at a density of $4.4\,\text{P/m}^2 \approx 0.7\,\rho_{\max}$, where spatial fluctuations in the density can be seen.

At this point, the model has been defined and a first comparison to empirical data been made. It will be applied to the simulation of realistic egress scenarios (for complete

[12] The empirical data was presented in table 2.3, fig. 2.9, and eqs. 2.23 and 2.24.

Fig. 3.6. Density for a square lattice with periodic boundary conditions and global density $\rho = 4.4\,\mathrm{P/m^2}$. The occupied cells are indicated by dark, the empty by white dots. Jam waves moving opposite to the walking direction, which is from left to right, can be observed.

buildings and ships) in chapters 4 and 5. In the remaining sections of this chapter, the model properties will be further investigated.

3.2 Distance Keeping and Paths for $\mathbf{v_{max} > 1}$

First, the influence of the distance kept by pedestrians is addressed. For $v_{\max} > 1$ there are paths of length $v_{\max} + 1$. The question in the case $v_{\max} > 1$ is: Does a pedestrian block all the cells he is using during one time-step? If a pedestrian blocks all the cells, then the person walking behind him automatically keeps a distance that is proportional to the walking speed of his predecessor. Since there is no empirical data available, this question cannot be decided directly. It can be motivated however, by comparison to the properties of the Nagel-Schreckenberg model (for $p_{\mathrm{dec}} = 0$), where the distance (gap) g_i to the preceeding car is v^i: $g^i \geq v^i$. The density ρ^* for which the highest flow occurs is therefore shifted to the left for increasing $v_{\max}$:

$$\rho^* = \frac{1}{v_{\max} + 1}. \tag{3.6}$$

The maximum flow is then $j_{\max} = \rho^* \cdot v_{\max} = \frac{v_{\max}}{v_{\max}+1}$. Distance keeping in the Nagel-Schreckenberg model is ensured by the parallel update (since there is a unique ordering of the cars) which effectively leads to blocking the cells used during one time-step.

In the 2D model there is no natural ordering of the pedestrians. If $v_{\max} > 1$ is used and the pedestrians are assumed to block their path (cf. fig. 3.7, version "no crossing paths") in analogy to the model for road traffic, then the movement has to be carried out in single steps, i.e., a time-step has to be divided into sub-time-steps (not to be confused with the version "sub–steps" in fig. 3.7). Furthermore, individual maximum walking speeds $v^i_{\max} \neq v^j_{\max}$ lead to individual maximum numbers of movement steps:

$$v^i_{\mathrm{sub}} = \begin{cases} 1 \;\text{ for }\; t = 1, 2, \ldots, v^i_{\max} \\ 0 \;\text{ for }\; t = v^i_{\max} + 1, \ldots, v_{\max} \end{cases} \tag{3.7}$$

where, $v_{\max} = \max_j v^j_{\max}$, i.e., the maximum walking speed of the fastest individual. Another alternative is the introduction of sub time-steps with $v_{\mathrm{sub}} = 1$ ("sub–steps" in fig. 3.7), i.e., movement to a direct neighbor. The difference to a genuine $v_{\max} = 1$–model is threefold:

- the path is determined for the complete number of sub-steps,
- $v^i_{\max} \neq v^j_{\max}$ in general, and
- the same pedestrian carries out $v^i_{\max}$ steps consecutively.

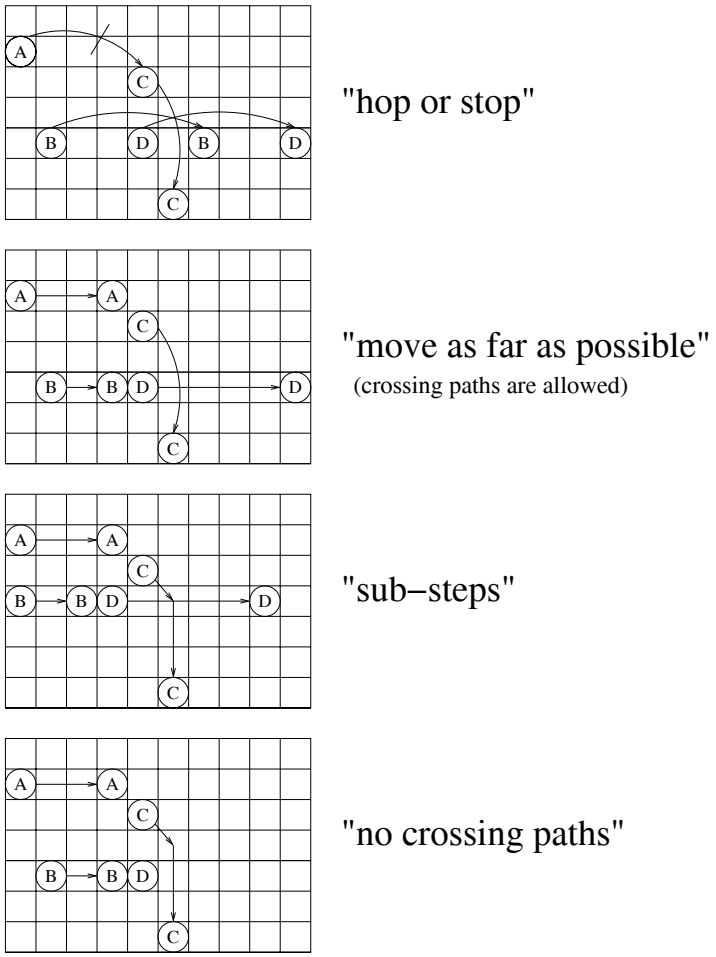

Fig. 3.7. Different ways to define a path (in the sense of blocked cells) for $v_{\max} > 1$. The circles a the origins of the arrows denote the current and the ones at the tip the desired final cells. For "hop or stop" movement is only allowed, if the final destination cell is empty, for all other versions, this is not the case. The second version (from top) allows crossing paths, the last one does not, and the third does, but only if at the same sub-time-step there is no "conflict". This last version can only be used if $v_{\text{sub}} = 1$, as shown in fig. 3.8. For case 4 ("no crossing paths") pedestrian D is not allowed to move, since his path is blocked by pedestrian C which is allowed to move first.

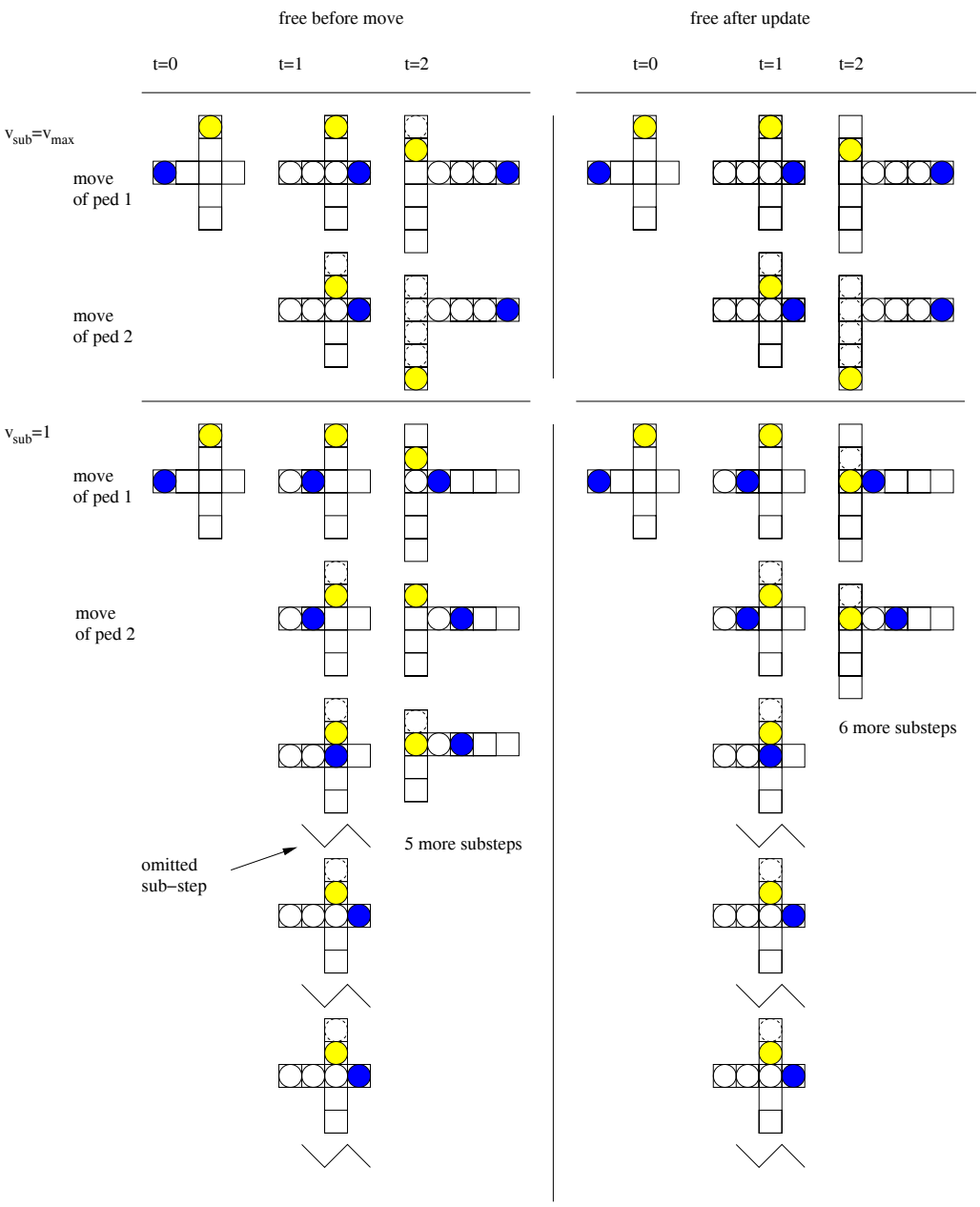

Fig. 3.8. Different possibilities for the definition of paths according to the number of cells a pedestrian is allowed to move in a sub-time-step (v_{sub}) and when $o(r)$ is set to zero. For $v_{\mathrm{sub}} = v_{\max}$, there is only one sub-time-step. The time steps are from left to right and the sub-time steps from top to bottom (two sketches for each sub-time-step). The black pedestrian is allowed to move first (resp. wins the conflict) at $t = 1$, gray at $t = 2$. The pedestrians are assumed to block all cells they pass (solid white circles for black, dashed circles for gray, corresponding to "no crossing paths" in fig. 3.7). The black pedestrian has $v_{\max} = 3$ and the white one $v_{\max} = 4$. The path is freed before the move (left), resp. after the update (right). This leads to an 'effective size' (number of cells blocked) of v^i_{current} for each pedestrian i. The left part of the figure ("free before move") is a shuffled (sequential) update, the right part ("free after update") can be viewed as parallel update.

The possibility that the paths of two pedestrians might intersect is excluded only for "no crossing paths" by setting $o(r_{il}) = 1$ for all r_{il} that belong to the path of a pedestrian. Alternative rules for the blockage of cells, can be used, though. In general, a matrix T can be defined, which is a $N \times (v_{\max} + 1)$ matrix containing the positions and paths (trajectories) of all pedestrians for one time step. $T_{ij} \in \{1, 2, \ldots x_{\max} \cdot y_{\max}\}$, $r_{i1} = T_{i1}$, e.g., the first column of T contains the positions. The entries of T are obtained by carrying out the procedure for determining the velocities repeatedly such that every pedestrian i has a path of length at most $v_{\max}$ stored in T_{ij}, $j = 2 \ldots v_{\max}$. If $v^i < v_{\max}$ then some of the rightmost entries in row i are equal.

$$\mathrm{T} = \begin{pmatrix} T_{10} & \cdots & T_{1v_{\max}} \\ \vdots & \ddots & \vdots \\ T_{N0} & \cdots & T_{Nv_{\max}} \end{pmatrix} \tag{3.8}$$

A cell can be occupied by at most one pedestrian, i.e., $T_{i1} \neq T_{j1} \,\forall\, i \neq j$. There are four major possibilities concerning the restrictions of the paths (cf. fig. 3.7 from top to bottom):

1. "Hop or stop"
   If $T_{iv_{\max}+1} = T_{j1}$ for any $j \neq i$, then $T_{iv_{\max}+1} = T_{i1}$. In this case pedestrians do not move at all, if the final destination cell is occupied (fig. 3.7, top).

2. "Move as far as possible"
   $T_{ir} \neq T_{jv_{\max}+1} \,\forall\, i \neq j, r$.
   This version does allow crossing paths. The final destination (which will eventually become the new position) is then $T_{iv_{\max}} = T_{ir}$ with $r = \max_{T_{is} \neq T_{jv_{\max}}}(s))$. This rule could also be formulated as "move as far as possible".

3. "Sub-steps"
   $T_{ir} \neq T_{jr} \,\forall\, r, i \neq j$.
   In this case two pedestrian are not allowed to access the same cell in the same sub-step. Since in the shuffled update this case is excluded, such this case is only relevant for a parallel update. This version would require the largest computational effort, since the tests have to be carried out for $v_{\max}$ sub-time-steps.

4. "No crossing paths"
   $T_{ir} \neq T_{js} \,\forall\, i \neq j, r, s$.
   This rule allows movement only, if the complete path is unused, i.e., there are no intersecting paths. This is the choice made for our model, motivated by the comparison with the empirical fundamental diagram.

This comparison is useful for assessing the choice made concerning the blockage of the paths of the pedestrians. As stated before, in the model used here, the complete path of a pedestrian is blocked. Whether or not this is the best choice to make, cannot yet be decided based on empirical investigations. The systematic approach presented allows to classify the different versions concerning the blockage of a pedestrian's path and use this comparison as a motivation for the specific choice made.

The CA model for crowd motion is based on a further assumption concerning the cell size. Even though the model parameters can be calibrated to reach agreement with empirical data, the question remains, how the dynamics will be influenced by a different discretization, i.e., smaller cells. This question will be addressed in the following section.

3.3 Cell Size and Discretization

The major assumption made in modeling pedestrian motion with a cellular automaton is the discrete space and especially the resulting limited freedom of motion. A point that is often mentioned in discussions is that it is not possible to realistically model small changes in the width of, e.g., a corridor or door. In the case of road traffic simulations, a finer discretization is motivated by attempting a smoother acceleration.[13] This is not a topic for pedestrian motion, since the maximum velocity can basically be reached immediately. The question is therefore mainly, how the flow is influenced by a finer discretization, especially, when the deviations stemming from mapping a real layout onto the grid of cells are decreased.

One possible choice is $a < A$, with A denoting the size of a pedestrian.[14] This is illustrated in figs. 3.9 and 3.10. In the second case, walls that are 10 cm wide can be represented accurately. For $a = 40$ cm those walls can only be represented by 'black' cells and would therefore be 40 cm wide.[15]

The following relation holds for the density ρ^* that provides the highest flow (only in the 1D case and for parallel update):

$$\rho^* = 1 - \frac{1}{1 + A/a}, \tag{3.9}$$

with A^2 denoting the size of a (quadratic) pedestrian. The velocity is still measured in units of a per time step, i.e., $v_{\max} = 1$ means that the maximum distance covered within Δt is a ($a \to a/2, \Delta t \to \Delta t/2$). The density ρ is defined by the ratio of the number of occupied (one ped occupies now $(A/a)^2$ cells) to the overall number of cells. The last equation can be seen from the fact, that the gap necessary for ensuring velocity $a/A \cdot a/\Delta t$ is a (the cell size), regardless of the density, which is given by eq. 3.9.

Simulations with a finer grid of size $a = 20$ cm have been carried out based on the model described in [Kirchner, 2002] in cooperation with these researchers [Kirchner et al., 2002]. The layout is a corridor with walking direction from left to right (increasing x). Transition is possible to the four next neighbors ($|\mathcal{N}| = 4$, $v_{\max} = 1$) and $p_{ij} = 1/N$ for a step up and down and $e^{\pm\beta}/N$ for a step to the right/left. β was set to 10 and N is the usual normalization constant. The parameter β is governing the transition probabilities. It can be interpreted as an information, since for $\beta = 0$ the pedestrian will perform a random walk and for $\beta \to \infty$ the movement is deterministic.

An additional application of a smaller cell size would be the use of rectangular instead of quadratic shapes for the pedestrians, which would be closer to the elliptic form of a human body. However, these aspects have to be postponed to further investigations.

The results for a discretization with $a = 20$ cm are shown in fig. 3.11. The curve for the corridor with width 120 cm shows that the peak of the fundamental diagram is shifted to the right, i.e., to a higher density ρ^* as expected (cf. eq. 3.9). On the other hand, the maximum flow $j_{\max} = j(\rho^*)$ is slightly decreased. This is due to the fact that two pedestrians can now block the hallway of width 3A, which is not possible for the case $A = a$, i.e., if the size of the pedestrians equals the size of the cells. The second aspect

[13] For the Nagel-Schreckenberg model with $\Delta t = 1$ s and $a = 7.5$ m the acceleration is $7.5\,\mathrm{m/s^2}$.

[14] The shape of the pedestrian is quadratic, too. Therefore his size is A^2.

[15] By using individual coordination numbers for each cell (i.e., different accessible neighborhoods), this problem could be avoided, since then walls would not have to be black cells but be represented by the missing 'links' to a neighboring cell. This would lead to a fairly different type of model, however.

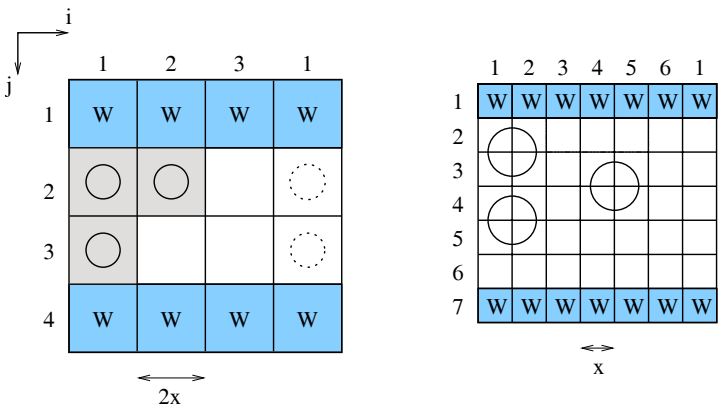

Fig. 3.9. This example shows the effect of a finer mesh with $A = 2\,a$: One pedestrian still occupies the same area. However, he then blocks a square of four cells. If $x = 20\,\text{cm}$, $b = 100\,\text{cm}$ (in reality), then $b' = 2\,a$ (in the model) for $a = 2\,x = 40\,\text{cm}$ and $b' = 5\,a$ for $a = x = 20\,\text{cm}$.

that can be seen from that figure is the influence of the more accurate representation of the layout. A width of 140 cm can be represented by either three or four cells, if $a = A = 40\,\text{cm}$. For $a = A/2 = 20\,\text{cm}$, this width can be represented accurately by $w = 7\,a$. The maximum specific flow in this case (width $7 \times 20\,\text{cm}$) is higher than 0.5, which would be the maximum flow for $a = A$. Therefore, a more accurate representation of the geometry leads in this case to a higher flow. The previous aspect ($w = 3$ or $w' = 6\,\text{cells}$) led to a smaller flow for the latter. Therefore, a finer discretization might produce a smaller as well as a higher specific flow depending on the details of the layout.

The question whether a finer discretization is necessary cannot be decided at this stage. Its influence will have to be investigated further. This could be done in the context of a comparison of discrete and continuous models, i.e., by taking the limit $a \to 0$.

3.4 Walking Direction and Orientation Based on a Potential

Based on assumption 2 in section 3.1.1, route-choice is reduced to orientation and the main problem remaining is to determine the shortest path to the exit, resp. the corresponding directions $V(r)$ for each cell r. $V(r)$ can take on eight possible values. For an empty room with a single exit, they could be determined via

$$\vec{V}(\vec{r}) = \frac{(\vec{r} - \vec{r}_{\text{exit}})}{|\vec{r} - \vec{r}_{\text{exit}}|}. \tag{3.10}$$

If $\vec{V}(\vec{r})$ is rounded to the closest of the eight possible discrete directions $\phi' = j \cdot \frac{\pi}{8}$, $j = 0, \ldots, 7$,

$$\phi = \arctan \frac{r_x}{r_y} + \Theta(-V_x) \cdot \pi, \tag{3.11}$$

$$\phi' = \phi - [(\phi + \pi/8) \mod \pi/4] + \pi/8, \tag{3.12}$$

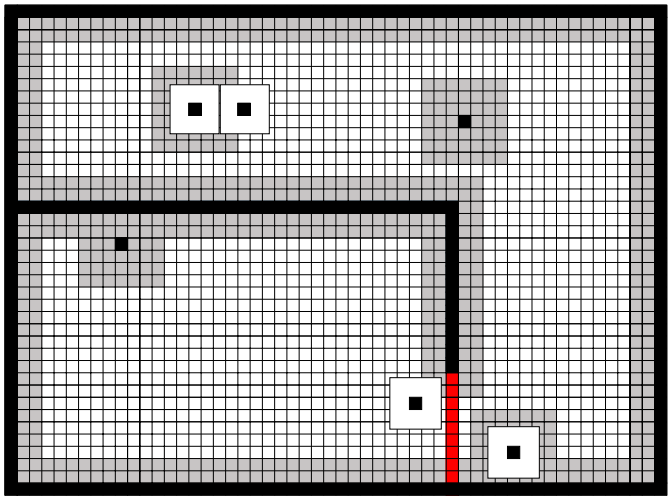

Fig. 3.10. This example shows a discretization with 10 cm cell length. It is constructed in such a way that pedestrians can still be assigned to only one cell, if they at the same time 'occupy' a square of cells surrounding this cell. The grey cells could then be represented by the occupation numbers o, resp. by w (for the walls and obstacles).

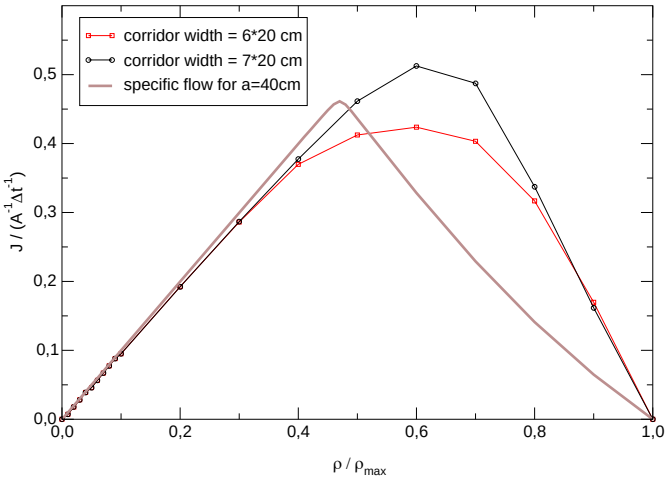

Fig. 3.11. Fundamental diagrams: $\beta = 10$ (cf. eq. 3.17), $v_{\max} = 1$ (parallel update), $a = 20$ cm, the length of the corridor is $186 \cdot 20$cm. The density is measured as percentage of $\rho_{\max}$ and the flow j in units of $(A \cdot \Delta t)^{-1}$, i.e. it is the specific flow (cf. eq. 3.5). The grey curve is for a corridor of width $3 \cdot 40$ cm.

then $V(r)$ gives the local direction in cell r.

For more complex geometries, like the one shown in fig. 3.2, this simple approach does not work. The room has then to be comparted and $V(r)$ determined for each compartment separately. This approach allows to simulate also complex structures like complete buildings and ships. In this way, it is possible to model exit signs that do not necessarily represent the shortest distance to the exit or that do lead to several exits. One major shortcoming of this approach, however, is that it is hard to implement into an algorithm that is able to cover complex geometries due to the problem of compartmentation.

An alternative approach, that does not suffer from this problem, is to use an appropriate metric M that assigns the distance to the exit to each cell or grid point

$$M(r) = d(r, r_{\text{exit}}) \tag{3.13}$$

and derive V via the 'gradient':

$$V(r) \sim \operatorname{grad} M(r) \tag{3.14}$$

The direction is given by the neighbour cell with the highest potential[16] value (d^*) minus the index of the current cell (r):

$$V(r) = (d^* - r) \cdot \frac{\pi}{8}, \tag{3.15}$$

$$d^* = \{j \in \mathcal{N} | M(j) = \max\}. \tag{3.16}$$

This is not well-defined for all cells. The ambiguities that occur could be resolved by using $P(d = d')$ instead of d in the movement algorithm:

$$P(d = d') = N \cdot \exp\Big(-\beta\big(M(d') - M(r)\big)\Big), \tag{3.17}$$

with $N = \sum_{i \in \mathcal{N}(r)} (\exp(\beta(M(i) - M(r)))$. For $\beta \to \infty$, the cell with the lowest M is chosen, if two or more cells have the same value, then one is chosen with equal probability.

M can be interpreted as a discrete potential ($\operatorname{curl} M = 0$), since

$$\oint_P V \, ds = \sum_{i=1}^{n} (M(P_i) - M(P_{i-1})) \cdot \frac{\pi}{8} = 0, \tag{3.18}$$

with P a closed path in $\mathcal{L}$: $P = \{P_1, P_2, \ldots, P_n\}$, $P_n = P_1$, and $P_{i+1} \in \mathcal{N}(P_i)$.

The procedure of determining M can be implemented as sort of wave propagation with absorption at the walls (cf. figs. 3.12) which is the most important advantage of this approach. However, if the potential spreads only across the edges ($k = 4$, von Neumann neighborhood), then the resulting potential is rather chiseled (fig. 3.12, top). This metric, which measures the steps across the edges is called Manhattan metric. The movement towards the exit would then for some areas be first towards the wall and then along this wall towards the exit (if the exit is in the center of a coordinate system and the room in the area $y > 0$, this would be the case for the areas $x < y$ and $-x > y$).

For an empty room with a single exit cell, one could use the metric

$$d(r, r_{\text{exit}}) = \sqrt{(r^x - r^x_{\text{exit}})^2 + (r^y - r^y_{\text{exit}})^2}, \tag{3.19}$$

[16] Potential is used as a synonym for the metric M.

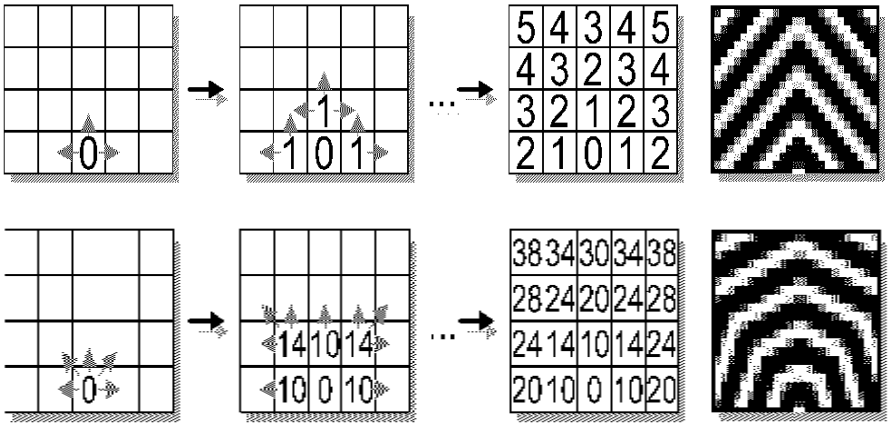

Fig. 3.12. Potential spread with von Neumann neighborhood ($k = 4$, top) and Moore neighborhood ($k = 8$, bottom). The source of the potential is the exit located at the center of the bottom wall. Shown are the evolution of the potential (comparable to wave propagation), the potential values, which are given by the distance to the exit based on the Manhattan metric ($k = 4$) or its extension $k = 8$, and the resulting equipotential lines (from left to right).

Such a metric, however, can only be used for a room without obstacles (cf. fig. 3.2) which would make – as for the case of assigning a direction to each cell as described above – compartmentation necessary.

The use of the Manhattan metric leads to artefacts in the motion that are a result of the definition of the metric and the discretization of space. This can be mitigated by allowing motion in diagonal direction ($k = 8$, Moore neighborhood). Since the potential M is a measure for the distance, a factor $\sqrt{2} \approx 1.4$ is used for diagonal spread (cf. fig. 3.12, bottom). In order to use integer numbers 10 and 14 were used instead of 1 and 1.4 for adding to the potential values. The rounding to integers can of course also be done after the orientation potential has been calculated – as is shown in fig. 3.13 for a further refined version taking into account an averaging process.

The example shown in fig. 3.14 is based on this approach that smooths out the pikes that caused the previous problems and thus comes closer to the 'natural' metric of eq. 3.19. The resulting path shown in fig. 3.13 can only be obtained via smoothing the potential, the path in the horizontal part of the hallway would otherwise advance along the bottom wall.

Based on M, the direction of movement, resp. the destination cell d in the algorithm (fig. 3.3) could be determined more directly via:

$$P(d = j) \sim \exp(-\beta(M_j - M_r)) \cdot (1 - w_j), \tag{3.20}$$

where $P(d = j)$ is the probability for choosing j as the destination cell d and β is a coupling constant ($\beta \in [0, \infty)$) to M. In this case, 'backward' movement would be possible, unless $\beta \to \infty$.[17]

[17]Even in this case backward movement is possible if all the cells closer to the exit than the current cell are occupied and $(1 - n_j) = (1 - o_j)(1 - w_j) = 1 - o_j - w_j$ is used instead of w_j in eq. 3.20.

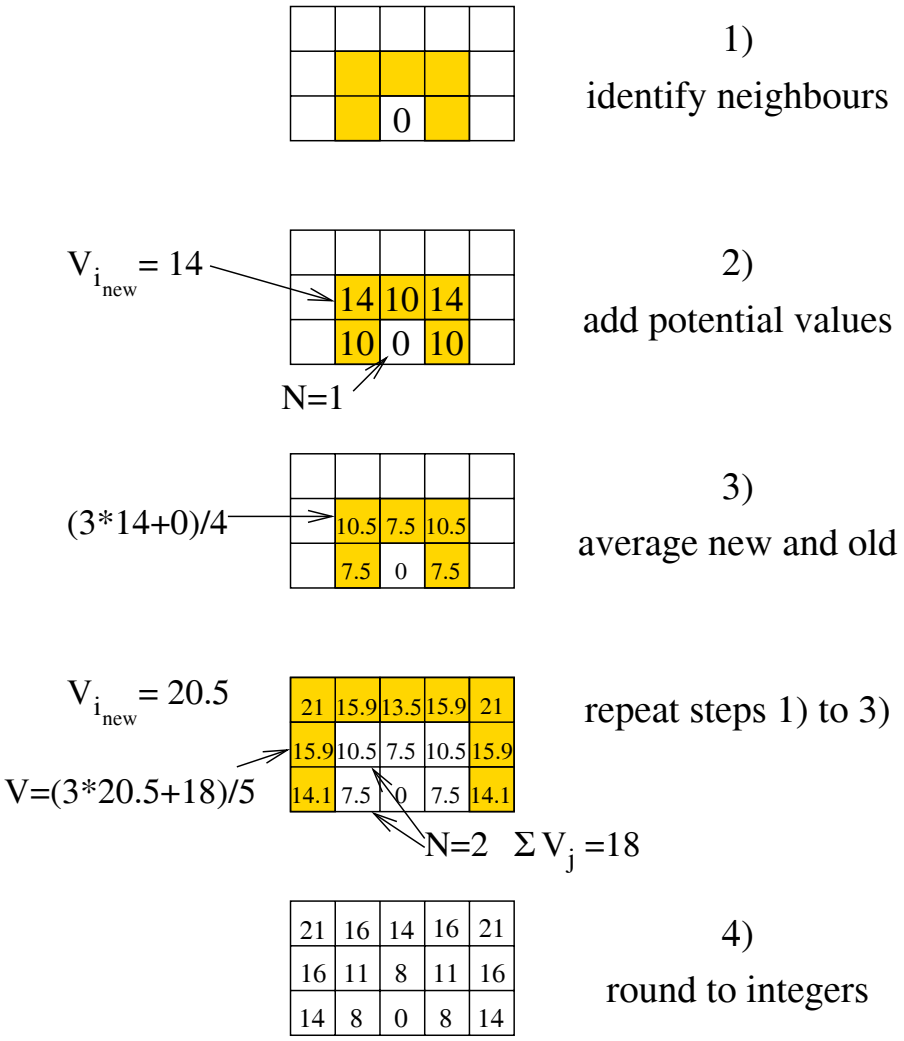

Fig. 3.13. Potential spread with Moore neighborhood ($k = 8$) and smoothing. The new potential values (step 2) are obtained by adding 10 to the one of the horizontal/vertical neighbor and 14 to the diagonal neighbor. If this is not unique (i.e., there are different neighboring cells already assigned a potential value) the lower result is taken. The average is $(3 \cdot V_{i_{\text{new}}} + \sum_{i \in \mathcal{N}} V_i)/(N+3)$, with $\mathcal{N}$ being the 'old' neighborhood cells of i_{new} and N the number of elements in $\mathcal{N}$.

Fig. 3.14. Potential (equipotential lines colored equally) spreading along a bended hallway (left). The right picture shows the trajectory along the gradient of the potential which is perpendicular to the equipotential lines. The generation of the potential is illustrated in fig. 3.13.

In summary, one can derive $V(r)$ from a metric $M(r)$ that assigns the distance to the exit to each cell. For complex geometries, however, this approach requires the definition of several potentials and groups of persons in order to allow exit allocation to exits other than the nearest one. Therefore, the direct assignment of the movement direction to each cell ($V(r)$) is more appropriate for evacuation scenarios, unless several potentials are used.

Nevertheless, the refined version of the potential spread with smoothing comes close to the metric defined in eq. 3.19 and if there is only one exit, or exit allocation is always to the nearest one, eq. 3.17 can be used to replace V by M in the movement algorithm. The major advantage is that M is easier to calculate than V. The disadvantage compared to the 'direct' assignment of directions is that there might occur artefacts in the paths due to the metric.

3.5 Transition Probabilities

An update step in the model corresponds to the movement of the entire population, where each pedestrian has moved (a move can consist of up to $v^i_{\max}$ steps). This is done determining the new position and then moving the pedestrian there. The movement of the pedestrians can also be interpreted in terms of transition probabilities, which enables a more systematic investigation. Transition probabilities are specific for stochastic cellular automata (the 'classical' update function of eq. 3.1 is deterministic).

The transition probabilities are based on the directions $V(r)$, ($r \in \mathcal{L}$). Apart from the set of rules that determine $p_{r\to r'}$ an equation could be used: $p_{r\to r'} = f(S(r), S(r'))$. The differences between the two approaches will be discussed in the following.

An example of the formulation with transition probabilities is

$$p_{r\to r'} = N \cdot e^{\beta(M(r')-M(r))} \cdot (1 - n_{r'})(t), \tag{3.21}$$

where $n'_r = o'_r + w'_r$, which is 1 only if $o(r') = w(r') = 0$ (N is a normalization constant).[18]

For the example of a hallway with walking direction in positive x-direction and the use of transition probabilities based on a metric $M(r) = r_x$ this leads in the simplest case to the following transition probabilities (for $n(r') \equiv 0$ for $r' = r$):

$$p_{r\to r'} = \begin{cases} N \cdot (1 - n(r')) & \text{if } r'_x = r_x, \\ N \cdot (1 - n(r')) \cdot e^{\pm\beta} & \text{if } r'_x = r_x \pm 1. \end{cases} \tag{3.22}$$

where $x_{\max}$ is the size of the lattice in the x–direction. $\mathcal{N}$ has eight elements, $N = (2 + e^{\beta} + e^{-\beta})^{-1}$, and β is governing the deviation from the optimal direction. As can

[18] o specifies if the cell is occupied by a pedestrian, w if it is a wall cell.

be seen from eq. 3.22 movement is possible also backwards. For $\beta = \infty$ the movement is deterministic.

By comparing this approach to the rule based movement algorithm (cf. fig. 3.3) the major differences can be identified:

1. Fluctuations in speed and direction are governed by the same parameter β in the one case and by two parameters p_{dec} and p_{sway} in the other case.
2. Movement across the corner is not distinct from movement across the edge.

For the example of the hallway the transition probabilities obtained from applying the movement rules of fig. 3.3 are (positions in the matrix correspond to the local neighborhood relationship and movement direction from left to right is assumed):

$$P = \begin{pmatrix} 0 & 0 & (1-p_{\text{dec}}) \cdot \frac{1}{2} p_{\text{sway}} \\ 0 & p_{\text{dec}} & (1-p_{\text{dec}}) \cdot (1-p_{\text{sway}}) \\ 0 & 0 & (1-p_{\text{dec}}) \cdot \frac{1}{2} p_{\text{sway}} \end{pmatrix} . \tag{3.23}$$

From these considerations, it can be seen again that the movement algorithm and the definition of the orientation potential V, resp. the metric M, are closely connected. However, the rule based approach is distinct from the one based directly on transition probabilities and they cannot be transformed into each other.

3.6 Comparison of the Different Update Types

The update that is used for the evacuation simulations in chapters 4 and 5 is a shuffled sequential one. Nevertheless, other types of updates could be used. Therefore, in this section, three different update types are investigated and their influence on the flow is compared.

3.6.1 Parallel Update

Parallel means that all pedestrians move synchronously. The situations that complicate the procedure are those where two or more pedestrians try to access the same cell (conflicts). Therefore, it has to be decided how to proceed in this case. One possibility would be to force all the peds that are involved in a conflict to stop. Another possibility is to allow one of them to move.[19] One possibility to do this is via 'throwing a dice', i.e., by choosing one with equal probability. In this case, the conflicts can be resolved in the following way (which has the additional advantage that it can be implemented via shuffling the sequence in which the pedestrians move):

1. Identification of conflicts:
   In this case and for $v_{\max} = 1$ each pedestrian can be involved in at most one conflict. The conflict parties are stored in a $m \times n_k$–matrix P, where m is the number of conflicts and n_k the coordination number (number of neighbor cells). Each row j contains the positions of the pedestrians involved in conflict i.

$$P_{j,l} = \begin{cases} i, & \text{if } r_i + v_i = k_j, \\ 0, & \text{otherwise.} \end{cases} \tag{3.24}$$

[19] The concept of friction introduced in this context by Kirchner [2002] (see also [Kirchner et al., 2002]) and employing an analogy to granular flow [Wolf and Grassberger, 1996] combines those two possibilities and is used in section 3.7.2 to distinguish competitive from cooperative behavior.

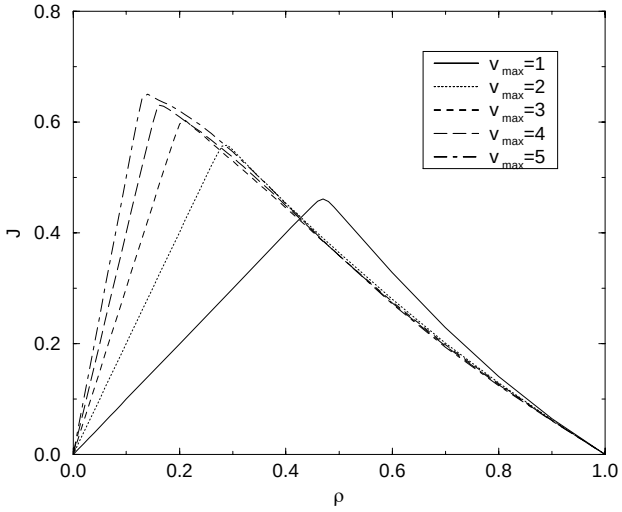

Fig. 3.15. Fundamental diagram for a hallway (parallel update) for $v_{\max} = 1 \ldots 5$ and $\beta = 10$ (cf. eq. 3.22). ρ is measured in units of $\rho_{\max}$ and j in units of $(a \cdot \Delta t)^{-1}$. As one can see, the shape of the curve for $v_{\max} = 1$ slightly deviates from the ASEP (cf. fig. 3.17, $v_{\max} = 1$, parallel update). This is due to the fact that interaction between different lanes destroys particle-hole-symmetry.

(k_j denotes the place (cell) of the conflict; l is the 'index' of the conflict party, i.e., if i tries to access k_j $P_{j,l} = i$ and $l \to l + 1$)

2. Resolution of conflicts:
   Choose randomly (uniform weights) one winner for each conflict
   $\mathrm{P} \to \vec{p} \in \mathbb{N}^m, p_j = P_{j,\mathrm{winner}}$.

3. Move.

From this a sequence in which the peds can be moved in the simulation one after the other can be obtained: $s^{\vec{p}} \in \mathbb{N}^N, s^{\vec{p}} = (\vec{p}, \{1, \ldots, N\} \setminus \{p\})$ (N is the overall number of pedestrians and $\{p\}$ denotes the set of the entries of $\vec{p}$, i.e., $\{1, \ldots, N\} \setminus \{p\}$ are the indices of the peds who lost a conflict or were not involved in a conflict). For a uniform conflict solution ($p_{\mathrm{move}} = \frac{1}{n_k}$, n_k the number of conflict parties) this can be implemented by shuffling the sequence $\vec{s} = (1, \ldots, N) \to s^{\vec{s}}$; $s^{\vec{s}} \sim s^{\vec{p}}$ concerning the dynamics, since the only relevant aspect is who wins the conflict, resp. moves first. Therefore, shuffling the sequence at the beginning of each time step is equivalent to a conflict solution with uniform weights. However, if another choice is made for the weights in the conflict solution (e.g., according to the differences $M(r') - M(r)$) this does not work anymore and the matrix P has to be explicitly stored when implementing the model.

Implementing the parallel update this way is easier, since the conflict parties do not have to be stored. Additionally, for high densities, the random numbers that have to be

drawn to resolve the conflicts will be as many or more as there are pedestrians, anyway.[20]

For the parallel update the route choice is made according to a 'frozen' situation, i.e., there is no difference in the situation pedestrian i and j see. The actual differences when the pedestrians move in a shuffled order are due to the pre-determined outcome of the conflicts, i.e., if pedestrian i occupies a cell which pedestrian j wanted to move to, then he has won the conflict and j has to stop. If one would apply iterative conflict solution, i.e., search for an alternative destination cell for the losers of a conflict, then j could access another cell.

A fundamental diagram for the model with parallel update for $v_{\max} = 1 \ldots 5$ is shown in fig. 3.15 [from Kirchner, 2002]. The peak is shifted to the left with increasing $v_{\max}$. For $v_{\max} = 1$ the flow density relation is very similar to that for the ASEP (cf. fig. 3.17). One interesting property is the slight deviation from the symmetric fundamental diagram of the ASEP (cf. eq. 2.12 and fig. 3.17) for $\rho > 1/2$. This is due to the fact that particle-hole symmetry is broken for multiple lanes. Roughly speaking, a particle can access the two different neighboring lanes. Therefore, the two corresponding holes would have to be able to access the lane of the particle, which is not possible. The fact that the deviation from the straight line for $\rho > 1/2$ is small corresponds to the low number of lane changes.

3.6.2 Shuffled Sequential Update

For the shuffled sequential update, the sequence in which the pedestrians move is shuffled at the beginning of each time step. The difference to the parallel update is not primarily the sequence of motion but the occupation of the cells. When choosing the destination cell in the shuffled sequential update, cells that have been accessed by another pedestrian within the same time step are not taken into account and therefore an alternative cell can be chosen.[21] For the parallel update, such a situation will lead to the pedestrian trying to access this cell and then – if he looses the conflict – stop. This is the reason why a shuffled sequential update produces a higher flow.

For the one dimensional case, the difference in the flows for high densities, i.e., the outflow from a jam, can be determined exactly. Consider the number l of pedestrians that move out of a queue (cf. fig. 3.16) of length n: $\langle l \rangle$ is then given by

$$\langle l \rangle = \sum_{l=1}^{n} l \cdot p_l, \tag{3.25}$$

where p_l is the probability of l pedestrians moving.

To count the configurations in which exactly l pedestrians are allowed to move, the construction of an appropriate configuration can be done in the following steps:

1. draw $l + 1$ different integer numbers (between 1 and n, $l < n$) randomly,
2. assign the largest of them to the pedestrian l,
3. assign any of the remaining l numbers to pedestrian $l + 1$,
4. assign the remaining $l - 1$ of the drawn numbers in an ascending order to the first $l - 1$ pedestrians, and

[20] For each conflict a random number has to be drawn and the number of conflicts for high densities is proportional to the number of pedestrians.

[21] This is similar to the iterative conflict solution in the previous section.

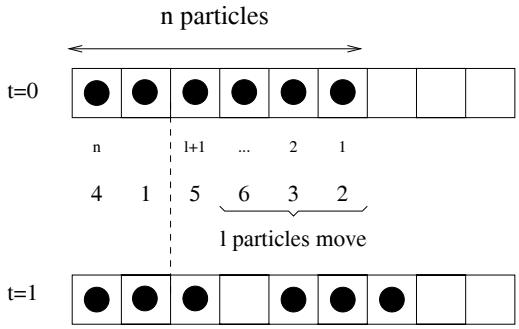

Fig. 3.16. Outflow from a cluster for the shuffled sequential update. The length of the cluster is n and the number of moving pedestrians l. The numbers below the cells for $t = 0$ indicate the sequence of motion.

5. assign the $n-l-1$ numbers $\{l+2,\ldots,n\}$ randomly to the pedestrians on the sites $(l+2)\ldots n$.

This procedure is illustrated in fig. 3.16. The count for the configurations that realize this procedure is shown in table 3.3.

Table 3.3. Construction of all sequences of motion that allow exactly l out of n pedestrians in the cluster to move (for the shuffled sequential update). However, this procedure works only for $l < n$.

	step	count	comment
1	draw $l+1$ different integer numbers $r_1,\ldots,r_{l+1}$ between 1 and n	$\binom{n}{l+1}$	$r_i < r_j$ for $i < j$
2	assign the largest to the pedestrian on site l: $s_l = r_{l+1}$	1	necessary, otherwise more $(s_i = r_i, i \in \{1,\ldots,l+1\})$ or less $(s_l = r_i, i < l)$ than l peds move
3	assign any of the remaining l to site $l+1$	l	$s_{l+1} = r_k$
4	$r_i = r_{i+1}$ for $i = k,\ldots,l-1$ $s_i = r_i$ for $i = 1,\ldots,l-1$	1	$\Rightarrow$ exactly l move
5	assign $r_{l+2},\ldots,r_n$ randomly to pedestrians $(l+2),\ldots,n$	(n-l-1)!	

The ways to do this are for step (1) $\binom{n}{l+1}$, for (2) one, for (3) l, for (4) one, and finally for (5) $(n-l-1)!$. The procedure works only for $l < n$, though. For $l = n$: $P(l = n) = 1/n!$, since there is only one configuration that allows all n pedestrians to move, namely $s_i = i\,\forall\, i$ ($n!$ is the number of all possible configurations). The details are shown in table 3.3 and the result in figure 3.16. Now, exactly l particles are allowed to move. This covers all the possible configurations where l peds move. Noting that the

number of all possible configurations is $n!$ and using (3.25) one obtains:

$$\begin{aligned}\langle l\rangle &= \left(\sum_{l=1}^{n-1} l\frac{\binom{n}{l+1}\cdot l\cdot(n-l-1)!}{n!}\right)+\frac{n}{n!} = \left(\sum_{l=1}^{n-1}\frac{l^2}{(l+1)!}\right)+\frac{1}{(n-1)!}\\ &= \sum_{l=1}^{n-1}\left(\frac{(l+1)(l-1)}{(l+1)!}+\frac{1}{(l+1)!}\right)+\frac{1}{(n-1)!}\\ &= \sum_{l=1}^{n-1}\left(\frac{l}{l!}-\frac{1}{l!}\right)+\sum_{l=2}^{n}\frac{1}{l!}+\frac{1}{(n-1)!}\end{aligned} \tag{3.26}$$

For $n\to\infty$ this expression can be further simplified using

$$e=\sum_{l=0}^{\infty}\frac{1}{l!}=\sum_{l=1}^{\infty}\frac{l}{l!}.$$

The first term in the last line of eq. 3.26 is e, the second $e-1$, the third $e-2$, and $\frac{1}{(n-1)!}\to 0$. Therefore

$$\lim_{n\to\infty}\langle l\rangle = e-1. \tag{3.27}$$

For the special case $l=1$ eq. 3.26 can be checked directly:

$$p_1 = P(l=1) = \frac{\binom{n}{2}(n-2)!}{n!} = \frac{1}{2}, \tag{3.28}$$

which is in accordance with the following argument: Exactly one pedestrian moves if and only if the place of the second pedestrian in the sequence of motion is lower (earlier) than that of the first (e.g., $s_2 < s_1$, cf. table 3.3).

In the limit $n\to\infty$ the average outflow from a compact cluster (mega-jam) is therefore for the shuffled sequential update $(e-1)/\Delta t$. This illustrates the higher flow compared to the parallel update, where the outflow is just one car, i.e., $j=1/\Delta t$ and that for the shuffled sequential update the flow is always higher than for the parallel update.

3.6.3 Ordered Sequential Update

Finally, a sequential update can be done based not on a shuffled, but some other sort of sequence. In reality synchronization effects can be observed, which lead to a high flow for high densities (platooning). The reason is probably the anticipation of the behavior of other pedestrians. An extreme example is the motion of soldiers in parades [Janosi, 1999]. The flow density relation for the ordered sequential update against the direction of motion for the ASEP is given in eq. 2.11. For $p=1$ (deterministic hopping) it holds $J_{\leftarrow}(\rho)=\rho$. Therefore, the fundamental diagram is just a straight line. It can be assumed that this result can be generalized to the fundamental diagram for 2D, if a pedestrian does not block his own path (for $v_{\max}>1$).[22] However, this occurs only in special situations and most empirical fundamental diagrams show a decrease in the flow for densities above around $2.5\,\mathrm{P/m^2}$, i.e., the highest flow is obtained for medium densities.

[22] If he does so, then the differences in the flow to the parallel update would be due only to the one origin cell that is blocked for the parallel update.

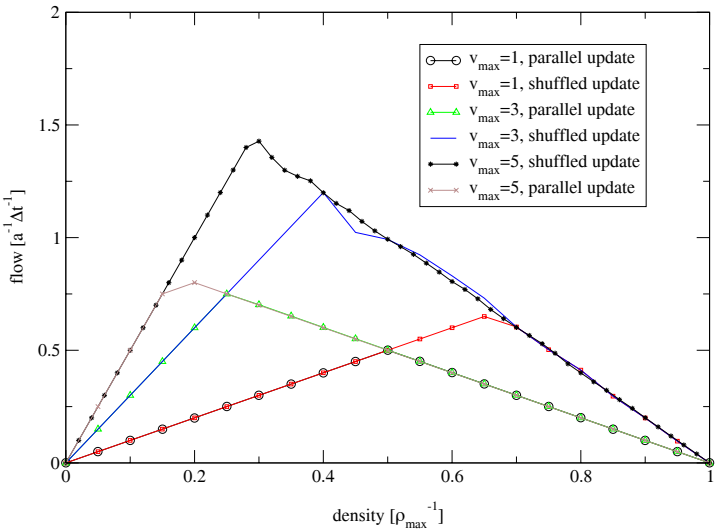

Fig. 3.17. Comparison of the flows for parallel and shuffled update obtained for the one dimensional Nagel-Schreckenberg model. The results are for $v_{\max} = 1$, 3, and 5 and the deceleration probability $p = 0$. The length was 1000 cells with periodic boundary conditions. One can clearly see that the shuffled updates produce higher flow rates in the high density region. The interpretation of the time scale depends on $v_{\max}$ via. eq. 3.3. Therefore, $j^{\text{emp}} \sim 1/v_{\max}$, i.e., the flow values for $v_{\max} = 1$ would have to be scaled by a factor 3 in order to compare them to the flows for $v_{\max} = 3$.

3.6.4 Influence of the Update on the Fundamental Diagram

From the previous considerations, the following relation between the flows can be conjectured (PU: parallel update, SSU: shuffled sequential update, SU: sequential update against the direction of motion, i.e., 'from the exit backwards'):

$$j_{\text{PU}} \leq j_{\text{SSU}} \leq j_{\text{SU,exit}} \tag{3.29}$$

The term $j_{\text{SU,exit}}$ denotes the flow for a sequential update against the direction of motion (for egress from a room, the sequence would be according to the distance from the exit). The differences in the flows are most prominent if only the destination (and origin for the PU) cells are blocked during one time-step (for $v_{\max} > 1$, otherwise, this is automatically the case). If the complete path is blocked, the differences become small. This can again be seen by comparison to the 1D case: If every car would block his trajectory for the time step Δt, then the sequence in which the pedestrians move is not important. This is the reason why the parallel update is implemented via a sequential update in the direction of motion.[23]

In summary, the type of the update is determined by the cells that are taken into account when choosing the destination cell and by the rules for blocking the path. For all different types of update, the path can be considered blocked or not (cf. the requirements concerning the matrix T in eq. 3.8). The classification of the updates can therefore be made according to the occupation numbers $o(r)$. If all $o(T_{1i})$ (i is the index of the

[23]This automatically considers the blocking of the path. For periodic boundary conditions, a special treatment for the first car is necessary to ensure parallelism also at the boundary.

Table 3.4. Comparison of the minimal distance between pedestrians for the different updates in the 1D case. The ordered sequential (smallest distance) update means that the pedestrian closest to the exit moves first. The minimal distance is for the high current phase and $v_{\max} = 1$, the flows are for $v_{\max} = 1$.

type of update	distance	maximum flow
ordered sequential	$d^i \geq 0$	$j = 1$
shuffled sequential	$d^i \geq \langle v \rangle - 1$	$j \approx 0.6$
parallel	$d^i \geq \langle v \rangle$	$j = 1/2$

pedestrian, $i = 1 \ldots N$) are set to zero only after all pedestrians have moved and cell T_{1i} is no longer occupied, this is called a parallel update. Therefore – technically – whether the update is parallel or sequential rather depends on the definition of $o(r)$ and not on the sequence in which the pedestrians move: If $o(r)$ is set to zero immediately after a pedestrian has left the cell and set to 1 as soon as a pedestrian moves onto a cell, this is called a sequential update.

Another reason for comparing the different update types is that in the continuum limit ($a \to 0$, $\Delta t \to 0$) the differences in the flow vanish. This can be seen from the fact that the headway (gap) $g_i = a \to 0$, i.e., the flow increases linearly with ρ:

$$j = \rho \cdot v = \rho \cdot \frac{\Delta x}{\Delta t} = \rho \cdot \frac{a}{\Delta t} \xrightarrow[a \to 0, \Delta t \to 0]{} \rho \cdot v_{\max} \,.$$

Therefore (without any restrictions concerning the path) the flow in this limit is given by: $j(\rho) = \rho$ (j measured in units of $(a \cdot \Delta t)^{-1}$).

Whether a parallel or sequential update is more realistic, cannot be decided by the fundamental diagram. The shuffled sequential update can be interpreted as pedestrians taking into account the outcome of a conflict when orientating (choosing the desired destination cell). This is the main difference to the parallel update. All the other features depend rather on the way a pedestrian blocks his path and when $o(r)$ is set to zero for all cells except those that are currently occupied by a pedestrian and not on the sequence in which the pedestrians are moved in the simulation. Further phenomena of crowd motion are necessary to assess the properties of a model. Those for which empirical data is available (cf. section 2.5) and that are important in the context of evacuation simulations will be addressed in the next section.

3.7 Model Extensions to Include Further Aspects of Crowd Motion

Obviously, the action of a crowd of people is not just the sum of individual motion. Additional phenomena are due to psychological and social influences that are connected to the character of crowd motion. However, the question is: Does the formation of a crowd change the rules for the movement of an individual or do the phenomena emerge from the interaction? As long as one does not simulate the decision making and the state of mind, it is sufficient to base an evacuation simulation on a model for crowd movement.

In the following, additional phenomena will be investigated together with potential model extensions to cover them. These extensions have not yet been implemented, but might become important when the scope of the model is extended to more complex

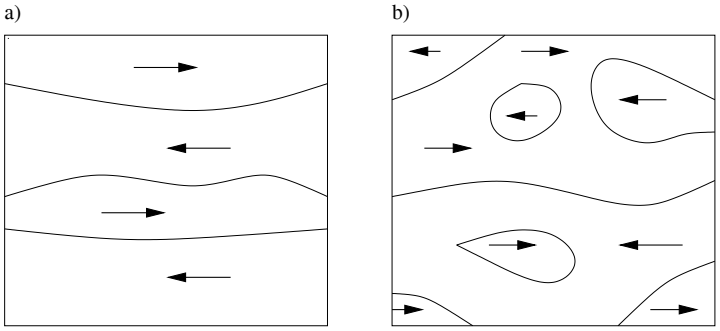

Fig. 3.18. A typical phenomenon in pedestrian movement is the formation of lanes (a) and clusters (b) with uniform movement direction. Yamori [2001] has introduced a band index, which is basically the ratio of pedestrians in lanes to the overall number. For a) this would be nearly 1. High band indices have only been observed for large numbers of pedestrians (100 and above).

situations. This is especially the case for simulations of non-emergency situations where people have various different goals and walking in opposite direction occurs frequently.

3.7.1 Lane Formation and Other Movement Patterns

Lane formation, the formation of walking patterns like trails, and other phenomena can be explained as self-organization processes. Pedestrian movement has a large degree of freedom. However, certain types of behaviors are reinforced and lead to the selection of macroscopic states. The micro-macro link, i.e., the connection between microscopic dynamics and macro-behavioral patterns was investigated by Yamori [2001].

To this end, the rectangular area observed (cf. fig 3.18) has been divided into small squares. A so called 'band index' is introduced, which is the ratio of the pedestrians walking in lanes spanning across the complete crosswalk to the total number of pedestrians. Typical lane widths observed were between 1 and 1.5m. The band index increases with the size of the crowd and for crowds of less than 100 persons the band index always was below 0.3. Furthermore, the time evolution of the band index shows certain characteristics. Usually, a high band index evolves only after the density has reached high values but then remains high even though the density goes down.

Lane-formation has been observed in continuous [Helbing et al., 2002] as well as CA-simulations [Burstedde et al., 2001]. The specific feature of the CA-model that is responsible for the formation of lanes is a so called 'dynamic floor field' D [Schadschneider, 2002b]. $D(r)$, $r \in \mathcal{L}$ is increased by one if a pedestrian leaves cell r. It can be used to increase the attractiveness of regions with high flow. Furthermore, D is subject to diffusion and decay, such that the information about the areas of high flow spreads. A detailed description can be found in [Kirchner, 2002, Schadschneider, 2002b]. Simulations show that the formation of lanes can be obtained by employing such a dynamic field D.

Another similar phenomenon is the formation of circulating traffic. AlGadhi et al. [2002] investigated the flow of pilgrims in Makkah. A static and dynamic model are proposed for the crowd flow. The latter takes, in addition to the speed-density relationship, also into account the dependency on the speed of the surrounders. This becomes important especially in the case of opposite walking directions. The major result is that

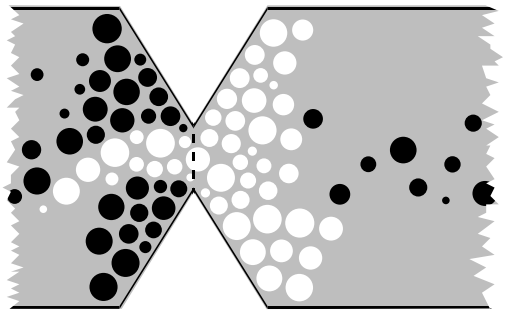

Fig. 3.19. Simulated oscillation at a bottleneck, where the walking direction through the passage varies periodically [from Helbing et al., 2002].

the speed reduction of people moving in the same direction is more than twice as much than for those moving in the opposite direction. This is mainly due to the fact that for opposite walking directions the formation of lanes occurs more frequently, whereas for the first case probably no lanes according to different walking speeds are formed and overtaking slows down the effective walking speed. Furthermore, the marginal impedance was scrutinized and a time of 32 seconds obtained for the relaxation of the average speed to its equilibrium.

From this investigation it can be seen that the case of bi-directional flow is fundamentally different from the uni-directional one. Another important aspect in this case is the behavior at bottlenecks as shown in fig. 3.19. Helbing et al. [2002] describe oscillation of the flow direction at bottlenecks as one of the characteristic features of crowd motion. The literature investigated contains no quantitative empirical results on this. It is likely that for very narrow passages, where only one person can pass at a time, an oscillation will occur. However, in reality, such a bottleneck would be rather uncomfortable or even dangerous and should be avoided. For wider bottlenecks the formation of lanes could lead to steady flows in both directions.

3.7.2 Simulation of Competition as Friction

In an experiment carried out by Muir [1996] with groups of 50 to 70 persons, competitive vs. non-competitive movement was investigated for aircraft evacuation. In one case (competitive) a bonus was paid for the first 30 persons; in the non-competitive case, no bonus was paid. The time of the 30th person reaching the exit was measured ($t_{\text{comp.}}$ and $t_{\text{non-comp.}}$, resp.) for variable exit widths w. There is a certain width w_0 where $t_{\text{comp.}} > t_{\text{non-comp.}}$ for $w < w_0$ and $t_{\text{comp.}} \leq t_{\text{non-comp.}}$ for $w \geq w_0$. This shows that competition or cooperation can be harmful or beneficial depending on the circumstances, especially the layout of the escape path. The scenario is different from a real emergency in some aspects: Most of all, the motivation of the persons being at the end of the queue might decrease when they realize that they will not receive the bonus. If there is a real emergency, the situation is different: The motivation or level of competition will increase with time and the pressure from the people at the end of the queue will be higher. Since already in the test situation some of the trials had to be terminated to avoid injuries, the importance of the exit width is even stressed. The egress times measured for competitive and non-competitive behavior are shown in fig. 3.20.

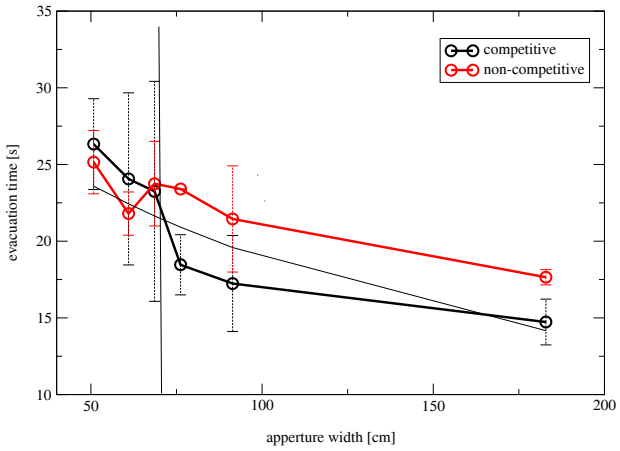

Fig. 3.20. The evacuation time increases with decreasing aperture width. For non-competitive situations, this decrease is rather smooth. However, if there is competition, at a certain aperture width ($w_c \approx 70\,\text{cm}$) the increase in the egress time is quite drastic and the performance is worse than in the case of non-competition [Muir, 1996].

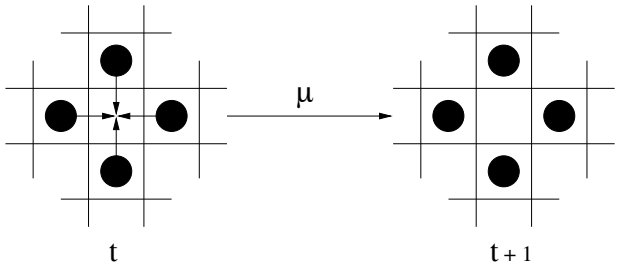

Fig. 3.21. Illustration of the friction concept and the parameter μ. For $\mu = 1$ there is no winner in a conflict, for $\mu = 0$, friction is turned off.

The main result is the existence of a certain door width w_0. Below w_0 non-competitive movement was beneficial, above competitive movement produced lower egress times. Competition is a typical social influence. However, here it is restricted to the movement behavior, i.e., only those aspects are considered that directly influence the motion. Simulations have been carried out based on the model described in [Kirchner, 2002, Kirchner et al., 2002] in cooperation with these researchers. As can be seen from fig. 3.23 the phenomenon can be reproduced qualitatively by utilizing a friction parameter μ in the simulation. This parameter μ gives the probability that for a conflict none of the parties is allowed to move (cf. fig. 3.21). A conflict is a situation where two or more pedestrians want to access the same cell. Since the probability for winning a conflict with k parties is $1/k$, the transition probabilities are then $p_{ij} = \frac{\mu}{k} \cdot N \cdot e^{\beta \cdot M_{ij}}$, with N as usual a normalization factor and M the Manhattan metric. Competitive is distinguished from cooperative behavior by increasing both, μ and β, for the first compared to the second.

It has to be noted that the model is based on $v_{\max} = 1$. Therefore, the time step ($\Delta t = \frac{a}{v_{\max}^{\text{emp}}}$) depends on the assumption about the maximum velocity of the evacuees in the experiment. If $v_{\max}^{\text{emp}} \approx 1.3\,\text{m/s}$, then $\Delta t \approx 0.3\,\text{s}$ (cf. eq. 3.3), which leads to an

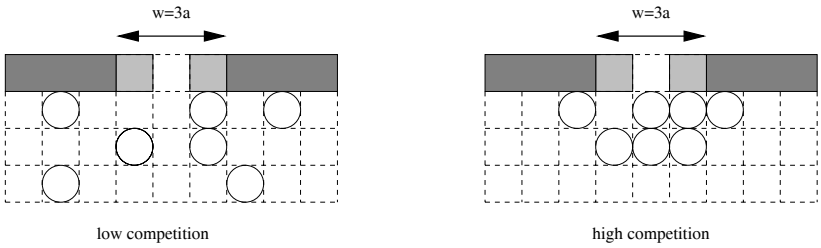

Fig. 3.22. At a narrow door the influence of the friction parameter μ can be dramatic. For a very narrow door (one cell) there is a drastic increase for the egress time for high μ due to the many conflicts which are not resolved but all parties have to stop.

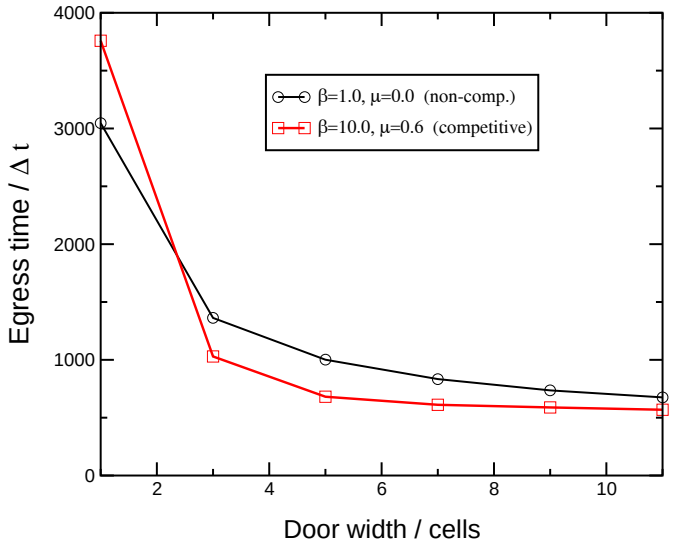

Fig. 3.23. Average egress times for variable door width. Competitive behavior is obtained by setting $\beta = 10$ and $\mu = 0.9$, non-competitive behavior by setting $\beta = 0.4$ and $\mu = 0.0$.

egress time $T = 300\,\mathrm{s}$ ($\approx 1000\ \Delta t$ for $w = 3\,\mathrm{cells}$). Furthermore, the size of the room in the simulation was 63×63 cells (with walls of thickness 1 cell) and the number of persons 111 ($\rho = 0.03$). If a steady outflow is assumed, the 30th person has left the room after $30/111 \cdot 1000\,\Delta t$, i.e., 81 s. This is then too high by a factor of 3.5. Even though some fine-tuning might be necessary to reach also quantitative agreement, these considerations show that a model including friction is able to reproduce the empirical findings quantitatively and distinguish between competitive and cooperative behavior in egress situations.

3.7.3 Route Choice Utilizing Networks

For more complex layouts, the orientation potentials become rather complex, especially, if many potentials are considered due to the inclusion of distinct groups. An alternative to the pure CA approach could be a combination of it with a more coarse grained network

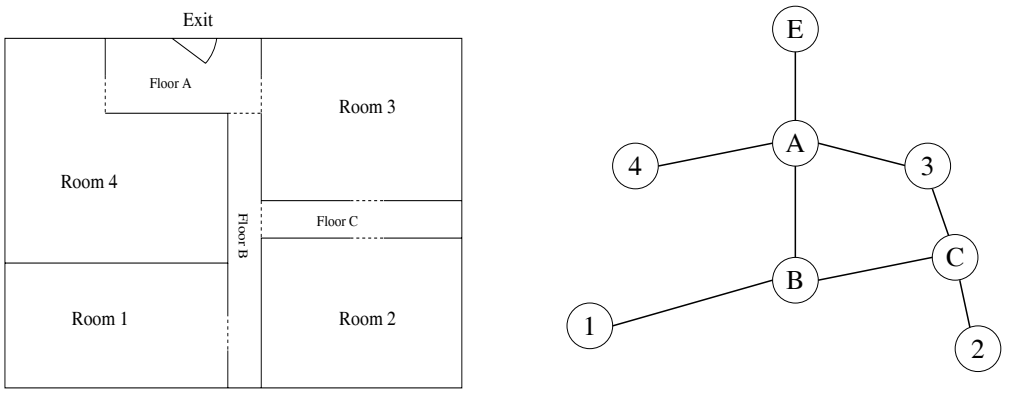

Fig. 3.24. A simple geometry and its graphical representation.

representation. The layout of a structure can be represented as a graph (cf. fig. 3.24), resp. directed graph (digraph). This is the approach used for queuing and network flow models [Hamacher and Tjandra, 2002]. This enables the application of standard graph theoretical tools like finding the shortest path or enumerating the paths [Kreyszig, 1999, Trudeau, 1993].

This combination of a CA with a graph would allow to define segmentations and related orientation potentials. Orientation would then be restricted to rooms (segmentations) and route choice would be done on the macroscopic level of the graph. The representation of a simple layout as a graph is shown in fig. 3.24. The rooms (and other two-dimensional elements like floors and stairs) are represented by knots, doors by edges. The resulting graph must not necessarily be simple, i.e., two vortices might be connected by more than one edge. Further investigations concerning this topic are not included here, but might be worthwhile investigating, especially from a technical point of view. It would make a connection between the microscopic models and the network flow approach and enable to cover more complex scenarios including proper route-choice.

A problem that might arise in a more complex simulation is that of deciding between different alternative routes. If route choice is restricted to orientation, i.e., there are no active decisions involved but route choice is pre-determined by taking the shortest path to the exit, certain aspects of reality are neglected and some scenarios cannot be covered by the model. There might, for example, be several routes to the same exit.

Nevertheless, based on the standard approach, all persons occupying the same area use the same route. This might not be true even for single rooms and more so for a complete building. This problem can be mitigated by defining several orientation potentials $V_1, V_2, \ldots V_n$. Those do only apply to the members of a certain group. For them

$$c_i = \begin{cases} 1 \text{ if } i \in G, \text{ where } G \text{ is the set of group members,} \\ 0 \text{ otherwise ,} \end{cases} \tag{3.30}$$

where c_i denotes the coupling to the potential i, i.e., they can follow only specific exit signs which must not necessarily lead directly (in the sense of minimizing the walking distance) to the exit but a sequence of potentials can basically reproduce any path. This generalizes the concept of the orientation potential to include different groups and can cover the choice of alternative paths by individuals.

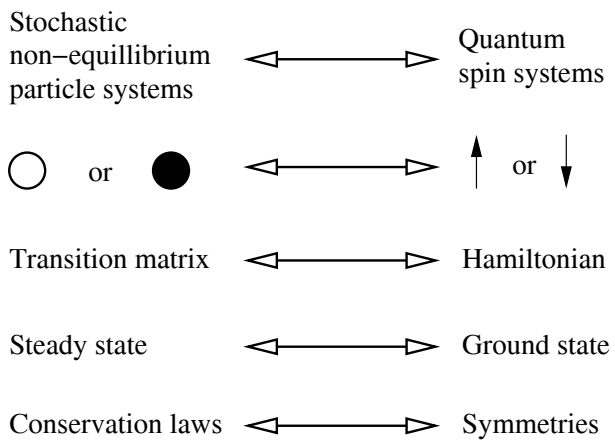

Fig. 3.25. Correspondence between stochastic non-equilibrium particle systems and quantum many body systems. For single-species exclusion processes the mapping can be to spin systems, as indicated in the second row [adapted from Stinchcombe, 2001].

By varying the c_i dynamically, i.e., forming a list of several consecutive potentials that direct a person or group of persons, a sequence of different destinations can be formed and more complex walking patterns represented. This allows also to overcome the restriction of taking the shortest path to the exit.

3.8 Relation to Other Lattice Based Models

3.8.1 Spin Models and Lattice Gases

Exclusion processes can be mapped onto spin models as shown in fig. 3.25. The time evolution can then be expressed in terms of a Hamiltonian:

$$e^{-H\delta t} = 1 - H\delta t \tag{3.31}$$

A particle at site i can hop to site j with probability $p_{ij}\delta t$ if j is unoccupied. This process takes $(n_i, n_j) = (1, 0)$ into $(0, 1)$ with probability $p_{ij}\delta t$ and into $(1, 0)$ with probability $1 - p_{ij}\delta t$. The Hamiltonian of the related spin system (cf. figs. 3.25 and 3.26) is given by

$$H = -\sum_{ij} p_{ij}\{\sigma_i^-\sigma_j^+ - \frac{1}{4}(1+\sigma_i^z)(1-\sigma_j^z)\} \tag{3.32}$$

Both terms contribute only when the state has $(n_i, n_j) = (1, 0)$, and the second term causes no change of configuration.

The steady state in the diffusion model then maps onto the ground state of the spin model. However, how the concept of a steady state would have to be defined in the context of crowd motion has not been investigated. This could provide an interesting topic for future research.

A standard model for diffusion processes is the ASEP. In this one dimensional case, i and j are neighbors. The totally asymmetric case $p_{i,i+1} = p$ and $p_{i+1,i} = 0$ is equivalent to the Nagel-Schreckenberg model with $v_{\max} = 1$. The connection between the ground

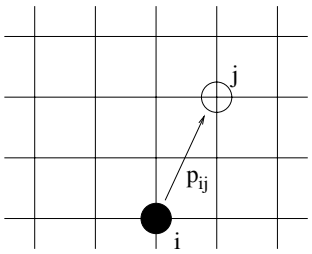

Fig. 3.26. A basic step and its transition rate p_{ij} in hard core diffusion.

state of a spin model and the dynamical equilibrium of diffusion models – if appropriately adapted to crowd motion – might lead to new insights concerning self-organization processes. This is, however, a different field of research and might be addressed in future investigations.

3.8.2 Phase Transitions and Critical Behavior

The question, whether there arises a phase transition in 1D CA depends on the specific type of the model. For traffic models there exist boundary induced phase transitions [Popkov et al., 2000] driven by the injection and removal of cars at the boundaries. The term dynamical transition [Biham et al., 1992] is used for changes in the relaxation behavior. A transition called 'jamming transition', which is driven by the density, is described in [Muramatsu et al., 1999]. Genuine 'phase transitions' are between stationary states. Those transitions are connected to the topic of self-organization [Fukui and Ishibashi, 1999, Helbing et al., 2001, Nagatani, 1993].

In order to find and characterize a genuine phase transition an order parameter has to be defined and its behavior close to the transition point investigated. It is known from other models, that phase transitions exist in 2D, but do not in 1D for $T > 0$ (e.g., the well-known Ising model). However, the time can be regarded as the second dimension in 1D CA. The generalization would then be to three dimensions for a 2D CA. Nevertheless, the search for critical behavior in this type of non-equilibrium CA might be fruitful. The application to evacuation processes could profit from such knowledge about self-organization phenomena, which are often connected to phase transitions and the emergence of macroscopic order parameters [Haken, 1983].

Chapter 4

Evacuation Simulations: Implementation and Validation

Egress simulations are not solely based on the dynamics of crowd movement but have to take into account further aspects like response times. When considering evacuation scenarios the number of influences and parameters increases. How these additional influences can be quantified and how simulations can be validated and used to assess evacuation processes are the main topics of this chapter. It also contains comments on the implementation of the model into a simulation and an overview over the programs that have been developed for evacuation simulations.

Contents

4.1 The Implementation of the Model Into a Simulation

4.1.1 Technical Aspects

The case of emergency situations is special with respect to the crowd movement (compared to normal situations) since it includes additional factors. This can be seen from the following equation:

$$t_{\text{egress}} = t_{\text{awareness}} + t_{\text{response}} + t_{\text{walk}} \tag{4.1}$$

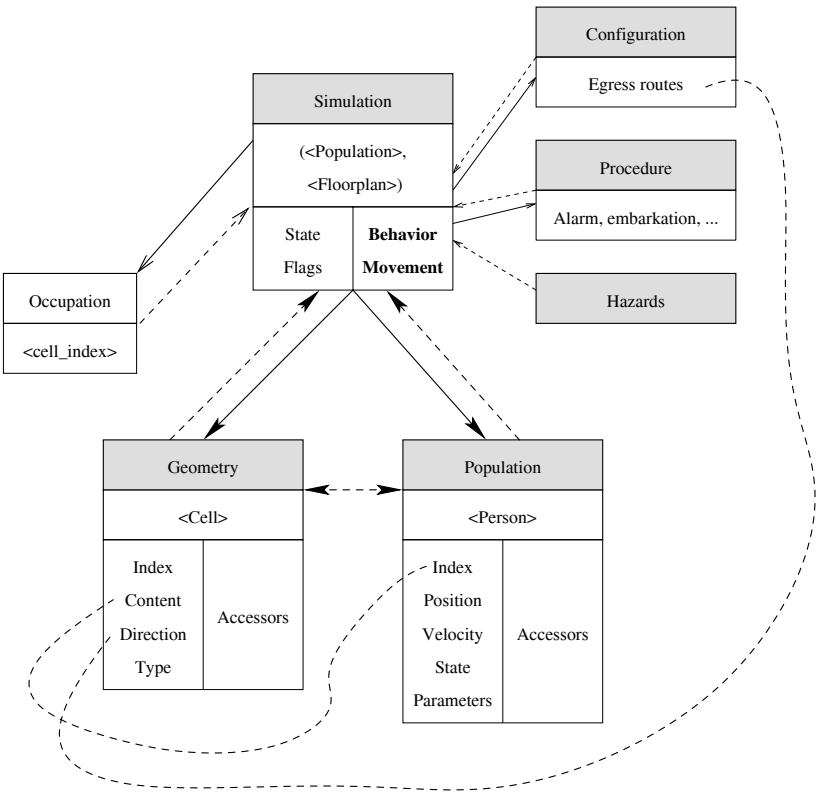

Fig. 4.1. Outline of the simulation components for a complete evacuation simulation.

As already stated in the previous chapter, the simulations presented here are mainly aiming at reproducing what could also be the outcome of an evacuation exercise. Therefore they focus on the action stage. This is also consistent with not explicitly modeling psychological aspects. However, they are of course represented indirectly by quantifying their average influence on the movement or behavior, for example by specifying a distribution for the response times. The proper movement is then based on the model introduced in the previous chapter.

If a pedestrian has reached the exit, he is rescued. For evacuation simulations, an exit can also be an embarkation station (where people enter a lifeboat or lifer-raft) or for aircraft a chute. In this case the embarkation cells are blocked for a certain time, the preparation time t_{prep}. Additionally, in an emergency case, not all persons start moving immediately after the alarm has been triggered. This is taken into account by a response time t^i_{response}. This parameter – like the other personal parameters – can vary among a population.

There are further aspects that have to be covered, if a realistic evacuation process is simulated [Meyer-König, 1999]: Different floors or decks must be connected via stairs. Within the framework of the CA, stairs are considered part of the lower floor and there are so-called 'jumping points' at the (upper) end of the stair. If stairs are used in two directions, a more intricate representation has to be used [Meyer-König, 2000]. The speed on stairs is reduced by a factor 1/2, which is the product of $\cos 35°$ (the average angle of

incline) and a reduction factor of 0.6, for the movement along the incline. Movement up- and downstairs usually proceeds with different speeds and therefore the reduction factors up- and downstairs could also be different. This fact might be considered in an extended version of the simulation. The simulations we have performed and that are presented in this chapter use this simplified reduction factor.

For movement through doors, there are only few empirical data. Since the opening (and closing) of doors is not explicitly modeled, there is a reduction factor of 0.25 for movement through doors. This factor is a rule of thumb.[1] Reduction factors r lead to a decrease of $v_{\max}$:

$$v^i_{\max} \to f_{\text{red}}(\mathcal{A}) \cdot v^i_{\max}, \text{ if } r_i \in \mathcal{A},$$

where $\mathcal{A}$ denotes a special area, i.e. stairs, doors, or assembly points, where the maximum speed is reduced. Due to the introduction of those special geometrical elements (doors, stairs, embarkation stations), the following additional rules have to be introduced:

1. When reaching the end of a stair, move to the next deck and continue there.
2. While on a stair, the maximum speed is reduced by a factor 0.5:
   stair: $v^i_{\max} = 0.5 \cdot v^i_{\max}$.
3. When moving through a door, reduce speed by a factor 0.25:
   door: $v^i_{\max} = 0.25 \cdot v^i_{\max}$.

The important point is that for an egress simulation there is a termination criterion which is the fact that all persons have reached a so called 'rescue cell' (exit, embarkation station, assembly point, place of safe refuge). This means that no fatalities are simulated. The connection between the single elements and influences that are relevant in an evacuation process and the corresponding simulation component is illustrated in fig. 4.1.

4.1.2 Evaluation of Simulation Results

In order to quantify simulation results, certain measures have to be defined. One that is well suit for judging the effectiveness of a layout and an evacuation procedure are queues. One might define significant queues either by the time they persist or by the densities that occur or by a mixture of both. For applications to ships, the term significant queue has been defined based on the ratio of the time the congestion ($\rho > 4\text{P}/\text{m}^2$) persists and the overall egress time [IMO, 2002a]. If this ratio is is larger than 0.1, then a queue is called 'significant queue'. The density can easily be measured in a CA by averaging for each cell the occupation number of the surrounding cells.

$$q_r = \frac{1}{k+1} \sum_{t=0}^{T} \sum_{j \in \mathcal{N}(r),\, j=r} o_j, \tag{4.2}$$

with $k = |\mathcal{N}| = 8$ being the coordination number and $\mathcal{N}(r)$ the neighborhood of cell r. The visual representation can then again easily be done via – like for the geometry itself – a grid of cells that are colored according to q_r. Apart from queues (which are a local and therefore microscopic measure) the overall evacuation time is the most important quantity for assessing an evacuation. There are several ways to define this time, which makes

[1] The literature investigated within this work did not contain any information about movement through doors.

the following distinction between the parameters and the variables of the simulation necessary.

The macroscopic variables measured (like evacuation time) are based on microscopic processes that take place on the level of single persons. Small letters denote individual parameters and variables, i.e., those that refer to single persons. The superscript i denotes the individual person. Capital letters are parameters and times referring to the whole process, e.g., overall evacuation time T.

1. Individual evacuation time t_i is the time a single person needs for the evacuation and is calculated during the simulation for every person.
2. Overall evacuation time T is usually the maximum of the individual evacuation times.
3. Preparation time T_{prep} is the time it takes to make the evacuation systems ready (for aircraft and ships).

The simulation runs until all persons have reached an exit or place of refuge which determines the overall evacuation time. Of course other measures for the success of the evacuation could be defined, e.g., the time when 95% of the persons have evacuated. Additionally, when there is pressure exerted on the persons or toxic combustion products are present, persons might become incapable of moving or die. In this case $T = \max_{i=1\ldots N} t_i$ cannot be used and, e.g., the time which is higher than 95% of the individual times is defined to be the overall evacuation time: $P(t_i \leq T) \geq 0.95$, where P denotes the relative frequency.

When interpreting the results of a simulation there are two separate topics of concern: (1) gaining information about the current situation and (2) deriving strategies for improvement. An optimization does directly provide information on (2), a simulation does not. Based on q_r and t_i the evacuation process can be assessed. Further information on the flow of persons at specific points could be used as an input for a systematic evaluation and the development of improvement strategies.

4.1.3 Monte–Carlo Simulation

Since the outcome of a real evacuation or an evacuation drill is not a single time but a probability distribution for the egress times, this should also be reflected in the simulation. A deterministic model will provide the same outcome if the initial conditions are not changed. In reality the outcome will differ even if a drill is repeated with the same initial conditions. Additionally, the characteristics of a population can usually only be specified in a statistical way. In the case of simulating crowd motion there are therefore two separate reasons for indeterminism: the current situation (initial configuration) can never be known exactly and the processes underlying decision making can not (either in principal or for the sake of describing them mathematically) be completely quantified. This lack of information is compensated by probabilistic parameters and algorithms in the simulation. This is of course the reason why the model presented in the previous chapter is a stochastic CA. In addition to this, the parameters are assigned randomly to the population within certain ranges to reflect the second source of indeterminism described above.

This leads to Monte-Carlo simulations where the uncertainties are taken into account by means of a random number generator.[2]

[2]The Monte-Carlo method for equillibria is usually based on detailed balance ($P(c \to c')p_c =$

Of course, a computer cannot produce genuine random numbers. However, a sequence of numbers that is 'statistically' random is sufficient [Kinzel and Reents, 1999]. It has to be kept in mind, however, that any sequence produced by a random number generator is periodic. Linear congruential generators are a good choice in this context [Knuth, 1997, Press et al., 2002]. The requirements for the random number generator are not as high as for other sorts of applications, since the length of the sequence of random numbers that has to be generated is in the order of 10^{10}.[3]

The two different influences mentioned above are both present in the simulation. On the one hand, there are stochastic parameters that represent the indeterministic nature of the motion, i.e., the influence of psychological factors not otherwise quantified (dawdling probability p^i_{dec}, swaying probability p^i_{sway}). On the other hand, the uncertainties regarding the initial conditions are taken into account by specifying the population in a statistical sense, i.e., by a distribution and its parameters. Effectively, the parameters of the persons are assigned freshly for each simulation run, which is equivalent to redistributing the initial positions. The outcome of the MC simulation is therefore a sample from which the characteristics of the probability distribution for the evacuation time can be derived. This will be carried out for the example in section 4.3.3.

4.2 Simulation Programs – Overview

As already stated in chapter 2 there is a variety of models for crowd motion. This does not contradict the fact that they all attempt to describe the same subject. It has already been outlined that different models can be in accordance with the same theory, especially, if it is such a complex and comprehensive one as for crowd movement. Therefore, a variety of different approaches have been developed to simulate crowd motion and evacuation processes. In the later field the first attempts date back to the 1970's [Stahl, 1978, 1982].

A classification of the different simulation approaches is shown in fig. 4.2. Some of the currently available simulation programs (software packages) are summarized in table 4.1. They can be roughly classified into the categories *simulations*, *optimizations*, and *risk assessment*. Optimization models are usually based on network flows, such that a quantity that should be minimized (e.g., travel time) can be stated explicitly as a function of the parameters. Similarly, risk assessment models allow to calculate probabilities and expectation values for certain incidents, resp. damages or fatalities.

Most of the models (except of EVACSim and Evi) are based either on a continuous or CA-type representation of space. For the CA the cells are usually quadratic (EGRESS is based on hexagonal cells). In Exodus, the movement is based on a grid of cells, where the connection between the cells is stored separately, such that any cell can be connected to any other, not only to its next neighbors.

As far as knowledge about the orientation could be obtained, it is based on a similar approach as the one described in chapter 3. This holds also for Simulex, where a so called 'distance map' based on a quadratic grid with a cell length of 25 cm is used. The motion is otherwise continuous. Information about EvacuShip and SPECS is scarce and it is not clear, whether the development still continues.

$P(c' \to c)p_{c'}$, where c and c' are certain configurations) and the appropriate choice of the transition probabilities: $P(c \to c') = e^{-\frac{1}{k_B T}(H_{c'} - H_c)}$, for $H_{c'} < H_c$, 0 otherwise, with H denoting the Hamiltonian (Metropolis algorithm). It can be shown that this method converges to the correct equilibrium state.

[3] The number of time-steps is in the order of 10^3 (i.e., hours, since $\Delta t = 1\,\text{s}$ in reality), $N \approx 10^4$, and the number of consecutive simulation runs (MC-simulation) around 500.

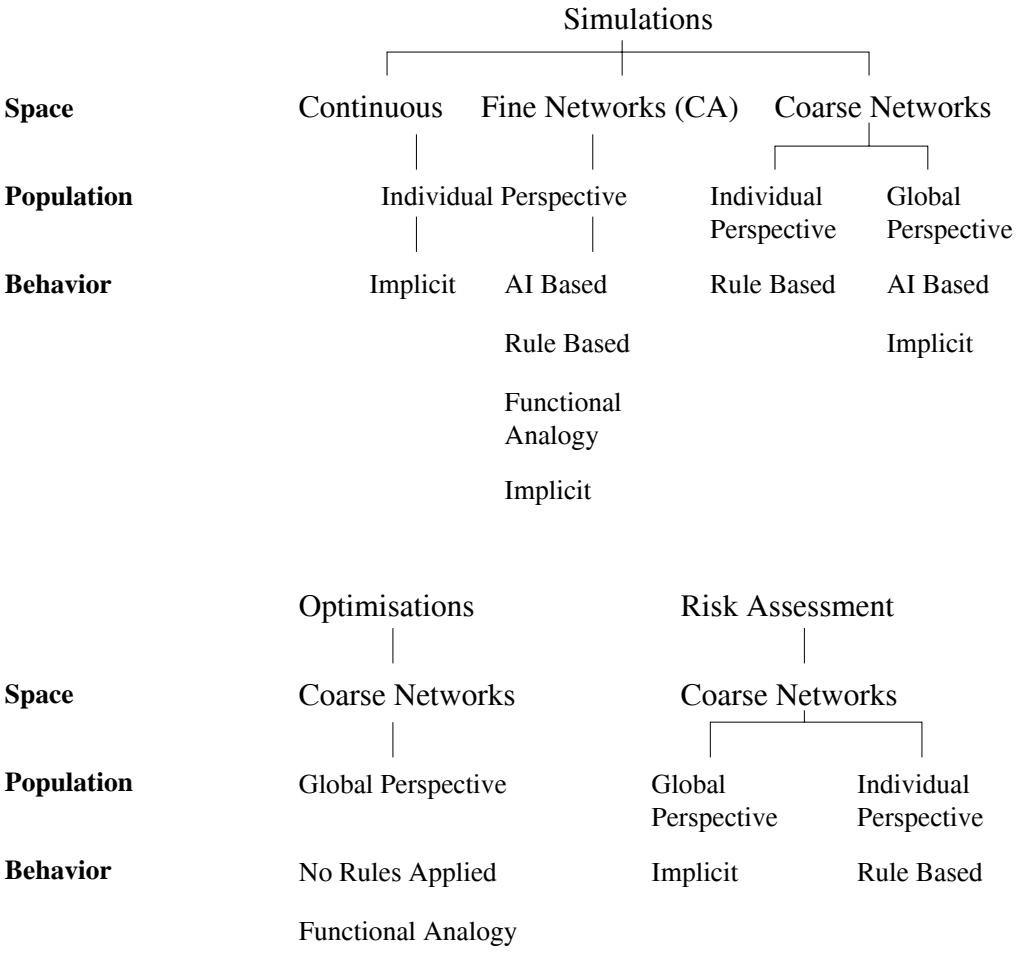

Fig. 4.2. Overview over the different approaches for modeling evacuation processes [from Gwynne et al., 1999]. Optimization and risk assessment are usually based on coarse networks, since the output, e.g. evacuation time, has to be specified explicitly as a function of the parameters and initial conditions. Simulations are more flexible with respect to the representation of geometry and population. On the other hand, they are no optimization tools. Most simulations are based on an individual perspective (microscopic). For continuous simulations, behavior is usually implicit in the equations of motion, whereas for CA a set of rules is specified. However, this is just a rule of thumb and exceptions are of course possible. An example for a coarse network with global perspective is the route choice based on a graph presented in section 3.7.3.

Table 4.1. Exemplary software packages for evacuation simulation that are currently available or under development. If certain entries in the table are blank this does indicate that the information could not be obtained; it does not imply that the respective feature is not implemented.

Name Developer	Geometry Population	Route Choice Ship Motion	Behavior Hazards
Exodus	discrete	potential	stochastic
Galea/FSEG	individual	under dev.	FED
	[Bukowski et al., 1998, Galea, 1998, and ref. therein]		
Simulex	continuous	distance map	deterministic
Thompson/IES4D	individual	-	
	[Thompson and Marchant, 1995a,b, Thompson et al., 1996]		
ASERI	continuous	distance	
ITS	individuals	-	
	[Schneider and Könnecke, 2002, Schneider and Weckman, 2000]		
SPECS	continuous	Multi-Agent System	
Principia Marine (IRCN)	individuals	-	
		[Pradillon and Ferry, 2001]	
Evi	mesoscopic	graph	stochastic
Vassalos/SSRC	individual	speed red.	
		[Vassalos et al., 2001, 2002]	
EVACSim	queuing netw.	graph	
Drager/Quasar	aggregate		
		[Drager et al., 1994]	
EvacuShip			
Brumley/Monash		speed red.	
		[Brumley and Koss, 1997, 2000a,b]	
PedGo	discrete	potential	stochastic
TraffGo	individual	under dev.	-
	[Meyer-König, 2000, Meyer-König et al., 2001, 2002, TraffGo GmbH, 2002]		
EGRESS	discrete (hex)		stochastic
AEA	individual		fire/smoke
		[de Vries, 1998, Webber et al., 1998]	
EXIT	continuous		
TU Wien/ÖISS	individual		no

A comparison of three simulation programs has been carried out by Weckman et al. [1999]. It is based on an evacuation exercise in a Finnish theater.[4] Results on evacuation times were obtained using hand calculations and simulations based on Exodus, ASERI, and Simulex. The overall evacuation times for the test, the calculation and the simulations were close to each other. This supports the conjecture, that simulations, even if they differ concerning the underlying model and the details of the implementation, basically represent the same theory for crowd movement.

4.3 Validation of Simulation Results by Comparison with Evacuation Exercises

Empirical data is used in two ways in the context of egress simulations: (1) calibration of the parameters and (2) validation of simulation results. For a phenomenological approach, the latter is sufficient. In this sense, calibration comprises the fundamental model properties like the flow-density relation. Data suitable for calibration has been shown in chapter 3. Here, the focus is on validation and therefore on data for egress scenarios. In [ISO, 1999] the following steps in validation are listed:

1. Component testing: checking of software subcomponents (the model).
2. Functional validation: checking of model capabilities and inherent assumptions.
3. Qualitative verification: comparison of predicted human behavior with informed expectations.
4. Quantitative verification: comparison of model predictions with reliable experimental data.

The underlying idea is that of a black box. However, since different models comply with a reasonable theory for crowd movement, this approach seems to be a good compromise. The first two of these items are usually based on simple test cases and do not require empirical data. The third is based on comparison with observations and the last on comparison with quantitative and experimental data. The data used in this chapter is based on video analysis. This analysis is done manually, i.e., there was no automatic device that extracted the information from the videotapes. This technique is on the one hand tedious, on the other hand it might be error-prone. The second aspect has been checked by repeating the countings for some of the evaluations (cf. section 4.3.3), which of course increases the time effort even further. There were no major deviations and therefore the procedure is reliable. Alternative approaches for data recording are briefly summarized in the next section. They have not yet been used, but will be indispensable when attempting the collection of extensive data on pedestrian movement (comparable to that available for road traffic).

4.3.1 Data Recording

The usual approach towards data recording is observation and counting. The use of technical devices is then restricted to video cameras which allow to separate the experiment

[4] An interesting aspect of the exercise was that people were not informed in advance, which makes the results of course more realistic, especially concerning the response times. Furthermore, they did not know that it was not a real emergency. Surprisingly, the audience did not complain about the interruption, but some of the actors did.

Table 4.2. Different techniques for pedestrian detection.

Video analysis	difficulties with obstruction
Pressure sensitive mats	expensive, high resolution possible
Active infrared	technically demanding
Passive infrared	better than video, more expensive
Laser scanner	high resolution, automatic detection

and the proper counting process. Further techniques for pedestrian detection can be found in table 4.2. If one aims at an automatic data recording there are many subtleties [Keßel et al., 2002]. A detailed discussion of this topic can be found in [Schirmacher, 2001].

There are two main problems when recording individual data: (1) recording the movement of individual persons automatically (like with turnstikes) does not measure free flow but strongly influences the motion and behavior and (2) 'contact-free' recording like video-taping can at the moment not be processed automatically for crowds. Light barriers or infrared detectors are usually not able to automatically detect, distinguish, and trace individuals.

The potential devices for pedestrian detection are:

Active infrared sensors emit infrared light and detect the transmitted part of the spectrum. This enforces a special mounting which is usually not possible for pedestrian movement measurements.

Passive infrared sensors are frequently used as motion detectors. A pyroelectric element produces a voltage when the light intensity changes. Therefore, they are only able to detect moving objects.

Microwave detectors are able to measure velocities by employing the Doppler effect.

Ultrasonic sensors can detect static objects. However, they depend on strong sound reflection and are therefore not appropriate.

Mat detectors allow a rather high spatial resolution. For counting persons, a high number of mats would be necessary, though.

Laser and radar scanners emit focused light and can compute the distance based on measuring the travel distance [Sick AG, 2000].

Video Analysis is the classic. It is very hard, though, to evaluate the tapes automatically, especially for the detection of moving pedestrians.

The recording and evaluation of data on pedestrian motion and evacuation exercises using video techniques is rather cumbersome and tedious. Therefore, a concept for simplifying this task would be helpful. However, up to now videotaping and manual evaluation can not be circumvented. The evaluation of the data presented below is based on the following assumptions and methods. If single persons are counted, for the flow holds $j = \frac{1}{\Delta t}$, where Δt is the time gap between two persons. If groups of n persons counted within Δt, however, the flow for the group is given by:

$$j_n = \frac{n}{\sum_{i=1}^{n} \Delta t_i} = \frac{n}{\Delta t}\,. \tag{4.3}$$

Taken to the extreme, n is set to the overall number of persons leaving a building N and $j = N/T = \text{const}$. It is therefore important to clearly distinguish this type of a priori averaging from the a posteriori averaging, where the mean of flows is calculated

$$\langle j \rangle = \frac{\sum_{i=1}^{n} 1/\Delta t_i}{n} \neq j_n \,. \tag{4.4}$$

For $j(t) = $const. (but only in this case) eqs. 4.3 and 4.4 provide the same result. However, eq. 4.3 can only be used for counting single persons. Therefore, eq. 4.3 is preferable. This is automatically considered when using the cumulative flow

$$n(t) = \sum_{i=1}^{N} f(t_i \leq t), \tag{4.5}$$

with N being the number of persons, $j(t) = \frac{\partial}{\partial t} n(t)$, and $f(A) = 1$, if A is true, 0 otherwise.

The specific flow is defined as the flow per width

$$j_{\text{spec}} = \frac{n}{\Delta t \cdot w}, \tag{4.6}$$

with w the width of the door, walkway, etc. Further information concerning the technical aspects of data recording and evaluation can be found in [Frantzich, 1996, Willis et al., 2002]. In the following section this will be applied to the evacuation analysis of a movie theater.[5]

4.3.2 Evacuation of a Movie Theater: Exercise and Simulations

In order to be able to compare simulation results with empirical data in detail, we carried out an evacuation exercise in a movie theater and recorded it on videotapes. This method provides information about the initial population distribution and the time each person reaches the exit. Furthermore, the appropriate parameters for the simulation can be obtained in two ways: (1) by measuring them – as far as possible – in the exercise (e.g., response times and walking speeds), and (2) by comparing simulations and exercise. First, the outcome of the exercise will be presented, then simulation results, and finally both will be compared to each other.

The layout of the building

The building was a so called multiplex movie theater. The layout is shown in figs. 4.3 and 4.4. It has altogether 8 halls. One of them, hall 5, was used for the exercise. The initial positions of the persons can be seen in table 4.5. The numbering of rows and seats in fig. 4.4 and table 4.5 are equivalent.

There are three escape routes available. In the figures 4.3 and 4.4 there are two marked (route A and route B). The third route is the one leading through the fire door. It was available but not used by the participants during the exercise. This might be due to the fact that the other two were explicitly marked as escape routes by the respective signs. The way the persons came in was via the stairs (fig. 4.3, left) from the ground floor. The fire door was shut when the alarm was triggered. Therefore, the route where the people came in and were familiar with looked different due to the closed fire door. Additionally, once the first person getting out at the back of hall 5 (fig. 4.4, bottom) had decided to use route B, all the other persons followed.

[5] UCI in Duisburg

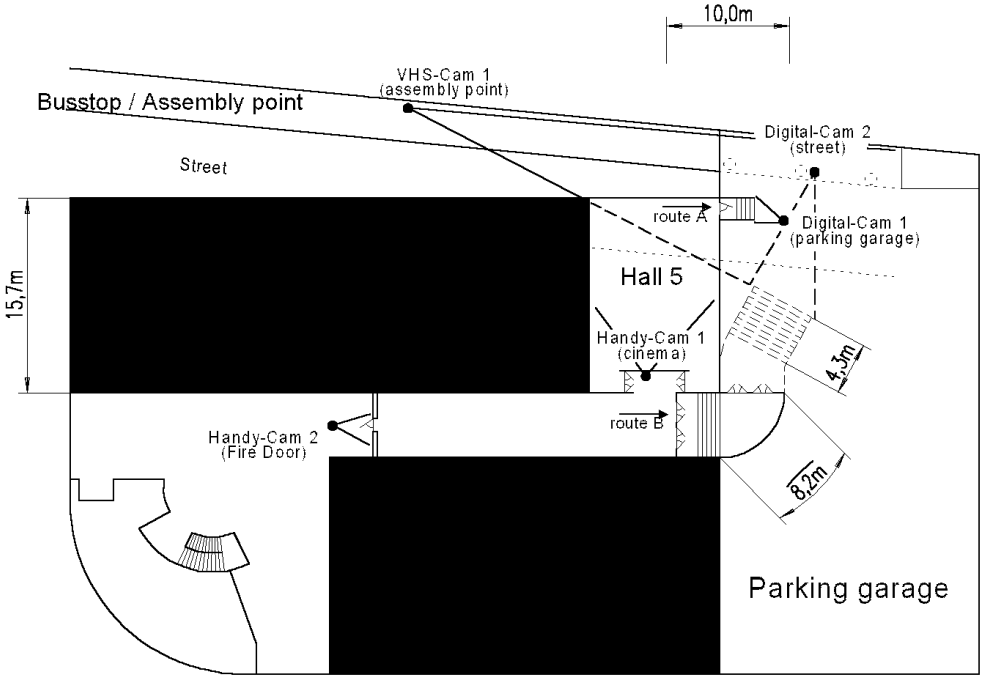

Fig. 4.3. Layout of the movie theater and positions of the cameras. The dashed lines represent two additional stairs separated by a terrace of length 3 m. All stairs lead downwards. The lines spreading from the cameras show their angle of vision (dashed lines indicate that they are on the ground floor below the theater).

Population

The participants were all students. 100 persons took part in the exercise, 27 of them female. Each person wore a hat with a unique number, such that an identification on the videotapes was possible afterwards. Four persons did not get a hat.[6] The homogeneous population (age between 20 and 30) is on the one hand a restriction concerning the generalization to an average population. On the other hand, this can be taken into account by an adapted distribution of walking speeds in a simulation.

Concerning a mixed ability population, the following differences (to a student population) might be expected:

- Walking speed: The average walking speed is probably lower.
- Route choice behavior: There seems to be no evidence that the route choice behavior is different from that of a homogeneous population. However, for persons with severe movement disabilities, especially those in a wheel-chair, neither route A nor route B are accessible. Therefore, they would either have to use the third route and then an elevator or escalator or other persons would have to assist or carry them. This influence cannot easily be quantified. Furthermore, it cannot be represented in the simulation at this stage.

[6] Two of the hats broke and one person of the staff used his for demonstration purposes. The number of hats was limited to 100.

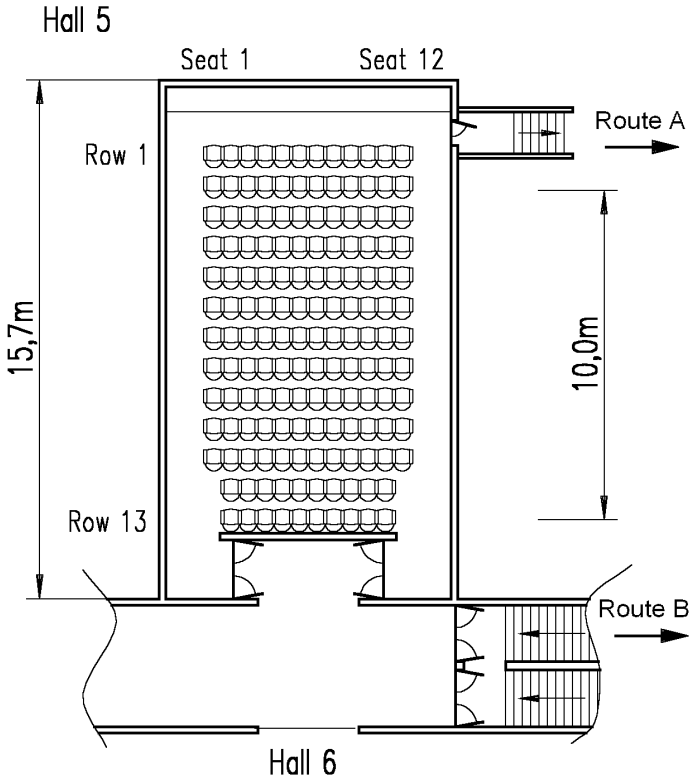

Fig. 4.4. Layout of the movie theater, hall 5. The drawing is in scale. The width of the front door (route A) is 90 cm and all the other doors and the stairs are 1.6 m wide.

- The population basically reacts as a whole and it is sort of a 'follow-the-leader' situation. In the exercise response was immediately. Students can be considered as performing optimal in this respect. Therefore, only slightly higher response times are expected for an average population.

- Orientation: the situation is similar to what has been said about the response time, i.e., increased p_{dec} and p_{sway}.

Therefore, the results could be generalized for a more diverse population by adapting the parameters.

Furthermore, the following deviations from a real emergency evacuation have to be kept in mind:

- The people were informed in advance. When marking every person unambiguously, this seems to be an unavoidable restriction, at least at the moment and with the equipment available.

- There were no hazards present.

- Everyone was urged to act carefully in order to avoid injuries.

Procedure

The procedure or sequence of events was the following:

1. Participants were advised in advance to move carefully and avoid injuries.
2. All participants wore hats which were sequentially numbered.
3. The number of the hat and the seat (starting position) of each person were recorded.
4. While the commercials were running the alarm was triggered.
5. The movie was stopped, full lighting turned on, and a message announced via the public address system: "There is a technical problem. Please leave the building via the marked exits and assemble outside the building at the bus stop in front of the east-entrance of the central station."
6. The persons started evacuating.
7. A person was considered evacuated when she reached the street, resp. the parking garage, where her egress was videotaped (Cams 1 and 2, cf. fig. 4.3).

For route A the counting point is the end of the stair (up) to the parking garage, for route B the end of the stair (down) to the street level. All the doors were closed before the exercise started. The emergency exits had been closed all the time until they were opened by an evacuee. There was no staff involved except of the operator who stopped the trailer (commercials before the proper movie), turned on the light, and made the announcement. Additional staff members were present at the assembly point. The first person to leave the room had to open the door. The doors did not have an automatic shutter, so they stayed open. They were all marked by luminous emergency exit signs above the doors.

There were three exit routes available (see figs. 4.3 and 4.4). On route B there was a first sign showing to the rear exit of hall 5 (fig. 4.4, bottom) and another one above the door at that end of the hallway. The distance from the main exit of hall 5 to the door leading to the stairs and then to the outside is much smaller than the one to the fire door. This is probably the main reason, why the persons leaving the theater via the rear exit exclusively chose this exit and nobody used the one via the fire door, even though this was the way people came in. However, due to the now closed fire door, it looked different.[7]

Egress Times and Comparison to Simulations

The results comprise data about the motion and egress times of each single person. In fig. 4.5 snapshots of the video camera that was placed in hall 5 at the back above the entrance (cf. fig. 4.3, bottom) at different times are shown. This gives an impression of the sequence of the exercise. Only part of the egress routes is covered by the camera (cf. figs. 4.4 and 4.5). There have been further cameras recording the events in the other parts of the theater. Altogether, five cameras were used, one in the theater and four

[7]The influence of the directions given via the public address system might have had an influence on this exit choice. However, since the two exits used were not familiar ones and only for emergencies, the persons could not have known which one was the shortest to the assembly point.

Table 4.3. Population parameters used in the simulation of the evacuation of the movie theater. Parameters are uniformly distributed within their range.

Parameter	Symbol	Value
Walking speed	$v_{\max} = 3 \ldots 5$	$1.2 \ldots 2.0\,\mathrm{m/s}$
Response time	t_{response}	$0 \ldots 4\,\mathrm{s}$
Dawdling probability	p_{dec}	$0 \ldots 0.3$
Swaying probability	p_{sway}	$0 \ldots 0.01$

Table 4.4. Comparison between exercise and simulation for the evacuation of a movie theater.

	Exercise	**Simulation**
Number of Persons	101	101
Number of Seats	174	174
Level of occupancy	0.58	0.58
Number of runs	1	20
Overall		
Time (last person)	66 seconds	68 seconds
Std.Dev.	-	2.5 seconds
Mean egress time	44.0 seconds	38.4 seconds
Median	45 seconds	39 seconds
Route A		
Time (last person)	45 seconds	68 seconds
Mean egress time	31.1 seconds	35.0 seconds
Median	31 seconds	35 seconds
Route B		
Time (last person)	66 seconds	63 seconds
Mean egress time	53.1 seconds	42.0 seconds
Median	53 seconds	44 seconds

for surveillance of the exits. One exit was not chosen, so Handy-Cam 2 did not record anything.

In accordance with the observations in the exercise, the response time was chosen rather short for the simulations (0 to 4 s) and the walking speed higher than for the average population (1.2 to 2.0 m/s). The population characteristics used in the simulation are summarized in table 4.3.

The progression of the exercise and the simulation is shown in fig. 4.5. The former covers only the inside of the movie theater, whereas the latter shows also the adjacent stairs. Please note that the third and fourth picture are for $t = 25\,\mathrm{s}$ and $t = 40\,\mathrm{s}$ for the exercise and $t = 40\,s$ and $t = 60\,s$ for the simulation. There is a difference in the flow at the inside door (top right) where a queue occurs in the exercise as well as in the simulation. However, it took a longer time until this queue had vanished in the simulation.

The results of the simulations and the exercise are summarized in table 4.4. There is a prominent difference in the time for route A (this is the exit where the queue occurred). The motion in the simulation did not proceed as effective as in reality. This is probably due to the lower average walking speed at high densities in the simulation than in reality. This is a hint for a synchronization effect which is not completely covered by the model.

Under certain circumstances, motion proceeds fast despite of high densities (which

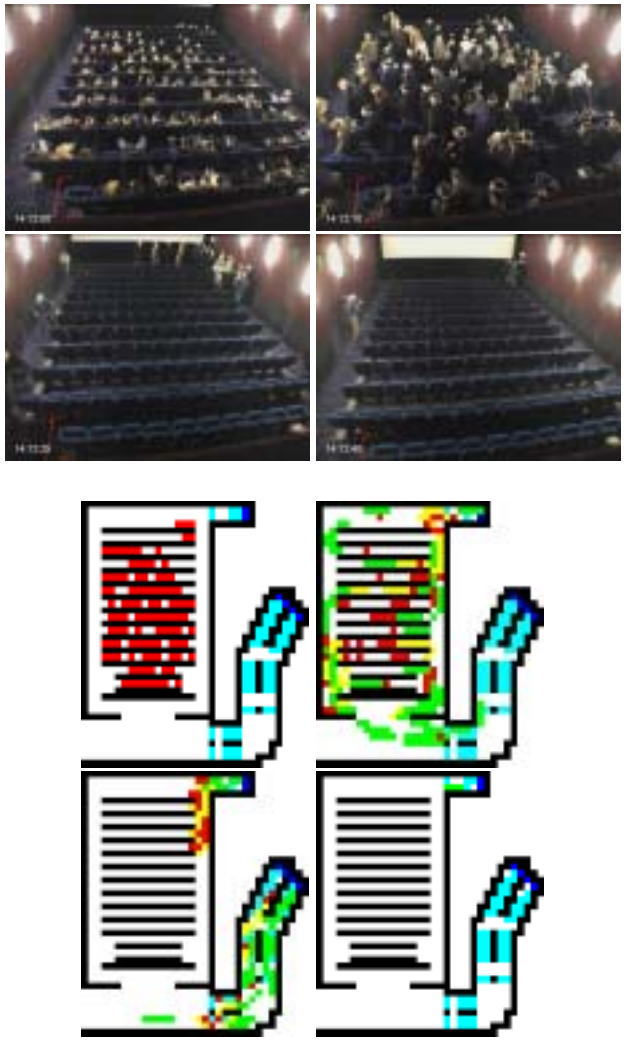

Fig. 4.5. Snapshots showing the evacuation exercise at times $t = 0s$, $t = 10s$, $t = 25s$, and $t = 40s$ (top part). The position of the camera can be seen in fig. 4.3 (Handy-Cam 1). The lower part shows snapshots of the simulation at times $t = 0s$, $t = 10s$, $t = 40s$, and $t = 65s$. The original output is colored. Here, the darker the shade, the lower the velocity. Walls and seats are black, stairs and doors light grey (as can be seen on the bottom right picture where the room is emptied). The directional field $\vec{V}(r)$ (cf. fig. 3.2) was assigned according to the evacuation plan.

could be called 'platooning'). This occurred in this case for the forward exit (A). For route B, where due to the wider doors no queues occurred, there is basically no difference in the overall time. However, comparing the mean individual times (cf. table 4.4), the same difference occurs for route B.

In summary, the walking for high densities is more effective in reality than in the simulation: For route A, where the highest densities occurred, the time in the simulation is longer than in the exercise. For route B, where the doors are wider and the densities

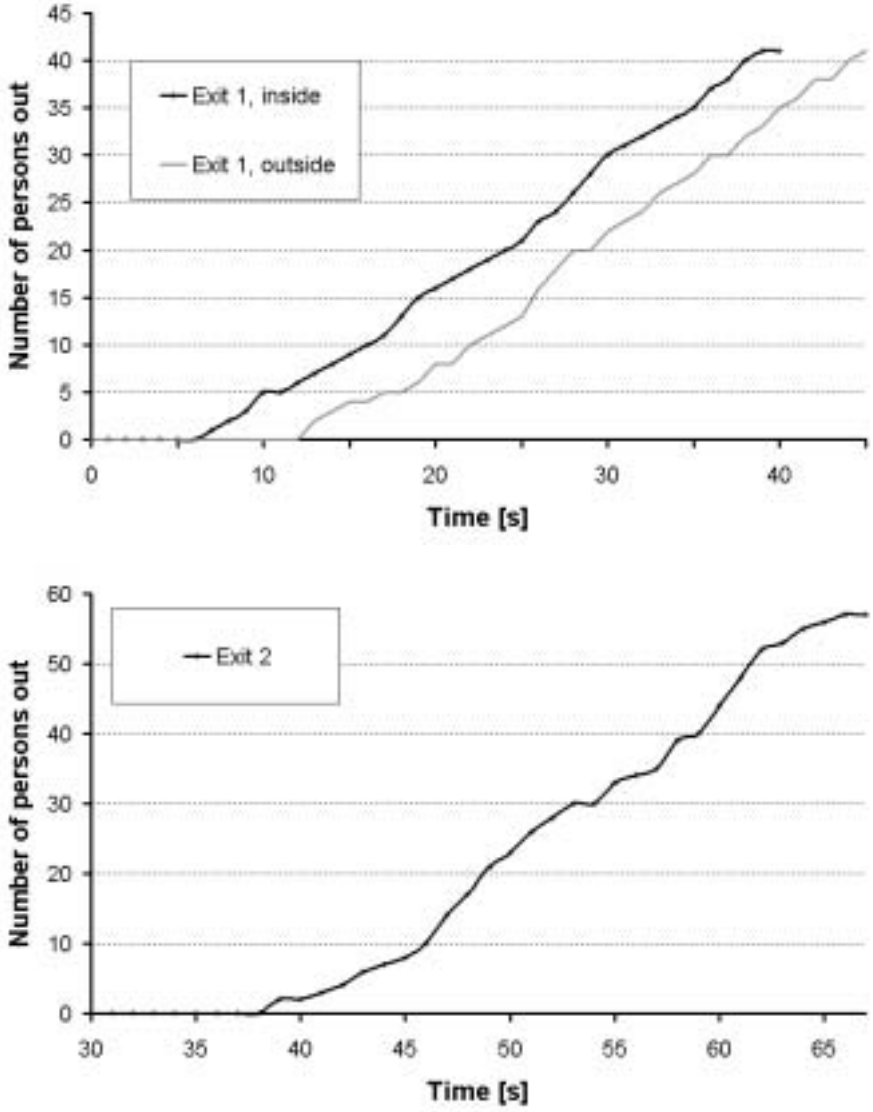

Fig. 4.6. Egress curve for route A obtained from the evacuation trial (inside and outside, top) and route B (end of the stair, street level, bottom). The difference between the two curves in the upper graph is the time it takes to walk from the door on route A to end of the staircase (cf. fig. 4.4).

are smaller, there is basically no difference in the times.

The reason for this difference, i.e., the synchronization effect (high flows at high densities) in the exercise but not in the simulation, can be seen from fig. 4.5, which shows the position of the evacuees at different time steps, and the the times in table 4.5 which shows the individual egress times.

The egress curves (number of persons out vs. time, cf. eq. 4.5) obtained from the

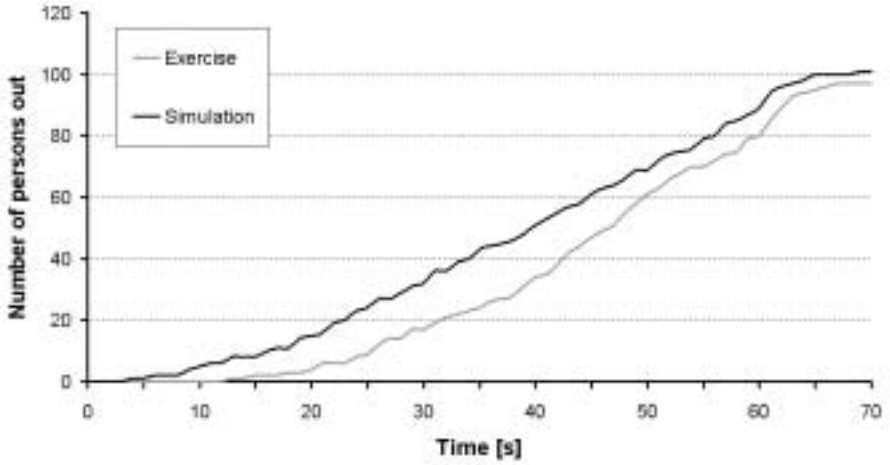

Fig. 4.7. Simulated evacuation time for the movie theater in comparison with the empirical results. Shown is the total number of persons out (both exits, cf. fig. 4.3) vs. time. The differences are explained in the text.

exercise for the two routes are shown in fig. 4.6. These curves contain the characteristic information about an evacuation. The flow rate vs. time can be obtained from this curve (by taking the derivative) as well as the overall time or information on fluctuations in the flow.

The two curves in the upper part are for route A at the inside and the outside (end of the stair to the parking garage, cf. fig. 4.4). The time distance is nearly constant, which shows that the queue is mainly due to the narrow door. Otherwise, the flow at the inside would decrease with time since at the beginning the flow at the door would be higher than that on the stairs and the distance between the two curves increase.

The second curve (fig. 4.6, bottom) shows the egress via the rear exit (route B). Here, no congestion occurs and the flow is determined by the walking speeds. Therefore, the fluctuations in the slope (which is the flow) are more prominent.

By adding the two flows one obtains the overall curve shown (together with the simulated egress curve) in fig. 4.7. The difference between simulation and exercise is small. However, in the simulation the offset in the time is smaller. Additionally, the difference in the times for the two exits are smaller in the simulation than in reality: $t_B^{\text{exerc}} - t_A^{\text{exerc}} = 21\,\text{s}$, whereas $t_A^{\text{sim}} - t_B^{\text{sim}} = -3\,\text{s}$ (cf. table 4.4). In summary, the simulation overestimated the time it took to pass the narrow door, where a queue formed.

Exit choice

The individual egress times and the exit choice have also been analyzed with respect to the initial positions. The results are shown in table 4.5. The rows in the table correspond to the rows of seats and the columns to the seat numbers. The underlines show those persons that have left the building via the rear exit (see fig. 4.4, exit B).

From the data shown in table 4.5 it can be hypothesized that there is a connection between the choice of the exit and the individual egress times. To quantify this connection

Table 4.5. Individual egress times (until the persons have left the building) and route choice for the exercise in the movie theater and the simulation. Underlines indicate the use of the rear exit (cf. fig. 4.4, exit B). The rows in the table correspond to the rows of seats and the columns to the seat numbers. Comparing the exercise and the simulation a difference in the route-choice can be identified: In the exercise nearly all person sitting at the rear and in the middle chose the rear exit. This is not completely reproduced in the simulation, since there the closest exit is taken. The times for exercise and simulation are summarized in table 4.4.

Exercise

Seat / Row	14	13	12	11	10	9	8	7	6	5	4	3	2	1
1										14		12		
2														
3	23	20	28	30	39	30			17					
4					35	31	32	25		24				
5	35	34	37	36		63	66		31	20	19			
6	25	28			60	61	61	41	38	38	28	26		
7		56		58	55	59		45	44		40	26	23	25
8		49	56	55		65	64	61	42	42	42		33	
9		48	48	46		43			44	60	60	60		41
10	47	44	47		49	57	62	62	51		53	58	42	
11	49	48	47		47		62	62	61		58	58		60
12					50	41	51	51		50	46			
13				53	52	39	38	39	45	43		52		

Simulation

1										8	8	5		
2													12	3
3	12	23	38	42	27	9			18					
4					47	51	39	23		10				
5	15	36	32	63		61	53		58	40	18			
6	15	41			20	52	56	56	34	24	25	16		
7		25		59	33	44		57	60		54	51	30	42
8		18	34	37		64	59	64	48	50	30	28	45	
9		30	44	35		61			46	50	54	43		21
10	40	32	50		45	68	32	60	41		60	21	19	
11	29	56	60		60		48	48	55		47	39		22
12					27	54	44	38		21	28			
13				25	23	56	58	62	30	39		34		

the mean of the times for each row and each seat number ('column') was computed as well as the ratio of persons in each row or column (same seat number) of table 4.5 that used the rear exit. The correlation coefficient for the egress time and the use of route B for the rows and seat numbers (the correlation coefficient is calculated as in eq. 5.8) is:

$$c_{\text{row,time}} = 0.81, \tag{4.7}$$

$$c_{\text{seat,time}} = 0.92. \tag{4.8}$$

As can be seen from table 4.5 the persons sitting in the middle usually took the backward exit. This might be due to the fact that there was a queue visible at the front exit (route A, cf. fig 4.5). This queue of course only formed over time and was not there right from the beginning. In the simulation (table 4.5) the exit choice is solely based on the geometry.

Therefore, the former connection cannot be found. Nevertheless, due to fluctuations not all persons in the same row chose the same exit.

4.3.3 Results for the Evacuation of a Primary School

We performed a similar exercise as the one described in the previous section in a primary school. This case is more complex than the previous one with respect to the layout. The question is therefore, whether there occur larger deviations between exercise and simulations or whether the simulations are still able to predict or reproduce the essential aspects of the evacuation exercise.

Layout, Population, and Procedure

The building consists of two separated parts. It houses a primary school with about 200 pupils (1st to 4th grade, i.e., 6 to 11 years old). The geometrical details together with the initial distribution of the persons are shown in fig. 4.8. The initial distribution is taken from the statistical records of the headmaster (class sizes and rooms, not taking into account absences).

The procedure for the exercise was as follows: After the alarm signal is triggered, staff (teachers guiding pupils) and pupils start immediately leaving the buildings via the nearest exits. A person was considered evacuated when she reached the outside, i.e., had left the building via its main exit. Route choice is determined/known beforehand according to the evacuation plan and exit signs; walking speed is rather high (2–7 m/s, running), pausing for orientation is negligible.

It has to be kept in mind that a single exercise does not provide statistical data. There is no "true evacuation time" but a distribution of times. The results presented here constitute at most three measurements (two repetitions). It would usually be desirable to carry out a series of measurements which is often not possible due to practical and time constraints.

The cameras were placed in building 1 in the top right corner of the room right next to the main exit on the ground floor (cf. fig. 4.8, right) and on the first floor at the door opposite to the staircase. This door was not used. In building 2 the camera was placed beneath the stair leading from the ground to the first floor. The camera filming the main exit of building 1 (from the inside) was fixed on a tripod placed on a table, i.e., its position above ground was about 2.20 m. All the other cameras were not mounted (hand-held), so their position was about 1.80 m above ground.

Therefore all the videotapes show the doors from the inside which has the disadvantage that counting might be complicated by obstruction (persons walking directly behind each other). On the other hand, the queues forming in front of the doors can be observed. It would be desirable to have both views (inside and outside the door). This was not possible in this case, due to the restricted number of cameras available.

The procedure allows to obtain data that covers some of the individual behavior. However, it is not as detailed as to allow direct observation of, e.g., the trajectories of all the persons.

The number of persons was reconstructed from the videotapes in the way that the sum for each building is in accordance with the total count. Those numbers are lower than those provided by the headmaster of the school for the class sizes. The number of persons in each room (class) was not counted at the day of the exercise. The participants were all children of the age 6 to 11 (first to fourth grade). Demographic data can be taken into account in the simulation by the parameter settings. One aim of this endeavor

Fig. 4.8. Layout of the school building. It is separated into two independent parts (building 1 and 2), building 1 having three, building 2 two floors. The numbers show the initial number of persons in the rooms according to the class sizes. The pupils gather on the playground just in front of each building.

was to determine (or at least get a feeling for) the appropriate parameter settings for such a special population.

In addition to the restrictions mentioned, some further limitations have to be pointed out:

- The population was special. However, this has the advantage that additional information about the parameters for such a population can be obtained.
- The population is naturally divided into groups (classes) lead by a teacher.
- There were no hazards present.
- Pupils knew the scenario and the procedure.
- Several runs were performed which might lead to learning or fatigue effects.

Table 4.6. Times obtained from the evacuation exercise.

Building 1		Building 2	
first run			
1st out	10 s	1st out	15 s
last from ground floor	37 s	last from 1st floor	35 s
1st from third floor	48 s	1st from 2nd floor	35 s
last out	77 s	last out	56 s
second run			
first out	4 s		
last from 1st floor	39 s		
first from 2nd floor	47 s		
last out	81 s		
third run			
first out	11 s		
last out	67 s		

Table 4.7. Simulated evacuation times (500 simulation runs).

Standard Parameters (Normal Population)	(160 ± 5.8)s
Adapted Parameters (Student Population)	(100 ± 4.0)s

- The cameras were visible and the whole procedure was videotaped. This might have distracted some of the pupils.

Therefore the results should be seen as representing an optimal case. This is the nature of such an evacuation drill. And this is reflected in the simulation, too.

Results of the Exercise and Comparison to Simulations

Figure 4.9 shows the number of persons having left the building vs. time (evacuation or egress curve $n(t)$) for building 1, fig. 4.10 for building 2. By taking the derivative of this curve, one can obtain the flow (resp. slope) vs. time. One can see that the flow is nearly constant except of the gap between the evacuees from the first and second floor. The evaluation was done for building 1 and 2 separately. The exercise was done twice for building 2 and three times for building 1. Due to the limited number of cameras, results for all runs are available only for building 1. The results are summarized in table 4.6

The evaluation is based on the videotapes. In order to check the validity of the counting procedure, it was repeated twice for building 2 (cf. fig. 4.10). It can be seen that there are only small deviations. These deviations are solely based on the counting, since the basis for the three counts is the same videotape.

For building 1, the drill was repeated twice, so there are three data sets altogether. Surprisingly, drill 2 proceeded slightly slower than drill 1. The gap at 40–50 s (fig. 4.9) is between the first and second class on the first floor (due to the different behavior of the teachers: one moving in front of and the other behind the class, cf. fig. 4.8 for the floor plan and table 4.6 for the times). The shorter time for drill 3 is mainly caused by the fact that then the teacher of the second class was also moving in front of the class, resulting in less congestion at the stair entry on the first floor, since the teacher moved slower than her class.

In contrast to the evacuation exercise, a simulation allows to do basically as many

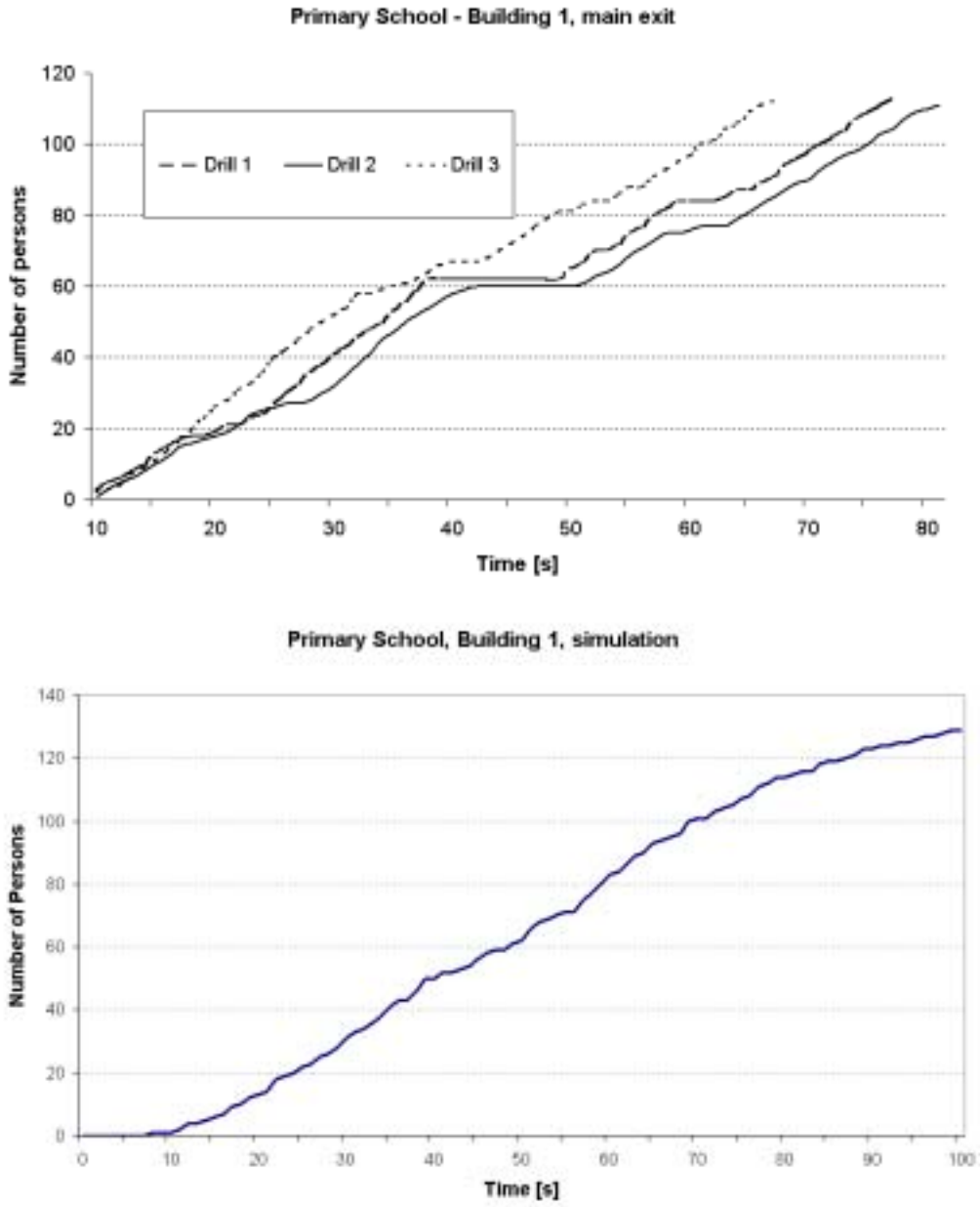

Fig. 4.9. Empirical and simulated egress curve (number of persons out vs. time) for building 1 (cf. fig. 4.8). Drill 1 to 3 are three different runs of the same scenario, with the same population and initial conditions. For an explanation of the differences, see text.

runs as one likes (cf. table 4.5). Then, the statistical properties of the distribution of egress times can be investigated. Since the egress time for the school was determined by building 1, the simulation was restricted to this building. Figure 4.11 shows the distribution of egress times for building 1.

Table 4.8. Parameter set used in the simulation (adapted parameters for pupils). The distributions are Gaussian with the tails cut off, i.e., parameter values lower than Min and larger than Max are rejected. Since the space is discrete (0.4 m ×0.4 m quadratic cells), and the time step is one second, speeds are always multiples of 0.4 m/s. Since orientation was optimal and also the young pupils did not hesitate while leaving the building, p_{dec} and p_{sway} were chosen very small.

Name	unit	Min	Max	Mean	StdDev	comment
Average Population						
Maximum Speed	m/s	1.2	2.0	1.2	0.4	$\Delta v_{\max} = 0.4\,\mathrm{m/s}$
Response time	s	0	10	5	2	
Deceleration	%	0	30	15	5	probability for stopping
Swaying	%	0	2	1	1	prob. for directional dev.
Adapted Parameters (Pupils)						
Speed	m/s	1.6	4.8	3.2	0.8	$\Delta v = 0.4$ m/s
Response time	s	0	10	5	2	
Deceleration	%	0	1	0	1	probability for stopping
Swaying	%	0	2	0	1	prob. for directional dev.

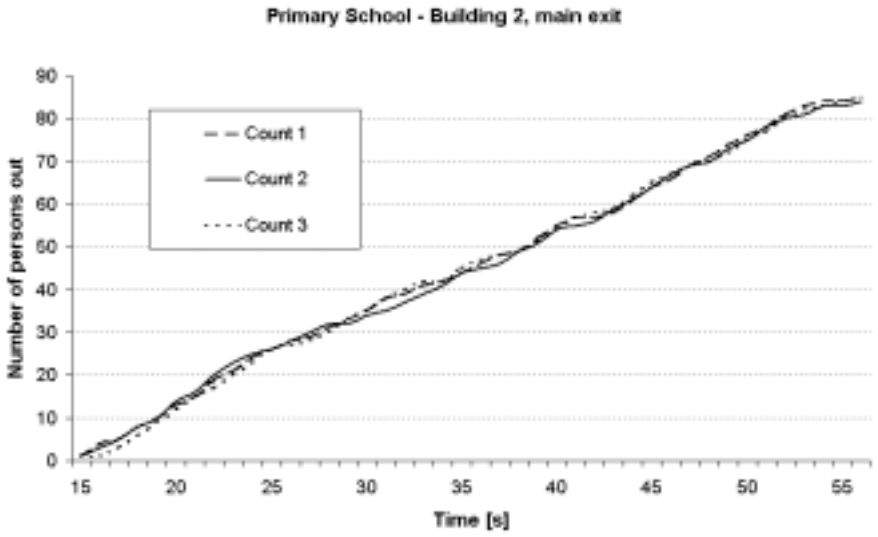

Fig. 4.10. Empirical evacuation curve: number of persons out vs. time for building 2 (cf. fig. 4.8). Count 1 to 3 are based on the same film. Therefore the deviations are due to counting errors (see text).

The population parameters in the simulation were chosen as shown in table 4.8. Using a parameter set derived from the capabilites for an average population, the simulation results deviated from the exercise. Therefore, the parameters were adapted and another simulation carried out. The parameter settings were based on the observations, e.g., the value for the parameter walking speed was derived from the time the first person left the building (see table 4.6 and figure 4.8).

The parameter values for a standard population led to an overall egress time too high by a factor of two (cf. table 4.6). Furthermore, walking speeds up to 5 m/s were observed

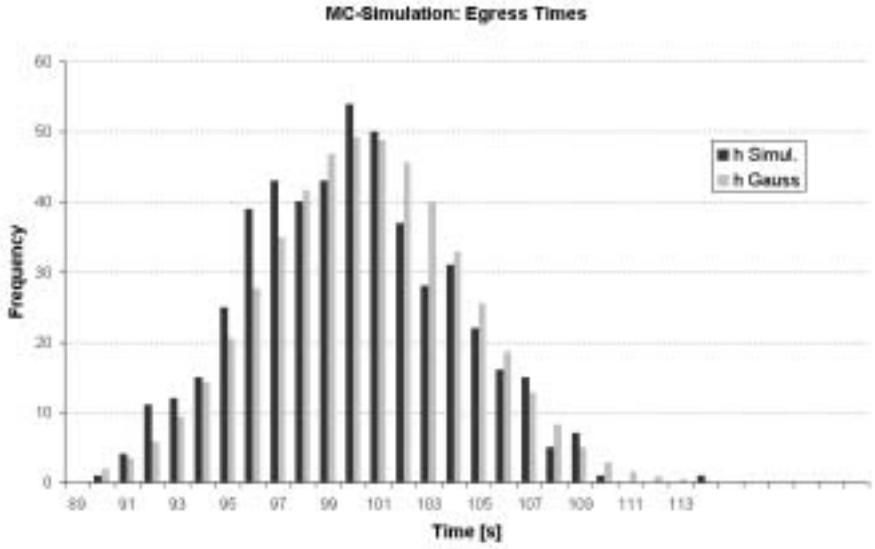

Fig. 4.11. Simulated egress times for building 1 (500 simulation runs). The parameters are shown in table 4.8 (adapted parameters for the student population).

during the exercise. Therefore, an adapted parameter set was used. The corresponding simulation results are shown in table 4.7 (for 500 simulation runs in each case).

Normal distributions were fitted to the distributions of egress times obtained by the simulations. In order to check the reliability of this approach, a χ^2-test was done [Kreyszig, 1999]. The results are shown in table 4.9. χ^2 is defined as follows:

$$\chi^2 = \sum_{j=1}^{n} \frac{(h_j - n \cdot p_j)^2}{n \cdot p_j}, \tag{4.9}$$

where h_j is the frequency in the simulation, n is the number of simulation runs, and p_j is the Gaussian probability for the occurrence, e.g., $p_j = \Phi(c_j) - \Phi(c_{j-1})$, where $\Phi(x)$ is the probability density and c_i is the class boundary for class i.

On the 5% significance level, the hypothesis that the distribution of the evacuation times is Gaussian cannot be rejected. This information is useful when interpreting the Monte Carlo results. Nevertheless, it probably depends on the scenario considered and especially the layout of the building, whether such an approach is useful. Furthermore, a 95% limit for the evacuation time (i.e., $P(t \geq t') \leq 0.05$) can be used without fitting a Gaussian distribution to the simulated times. Nevertheless, in the latter case, the information is restricted to the sample, whereas otherwise, the sample is used to extract information about the distribution of the evacuation times.[8]

The simulation run that corresponds to the median of the simulation times (cf. fig. 4.11) was evaluated in detail. Figure 4.9 shows the simulated evacuation curve. Another way of representing this data is by plotting the frequency of the individual egress times (cf. fig. 4.12). For an egress curve with constant slope, these times would be uniformly distributed between the minimum and the maximum value.

[8]The calculation of a standard deviation basically only makes sense if information about the type of the distribution is available, too.

Table 4.9. χ^2–Test for the simulation results for building 1.

Normal Parameters (Standard Population)		
k	32	number of classes
α	0,05	level of significance
1-α	0,95	level of certainty
χ^2	42.1	see eq. 4.9
$\chi^2_{32,0.05}$	46.2	quantile
$P(x^2 \geq \chi^2)$	0.11	error probability

Adapted Parameters (Student Population)		
k	26	number of classes
α	0,05	level of significance
1-α	0,95	level of certainty
χ^2	32.3	see eq. 4.9
$\chi^2_{26,0.05}$	38.9	quantile
$P(x^2 \geq \chi^2)$	0.18	error probability

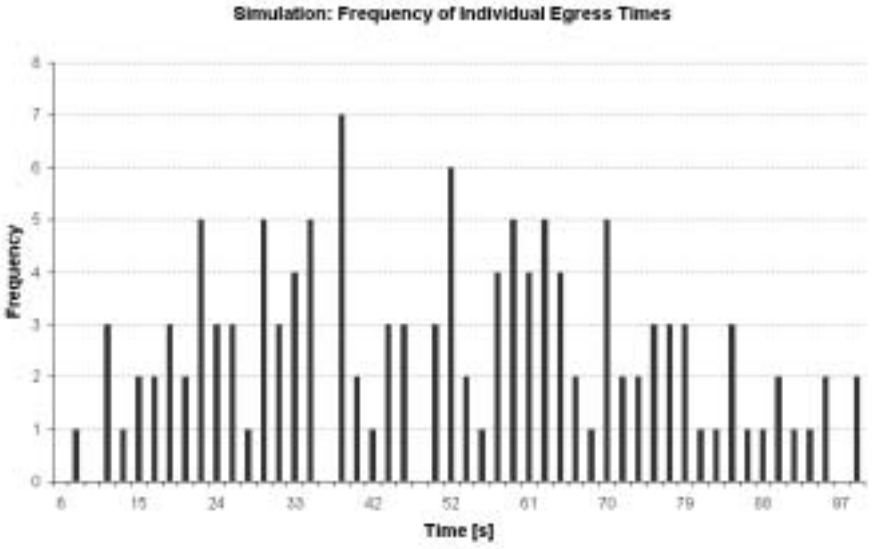

Fig. 4.12. Individual egress times obtained for the simulation.

The egress times do not provide information about congestion, which is useful for assessing (and improving) the layout. The values for q_r defined in eq. 4.2 are shown in fig. 4.13. Congestion occurred mainly on the stairs from the first to the ground floor and at the final door to the exit.

In summary, the agreement between the simulation and the exercise is sufficient when adapting the parameters to represent the high fitness, familiarity with the building, and effective egress behavior. A further decrease of the egress time in the simulation could be reached by an increase of the walking speeds. Decreasing the response times does not have any 'positive' effect, since the lower limit of the distribution is 0 anyway, and it is beneficial if not everyone starts immediately, which leads to increased congestion. Further increasing the walking speeds does not seem to be justified, however.

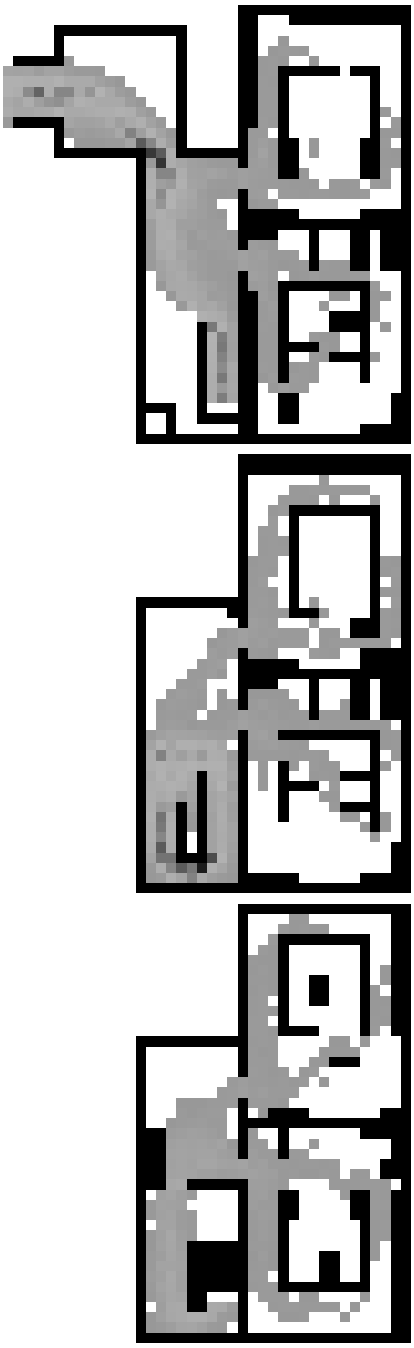

Fig. 4.13. Plot of the densities that occurred during the egress simulation for the primary school building 2 (cf. fig. 4.8). Dark areas are those of high densities. There are four shades of gray, from dark to light gray: $q_r > 5$ ($\rho > 4\mathrm{P/m^2}$ for at least 0.1 T, 0.25 T, 0.5 T, 0.75 T. For the identification of congestion see also section 5.3.2.

4.3.4 Aircraft Evacuation

For aircraft there is a regulation stating that they have to be evacuated in 90 s [Federal Aviation Administration, 1990]. The fulfillment of this requirement is usually demonstrated in full scale evacuation trials. Empirical data concerning these trials can be compared to simulation results. Empirical results are presented in [Galea et al., 1996] and compared to simulation results for various populations and scenarios. The simulations presented here are based on a population with walking speeds between 3 and 4 cells per second (i.e., 1.2 to 1.6 m/s), and zero response time (the other parameters are as in table 4.8, average population). The exit blockage, i.e., the time one person stays on the evacuation slide, was assumed to be 1s. There are four exits on each side. However, only one side was used in the simulation as can be seen in fig. 4.14. This is in accordance with the trial, where the same scenario (available exits) is assumed. The evacuation curve is shown in fig. 4.15. These simulations are intented as a further illustration of the application of the simulation. Most of all, only one scenario (concerning the population characteristics) was considered. Especially the influence of the crew was not explicitly simulated. The exit blocking time has of course a major influence on the overall evacuation time. There were four exits, each two cells wide (80 cm), available. If they are used as efficiently as possible, the lower limit for the overall time imposed by this factor is $\frac{444\,s}{8} \approx 56\,\mathrm{s}$.

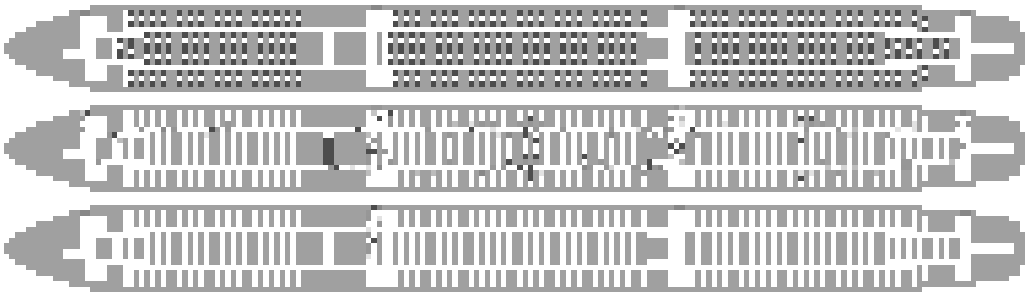

Fig. 4.14. Snapshots of the simulation for the evacuation of an A340 aircraft. The initial occupation is 444 persons. The times are $t = 0$ (top), $t = 60\,s$, and $t = 100\,s$ (bottom).

Nevertheless, as can bee seen from fig. 4.14 (bottom) and 4.15 there is space (in the simulation) for increasing the effectiveness by ensuring optimal route choice and orientation. The ideal curve would be a straight line. If the initial slope in fig. 4.15 is extrapolated, an overall time of 80 s is obtained. When comparing this to the 56 s on the slide, it becomes clear that the major constraint are the evacuation slides.

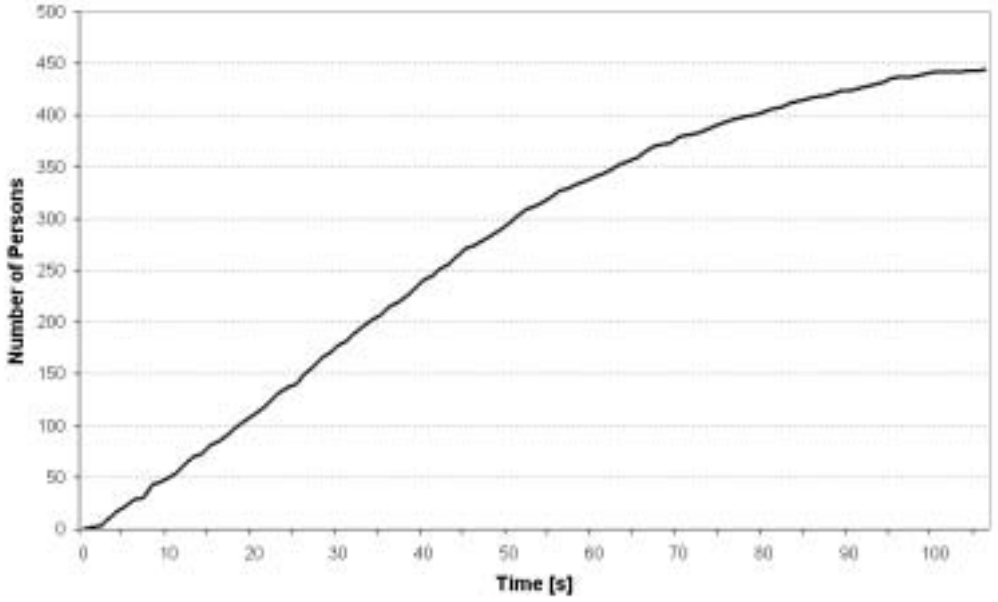

Fig. 4.15. Evacuation curve for an A340 aircraft (simulation, cf. fig. 4.14).

Chapter 5

Evacuation Analysis for Passenger Ships

Safety of ships is achieved by ensuring the dynamic stability of the ship even under difficult conditions and by avoiding hazards like fire or structural damages. Evacuation remains as the last measure. As will be argued in this chapter, ships are a case more complex than buildings or other passenger vessels with respect to evacuation. Evacuation simulations as presented in the previous chapter can nevertheless also be applied to ships. There are some additional influences that have to be taken into account, mainly ship motion and the procedure divided into assembly and embarkation phase.

Contents

5.1 Why the Case of a Ship is the Most Complex

This chapter presents a further area of application for the model presented in chapter 3. Similar to the previous chapter, where the simulation was mainly applied to the evacuation of buildings, the basic principles of the model remain the same and the special circumstances for the evacuation of ships are taken into account by introducing few additional parameters. In order to do that in a systematic way, the special influences in the case of ships are briefly summarized. Another important point is that the guidelines

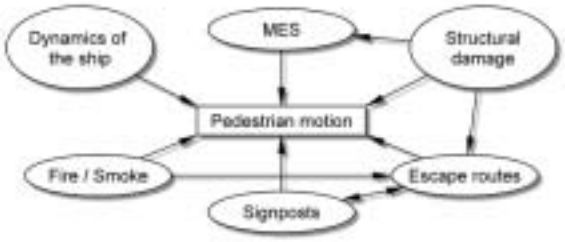

Fig. 5.1. The different influences on ship evacuation. MES is short for Marine Evacuation System.

for the safety of ships are based on international standards, which is a very special and beneficial situation.[1] Furthermore, just recently, guidelines have been developed (partially based on results presented here) that allow to perform the required evacuation analysis for passenger ships on the basis of computer simulations.

Compared to other passenger vessels, ships are the most complex case with respect to geometry, procedure, environment and hazards. The layout of aircraft is simpler than that of ships. And most buildings (except of maybe skyscrapers) are less complex than a large passenger ship. With respect to the procedure (assembly and embarkation phase), the environment (ships sail in very different environments), the ship motion, the technical equipment (life boats, inflatable slides and rafts, davits, free fall boats, etc.), and the complexity of the structure with many hallways and stairs and escape routes leading up- and downstairs.

Furthermore, the survivability of the ship [Chang, 1998] sets a strict upper limit for the available evacuation time. The different factors on the evacuation of ships are illustrated in fig. 5.1. However, the factors described either influence the movement ability of the evacuees (e.g., motion of the ship) or can be represented as a delay at the embarkation stations (time for preparing the evacuation system and time for getting into the life-boat or life-raft). Therefore, the general concept of the evacuation simulation based on the cellular automaton remains valid and can be extended to take into account the special factors by introducing a preparation time t_{prepare} and an embarkation time t^i_{embark}[2], the former leading to a blockage of the exit or embarkation cells for $t < t_{\text{prepare}}$ and the latter to a waiting time at the exit as long as it is occupied by the person i.

The complete chain of events leading to an evacuation and the search and rescue after the ship has been abandoned (fig. 5.2) are not part of the simulation. However, except of the first and the last element (Evacuation Need and SAR Recovery) all the others are present in the simulation.

5.2 The Procedure: Assembly and Evacuation Phase

In general, the evacuation procedure for passenger ships is comparable to buildings. There is one major difference, however: the separation into an assembly and embarkation phase. First, all passengers assemble at specific locations on-board the ship. Then groups are formed and the embarkation proceeds in groups. The assembly points are

[1] For buildings the standards even differ between states within the same country.

[2] This time is relevant mainly for High Speed Craft, which are evacuated via slides.

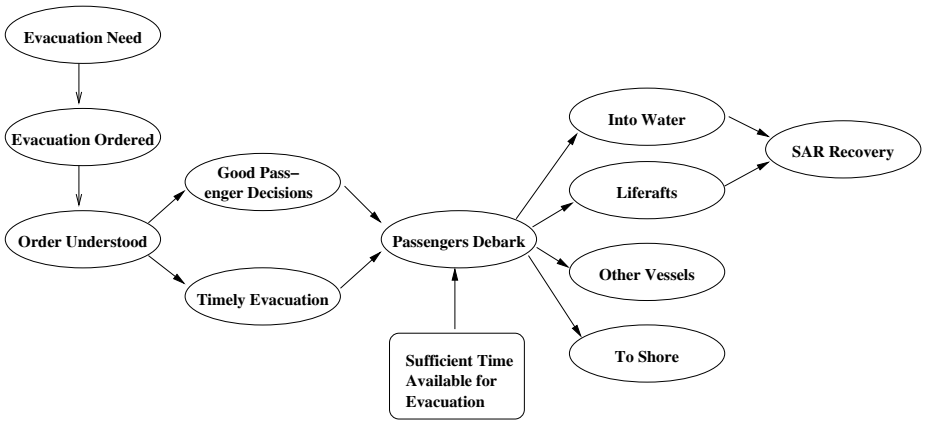

Fig. 5.2. Sequence of events in an evacuation (adapted from the US Coast Guard Evacuation Analysis Plan, see `www.uscg.mil/hq/g-m/nmc/evacuation/nfpapers.htm`).

usually public spaces. For the case of high speed passenger craft[3] the assembly stations might be the seating areas and therefore there is no separate assembly phase. The situation becomes completely different from buildings for cruise ships. The sequence of the evacuation in this case is outlined in fig. 5.3. In this case, the necessary model extensions would be quite extensive and are therefore not treated in detail here.

In order to specify the different phases (assembly and embarkation) in detail, and to be able make the connection to the terms used in the guidelines [IMO, 2002a] the following definitions are used:

1. Response time t^i_{response} is the time it takes a person to respond (processed the information and decide to start walking towards the assembly station, resp., for cruise-ships to the cabin). This resembles the fact that even if all persons are informed what to do, not all will start moving simultaneously.

2. Walking time t_i is the time it takes a passenger to get to the assembly station and is calculated (simulated) during the analysis for every passenger individually. It includes the response time t^i_{response}, which is basically an offset in t_i.

3. Preparation time t_{prepare} is the time it takes to make the life boat or life raft and slides ready for embarkation. After the time t_{prepare} the lifeboats or MES are ready for embarkation. This parameter is specific for the simulation of ship evacuation.

4. Embarkation time t^i_{embark} is the time it takes a single person to embark the life boat or life raft. The embarkation station (cell) is blocked by one person for the time t^i_{embark} during embarkation. This parameter is also only relevant for ships.

The analysis is restricted to the assembly and embarkation phase. It does therefore not consider the probability for an incident. These factors have to be put in from the outside. However, they play an important role. There might be even only a restricted number of scenarios of all those that actually occur, where evacuation simulation are

[3]High Speed Passenger Craft (HSC) do not have cabins and the arrangement of the seats is similar to aircraft.

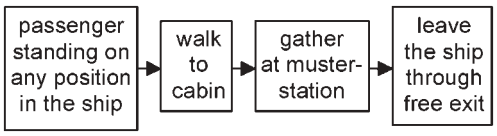

Fig. 5.3. Time sequence of an evacuation for the case of a cruise ship. Since the life-vests are usually stored in the cabins and the passengers might have to re-dress, they first have to go back to the cabin and then proceed towards the assembly stations.

useful. If a ship sinks rapidly or the alarm is not triggered, then this is outside the scope of an evacuation simulation.

5.3 Regulations Concerning the Safety of Ships

Progress in safety of passenger ships was often triggered by accidents. The most notorious examples are the "Titanic" which sank in 1912 and lead to the implementation of SOLAS (International Convention on the Safety of Life at Sea) and the "Estonia" [Björkman, 1999] which sank in 1994 and lead to SOLAS ammendments, the Stockholm Agreement and the implementation of a working group at the International Maritime Organization (IMO) concerned with evacuation analysis for Ro-Ro passenger ships.

> "At an international conference in Geneva in 1948, the Inter-Governmental Maritime Consultative Organization (IMCO) was founded. Its name was altered to the International Maritime Organization (IMO) in 1982.[4] The Organization is attached to the UN and functions as a forum for work on international rules for safety at sea.
>
> The Organization has developed a number of conventions designed to promote safety at sea and prevent pollution. A central set of rules is the International Convention for Safety of Life at Sea (SOLAS). The first SOLAS Convention was adopted in 1914, i.e., before the organization was founded. It was occasioned by the Titanic disaster. New versions of the Convention were adopted in 1929 and 1948. The first version issued under IMCO was adopted in 1960.
>
> The present SOLAS convention is from 1974. It entered into force on 25 May 1980. The Convention contains safety rules in the form of minimum standards binding under international law, which the ratifying States are obliged to incorporate in their national law."
> [SleipnerReport, 2000]

The documents concerning the evacuation procedure and analysis for ships are summarized in table 5.1.

The starting point were prescriptive rules specifying minimal door and stair widths [IMO, 2000a]. However, the prescriptive regulations focus on single aspects of the evacuation process and neglect the interaction between the various parts of the evacuation system. To get a more realistic description a comprehensive approach is desirable, which requires the analysis to be based on simulations.

[4]For more information concerning IMO, see www.imo.org.

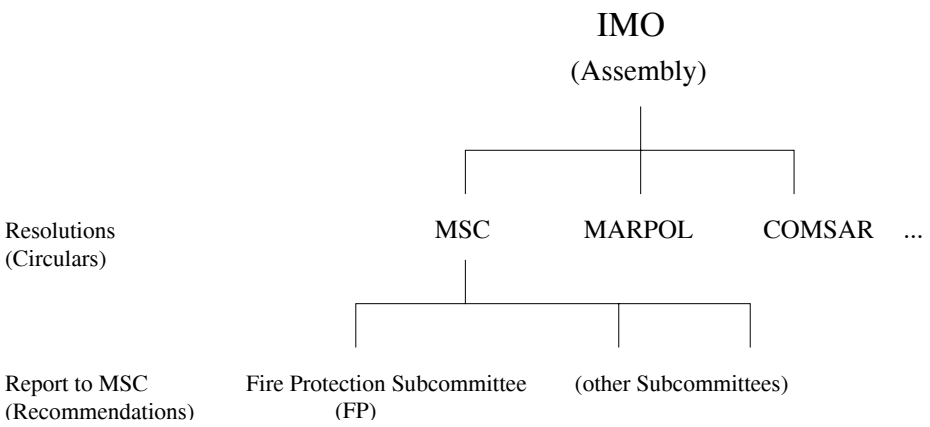

Fig. 5.4. The International Maritime Organization is a sub-organization of the UNO and responsible for the maritime sector. The Marine Safety Committee (MSC) develops guidelines for the safety of passenger ships, including evacuation analysis.

Table 5.1. Relevant IMO Documents concerning the safety of passenger ships with respect to evacuation. The main source is "Safety of Life at Sea" (SOLAS). The other documents contain interpretations or guidelines referring to it. HSC is short for High Speed Passenger Craft and Ro-Pax is short for Ro-Ro-passenger ships (roll on/roll off).

Document	Content	Reference
SOLAS	Ship Safety	[IMO, 2000c]
FSS Code	Fire Safety Systems	[IMO, 2000a][1]
HSC Code	High Speed Craft Safety	
MSC/Circ.909	Evacuation Analysis for Ro-Pax	[IMO, 1999][2]
MSC/Circ.1001	Evacuation Analysis for HSC	[IMO, 2001][3]
MSC/Circ.1033	Evacuation Analysis for Passenger Ships	[IMO, 2002a][4]

[1]Implementation of SOLAS II-2/28.1, contains regulations of Res. A 757(18)
[2]Replaced by MSC/Circ.1033
[3]Implementation of HSC-Code 4.8.2
[4]Implementation of SOLAS II-2/28-1.3

Recently, rules have been introduced that focus on the performance of the evacuation system and set an upper limit for the allowable evacuation time (cf. table 5.2). The first approach used to perform the respective analysis during the early stage of design was based on a hydraulic (macroscopic) model [IMO, 1999], where the egress routes are transformed into a system of pipes and vents (so called transition points).

Within the BYPASS project[5] we developed and analyzed alternative approaches towards such an evacuation analysis. These results contributed to extensions of the guidelines, which enable evacuation analysis based on computer simulations. They comprise a method for calculating the overall evacuation time and identifying congestions, as well as guidance on the validation of simulation models [IMO, 2002a].

The aims of an evacuation analysis according to the relevant guidelines are the

[5]`www.traffic.uni-duisburg.de/bypass`

Table 5.2. Limits that the evacuation time of a ship has to comply with in the analysis.

Type of ship	Limit	Reference	Comment
HSC	17 min	[IMO, 2000b]	full scale tests required
Ro-Pax	60 min	[IMO, 2000c]	
Cruise	60 min	[IMO, 2002a]	suggestion for less or equal to and
	80 min		for more than three main vertical zones

following [IMO, 2002a]:

1. Identify and eliminate, as far as practicable, congestion which may develop during an abandonment, due to the movement of passengers along escape routes,
2. provide hints for an effective employment of the crew, especially at critical points, and assure the efficient use of the available arrangements,
3. give insight into the role of the parts of the system and take into account the fact that events during an evacuation take place in parallel,
4. demonstrate that escape arrangements are sufficiently flexible to provide for the possibility that certain escape routes, assembly stations, embarkation stations or life-saving appliances and arrangements may be unavailable as a result of a casualty.

5.3.1 Calculation of the Evacuation Time

In the regulation [IMO, 2002a] the following equation is used to calculate the overall evacuation time:

$$T = t + \frac{2}{3}(E + L) + S, \tag{5.1}$$

with t being the assembly time and S a safety margin set to 10 minutes for the night case and 5 minutes for the day case.[6] This safety margin is intented to cover influences not otherwise quantified, like the dynamics of the ship. The next section 5.4 will review some of the concepts that have been proposed for taking ship motion into account directly via its influence on the walking speed. E is the total embarkation and L the launching time. $E + L$ can be assumed to be 30 minutes, if no other data is available. In this case, embarkation and launching are covered by $E + L$ and T_{prepare} and t_{embark} are not necessary. The requirement for the overall evacuation time is then

$$T \leq 60\,\text{min} \tag{5.2}$$

for Ro-Ro (roll on/roll off) passenger ships. This leads to the following condition concerning t:

$$t \leq 30\,\text{min}. \tag{5.3}$$

(E+L) takes into account the times for preparation and launching of the lifeboats. It is also possible to simulate this process by blocking the embarkation stations for a certain time t_{prepare}. The embarkation time t_{embark} is then usually assumed to be equal

[6] There are basically two standard cases that must be analyzed: day and night case. For both cases the initial distribution of passengers and crew is specified in [IMO, 2002a].

for everyone. T_{prepare} is the time it takes to prepare the lifeboats or marine evacuation system (MES).

t is obtained based on a Monte-Carlo simulation. The longest individual assembly time determines the overall assembly time for a single run:

$$t' = \max_i t_i. \tag{5.4}$$

This makes sense, since the analysis is intented mainly to assess the performance of the layout and the procedure and should show that all persons are able to leave the ship within the available time-span. t is then the time which is exceeded by at most 5% of the values of t'. This value is used for comparison with the performance standard in eq. 5.1.

The knowledge of the evacuation time T, resp. the individual times t_i is not sufficient to fulfill the requirements stated in the previous section concerning the evacuation analysis. Especially the identification of congestion requires information about the coordinates and duration of queues.

5.3.2 Identification of Congestion

According to IMO [2002a], the presence of congestion should be identified on the basis of the following criterion:

- the local density exceeds 4 persons per square meter ($\rho_{\text{local}} \geq 4\,\text{P/m}^2$) for at least 10% of the assembly time.

This situation is called a significant queue. The local density q_r defined in eq. 4.2 is tailored to check this condition. For $q_r \geq 6$ (i.e., $\rho_{\text{local}} \geq 6/9\,\rho_{\max} \approx 0.55 \times 6.25\,\text{P/m}^2 \approx 4.1\,\text{P/m}^2$ significant queues are identified at cell r. For further considerations concerning the evaluation of simulation results please refer to section 4.1.2.

The unavailability of a single embarkation station or any life-saving appliance and arrangement should be fully compensated by the capacity of the other embarkation stations or life-saving appliances and arrangements on the same embarkation deck. Unavailability of corridors, stairways, doors, etc. due to fire, smoke, or structural damage can be taken into account by performing a simulation where the floor plan is modified accordingly. The consequences of structural damage are therefore transformed into geometrical constraints. The unavailability of part of the escape route that is used by the person with the longest walking time to the assembly station should be simulated as well as of the embarkation station that is used by that person. Details can be found in the guidelines [IMO, 2002a]. This approach takes away the weakest element of the escape route system. It therefore does not consider the worst case which would be blocking the strongest element (i.e., the one with the highest capacity).

5.4 Ship Motion and Further Influences

It has already been mentioned that ship motion is not directly taken into account when performing an evacuation analysis according to the relevant guidelines. This is mainly due to the fact, that there are only few results available on the influence of ship motion on the walking speed. Two approaches will be reviewed in the following subsection. Furthermore, the remaining extensions that are necessary to complete the model in the sense of covering all relevant aspects for evacuation simulation on ships (cf. figs. 5.3 and 5.1) are addressed.

5.4.1 Dynamics of the Ship

In the following, the quantitative results on speed reduction due to ship motion will be briefly reviewed. The influence of ship motion is usually included via a reduction factor, i.e., the walking speed is reduced in the simulation. It is given as a function of the angle of the roll motion Θ by Vassalos et al. [2001].

$$f(\Theta) = \begin{cases} \frac{e^{1-\|\Theta\|/\Theta_{\max}}-1}{e-1} & 0 \le \Theta \le \Theta_{\max}, \\ 0 & \Theta > \Theta_{\max}. \end{cases} \tag{5.5}$$

$\Theta_{\max}$ is the amplitude of the roll motion. The graph of this function is plotted in fig. 5.5 with $\Theta_{\max} = 20°$. This parameter is fixed for this type of speed reduction, since $f(\Theta_{\max}) \equiv 0$.

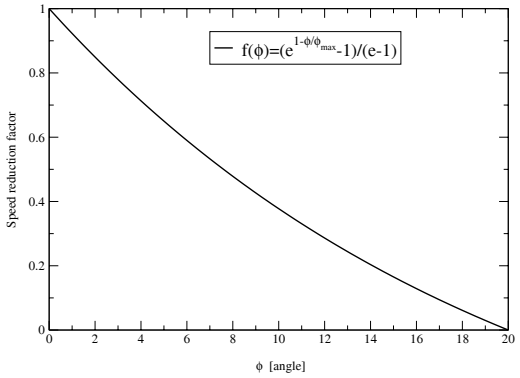

Fig. 5.5. Reduction factor for roll motion. The maximal amplitude $\Theta_{\max}$ is 20°. The analytic expression for the speed reduction factor is shown in eq. 5.5. Another result concerning speed reduction due to list or roll motion is shown in fig. 5.6.

Brumley and Koss [1998, 2000b] investigated the influence of the ship's motion with respect to three separate aspects: route choice, motor ability, and influence on overall evacuation time. Four scenarios were used in this investigation: harbor, bay, overseas ferry, and cruise ship.

It is assumed that the influence of static list and motion of the ship can be represented by a speed reduction factor (it is called egress reduction factor there):

$$r_v = c_1 \cdot \frac{M_1}{M_2} + c_2, \tag{5.6}$$

where $M_1 = f(m, h, A, g, \phi, \omega)$ is the environmental moment, $M_2 = f(h, F_r)$ the resisting moment of the pedestrian, h the height of the center of gravity of the person, F_r the measured individual resisting force, m the mass of the person, ϕ the mean list, A the amplitude of roll motion, ω the frequency of roll motion, and c_1, c_2 are regression parameters.

Using $M_1 = m \cdot g \cdot h \cdot \sin(A \cdot \sin\omega + \phi)$ this leads to the following equations for the

speed reduction factors ($\Theta = A \cdot \sin\omega + \phi$):

$$r_v = \begin{cases} 1 & \text{for} \quad M_1 \leq M_2 \quad (\theta \leq 15^\circ)\,, \\ 1 - 0.25\,(\frac{M_1}{M_2} - 1) & \text{for} \quad M_2 \leq M_1 \leq 2\,M_2\,, \\ 0.25 & \text{for} \quad M_2 > M_1\,, \\ 0 & \text{for} \quad \Theta > 35^\circ\,. \end{cases} \tag{5.7}$$

These results were obtained by linear regression, where the correlation coefficient is

$$\rho_{\frac{M_1}{M_2} r_v} = 0.91^2,\ \rho_{xy} = \frac{\overline{(x - \overline{x})(y - \overline{y})}}{\sqrt{\overline{x - \overline{x}} \cdot \overline{y - \overline{y}}}}. \tag{5.8}$$

At 25° list the persons were found to frequently pause momentarily. Above 35° the persons were not able to make forward progress without the use of hand-rails. A graphical representation is given in figure 5.6.

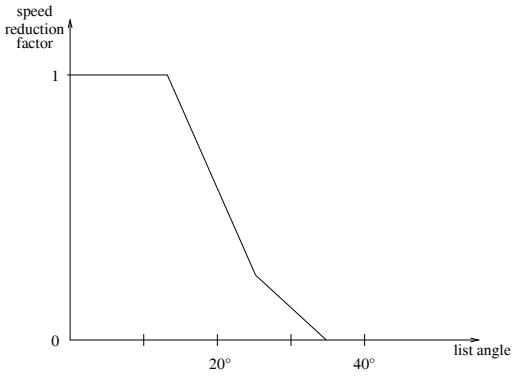

Fig. 5.6. Relation between the roll/list angle and the speed expressed via a speed reduction factor $r_v(\Theta)$ (cf. eq. 5.7).

Bles et al. [2001] have investigated the influence of an inclined floor on the motor ability. One of the major findings is that the visual vertical line is equally important for keeping the balance as the actual inclination. There is currently research going on in Canada with another cabin section simulator (SHEBA) that will provide additional results on the influence of the motor ability in a non steady environment.

5.4.2 Familiarity with the Ship

There is one factor remaining to complete the investigation of the potential influences on the evacuation performance, namely familiarity with the procedure and layout. This is of course not only relevant for ship evacuation but also for buildings. However, in the case of ships the quantification of this influence is complicated by the different types of ships and the environments they sail in. High Speed Craft on the one hand have a simple layout and the distances are short, cruise ships on the other hand a very complex layout, an elaborate evacuation procedure (cf. fig. 5.3), and the trips are usually a few weeks.

This of course has an impact on the familiarity with the ship and therefore the behavior in an emergency situation. The classification into different types of ships and environments was done using a so called media and experience factor by Brumley and

Koss [2000a]. The influence is represented by a probability for choosing the correct assembly station taking into account the familiarity with the surroundings and procedures:

$$f_{\mathrm{m+e}} = 0.85\sqrt{L^2 + A^2 + N^2} + 0.15\,T, \tag{5.9}$$

with the ratios of passengers who have looked at the layout, listened to announcements and drills, looked at notices and pamphlets, and having previous experience being L, A, N, and T. The factors 0.85 and 0.15 are parameters of the fit to the empirical data. This relationship can of course only be used if the knowledge about the experience of the passengers is available. Nevertheless, it provides a starting point for transferring this experience into a qualitative statement. Since this probability of choosing the correct assembly station cannot directly be represented by the parameters available in the model, the media and experience factor would have to be transformed into a reduction of walking speed or increased p_{dec} or p_{sway}. Nevertheless, for an extension that uses the representation of the layout as a graph (cf. section 3.7.3), such a factor could be introduced as an additional parameter.

This would also take into account the comprehensibility of the exit signs and related topics. Boer [2000] has investigated the sequence of mustering and evacuation phases for ship evacuation with respect to signs and devices like low location lighting and their perception. This study concludes that dynamic low location lighting[7] is hard to understand. It also quantifies the frequency of orientation problems that occurred in a mockup of a cabin section. Low location lighting (LLL) is intended to provide orientation and guidance towards the exit if the visibility is restricted due to smoke or the smoke filled zone is large and crawling is necessary to be able to move. It has first been used in aircraft but become mandatory for ships, too. It has also been investigated in the previous study [Boer, 2000], if dynamic route guidance is possible. However, the result was that it mainly caused confusion.

Furthermore, systems for route guidance based on sound have been developed [Withington, 2002] which are at the moment still tested. So called 'directional sound' uses sounders placed above exit signs and guiding the persons to the exit even if visibility is severely restricted (cf. fig. 5.7).[8]

For the simulations we performed for ships and that will be presented in the remaining sections of this chapter, the influences and results just described were not considered. One problem that arises – like for other deviations from the intended evacuation procedure – is that choosing the wrong path might produce infinite egress times. In reality, this will either be prevented by the crew which assists the evacuees and searches for lost persons or it will lead to persons loosing their lifes. Since a modification of the layout does not change this situation, it is more helpful to ensure that the requirements are met and using the simulation to determine the influence of the layout. This is also in accordance with the spirit underlying the guidelines for evacuation analysis issued by IMO. Additionally, taking into account these possibilities (wrong decisions, route-choice failure) in the simulation would require to also include the counter measures taken in reality. This exceeds the scope of the model presented here. To simulate fire-fighters checking whether certain cabin sections are empty and taking persons to a safe place will require an 'Artificial Intelligence' approach.

[7] Low location lighting is usually fixed. However, dynamic low location lighting is adapted to the situation and intented to provide dynamic route-guidance (like variable message signs).

[8] At IMO the equivalence of directional sound and low location lighting is currently discussed [IMO, 2002b].

Fig. 5.7. Directional sound is based on sounders (right) that are integrated in the exit signs and allow sort of an intuitive orientation based on sound beacons.

5.4.3 Counterflow

What has not been considered up to now is the influence of the crew (apart from the general remarks at the end of the previous section[9]). On the one hand, it assists the passengers in finding their ways. On the other hand, counterflow occurs as can be seen from fig. 5.8. Counterflow is also common in the evacuation of cruise-ships, where the passengers first return to their cabins to gather their life-vests (cf. 5.3). Assigning different groups of persons (e.g., passengers and crew) to different orientation potentials can be used to represent this situation in the simulation. This is only possible in an extended and more complex version of the model [TraffGo GmbH, 2002].

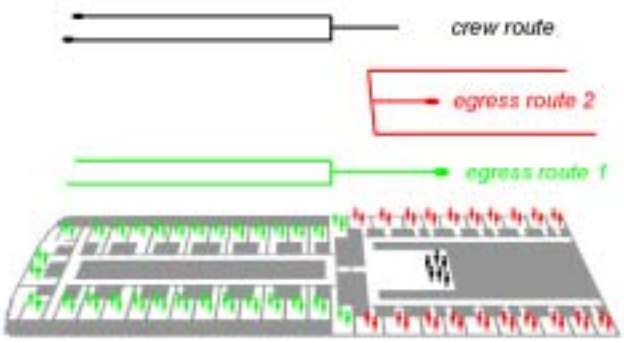

Fig. 5.8. Crew and passengers might have different routes which leads to counterflow. Additionally, if the life-vests are not stored at the assembly stations, which is usually the case for passenger ships other than Ro-Ro passenger ships, the persons first have to go back to the cabins. This also produces counterflow. (Graphics courtesy of TraffGo GmbH [2002])

[9] Fire fighters on a ship are members of the crew specially trained for that task.

5.5 Results from Full Scale Tests and Simulations

What has been presented in this chapter up to now were the special rules that apply for the evacuation of passenger ships (mainly the procedure and external influences like ship motion) and the corresponding regulations for an evacuation analysis. In analogy to the previous chapter on building evacuation, we have performed simulations for various types of ships and compared them to empirical data. The data does in this case not stem from exercises we carried out ourselves, but was provided mainly by the See-Berufsgenossenschaft. Where such data is not available and quantitative validation is not possible, at least the plausibility of the results can be checked.

Table 5.3. Reports containing detailed data about drills and accidents. An overview over cruise ship evacuations can be found in [de Vries, 1998].

Name	Type	Ref.
Stena Invicta	Ro-Pax	[Marine Safety Agency, 1997]
MS Sleipner	HSC	[SleipnerReport, 2000]
Scandinavian Sea	Cruise ship	[Harbst and Madsen, 1996]

There are two major categories of data concerning evacuations: drills or exercises and actual emergency evacuations. Using data from accidents for model development or calibration is usually not possible. However, they are useful for judging the restrictions and limitations of simulations. In each incident usually one major influence can be identified which leads to the emergency situation. This is important when considering the limitations of an evacuation simulation. It does not quantify the probability and severity of an accident.

Table 5.4. Results for the evacuation time of different passenger ships obtained by calculation according to the simplified evacuation analysis [IMO, 2002a], simulations, and actual evacuation tests. A double apostrophe denotes minutes, a single seconds. The time T_{calc} contains a safety factor of 2.3 [IMO, 2002a]. The time of the simulation T_{sim} has to be increased by the safety margin of 10 minutes (cf. eq. 5.1) to be comparable to T_{calc} (the night case was considered in the analyses) except of the case of HSC. The drills were done once, i.e., not repeatedly. The time for the simulation is the mean value for 500 runs. Manual calculations using the hydraulic model were not performed in all cases. Since the method is deterministic, the result of the calculation is a single time.

Type	pass.	crew	T_{test}	T_{sim}	T_{calc}	scenario	limit
Ro-Pax (section 5.5.2)	1482	118	-	9”11’	22”28’	assembly	30”
Ro-Pax “Stena Invicta”	723	119	65”	-	-	complete	60”
HSC “Cat No 1” (sec. 5.1.1.1)	100	-	12”57’	13”27’	-	complete	17”
HSC “Polarstern” (sec. 5.1.1.2)	400	8	11”26’	11”15’	-	complete	17”
HSC (detailed results omitted)	171	4	17”02’	15”20’	11”35’	complete	17”
Cruise-ship (detailed results omitted)	650	210	-	9’44”	18”56’	assembly	30”

This must be put into the simulation as an initial condition. This is similar to psychological and social influences mentioned before like the familiarity with the vessel. Some of the more extensive and detailed sources for data about drills and accident records are summarized in table 5.3.

It is clear from the arguments considered in the previous paragraphs that empirical data are important for quantitative validation. In table 5.4 results from calculations based on a simplified method of analysis [IMO, 2002a] and simulations we carried out for different kinds of ships, new-buildings as well as ships that are already in use, are presented. Where results of evacuation tests were available[10] they have been compared to the simulation results (see table 5.4). Since tests are mandatory for new High-Speed-Craft there is more data available for this type of ship than for Ro-Ro-ferries and cruise ships. An additional overview for data on cruise ship evacuation (causes and results of accidents concerning fatalities, etc.) is given by de Vries [1998].

5.5.1 Evacuation Trials and Comparison to Simulation Results for High Speed Passenger Craft

The case of high speed craft (HSC) is different from other passenger ships. This is mainly due to their higher speed, resulting in different construction and the short travel distance leading to a seating configuration similar to aircraft. This poses special problems with respect to safety to the designer and operator [Grossi and Farinetti, 1999, SleipnerReport, 2000].

High Speed Passenger Craft are similar to aircraft concerning the layout and the evacuation procedure. The marine evacuation system (MES) usually consists of inflatable chutes and life-rafts, i.e., there are no life-boats. For HSC evacuation trials are mandatory. They are – due to financial and practical constraints – not always carried out with the full load of the ship, which can be up to 1000 persons. In the following, results from such evacuation exercises provided by the See-Berufsgenossenschaft[11] are compared to simulation results. There are no cabins and the passengers are seated in open public spaces. These are usually also the assembly points and the number of crew is small (around 10).

5.5.1.1 Cat No 1

In the following, results for an evacuation trial on the High Speed Craft "Cat No 1" are used for comparison with and validation of simulation results. The evacuation exercise was carried out with 100 persons that were distributed over two decks on the starboard side of the ship (cf. fig. 5.9). Therefore, we performed the simulation also with a restricted number of persons and not with the full load of the craft. The parameters that were used were the following: $v_{\max} = 2 \ldots 5$, $t_{\text{response}} = 0 \ldots 10\,\text{s}$, $p_{\text{dec}} = 0 \ldots 0.3$, $p_{\text{sway}} = 0 \ldots 0.02$ (equally distributed). These parameters correspond to a standard population. The embarkation time was set to 4 s/P, since the time for the embarkation of 50 persons was specified with 3 minutes by the manufacturer. Additionally, the preparation time was set to 5 minutes (300 s).

As can be seen from table 5.5 the simulation results agree well with the exercise. However, when analyzing the evacuation curve shown in fig. 5.10, the embarkation stations can be identified as being the bottleneck. The embarkation time t_{embark} is 4 s per

[10] comprising a detailed plan of the general arrangement, a description of the initial distribution of persons, and the procedure

[11] The See-Berufsgenossenschaft is responsible for enforcing the safety standards in Germany.

Table 5.5. Data for the evacuation of the High Speed Craft "Cat No 1" with standard parameters. The higher value for the 1st person out in the test probably results from the different procedure: in the simulation, the persons start moving to the embarkation station as soon as they have reacted to the alarm, whereas in the trial, the persons probably wait until the embarkation stations are ready. Otherwise, there would not be such a large time for the first person in the raft (in the trial).

	Exercise	Simulation
Persons	100	100
Runs	1	500
Time	777 s	807 s
Min		796 s
Max		825 s
1st person	338 s	301 s
50th person	485 s	543 s

Table 5.6. Overall times for the evacuation of the High Speed Craft "Cat No 1" with standard parameters ($T_{\text{prepare}} = 4\,\text{min}$ and $t_{\text{embark}} = 4\,\text{s}$) and $t_{\text{prepare}} = 4\,\text{min}$, $t_{\text{embark}} = 3\,\text{s/P}$. For the second case, the distribution of the evacuation times was not analyzed.

Case	Mean	Min	Max
Standard parameters	807 s	796 s	825 s
$t_{\text{embark}} = 3\,\text{s/P}$	686 s		

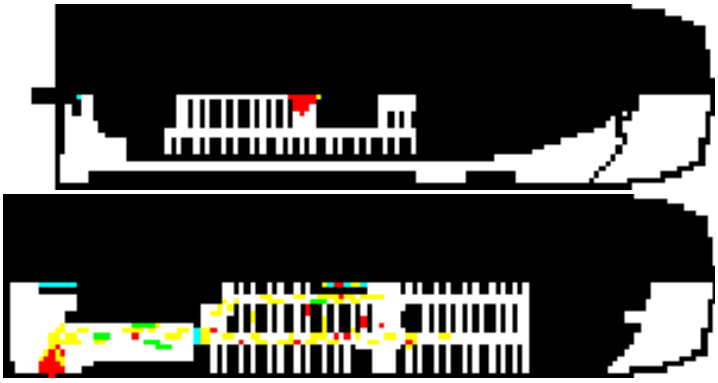

Fig. 5.9. Layout of the High Speed Craft "Cat No 1". This shows a snapshot after 80 s for a simulation with $t_{\text{embark}} = T_{\text{prepare}} = 0$. The colors are according to the walking speed (the darker, the slower). For the exercise only half of the craft was used to save costs. Therefore, in addition to the walls, also half of the craft is black.

person and the overall evacuation time is basically the sum of the preparation time and the sum of the individual embarkation times:

$$T = T_{\text{prepare}} + n \cdot t_{\text{embark}} \,. \tag{5.10}$$

This fact is due to the special conditions of the exercise: there was only one embarkation station on the lower deck (since only one half of the craft was used) as can be seen in fig. 5.9. We performed an analysis for another HSC with full load, where this distinct feature is not present since then there are four embarkation stations available.

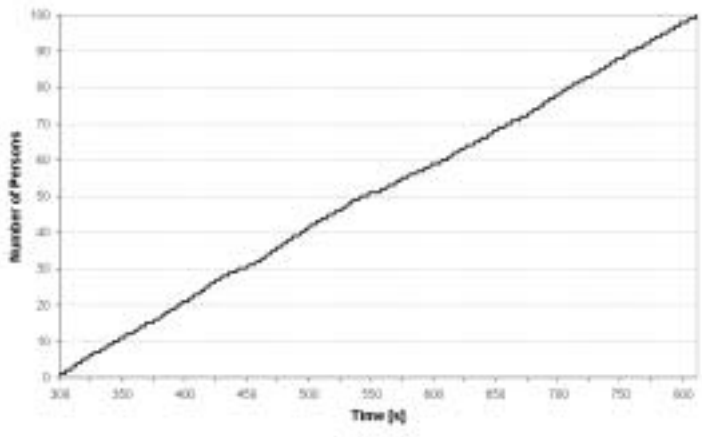

Fig. 5.10. Simulated evacuation curve for the High Speed Craft "Cat No 1". The preparation time was 300 s and the individual embarkation time 4 s per person.

5.5.1.2 Polarstern

Knowing the results of an evacuation trial and performing a simulation afterwards is – at least from the external point of view – different from predicting the results of an exercise. In order to do this we carried out simulations for a vessel where data about an exercise with 408 persons was provided by the See-Berufsgenossenschaft comprising the population characteristics, layout, procedure, and configuration of the MES, but not the results of the exercise. Therefore, the evacuation time was predicted by the simulation and afterwards compared to the exercise. The parameters that were used were the following: $v_{\max} = 2 \ldots 5$, $t_{\text{response}} = 0 \ldots 10\,\text{s}$, $p_{\text{dec}} = 0 \ldots 0.3$, $p_{\text{sway}} = 0 \ldots 0.02$. These parameters correspond to a standard population. The preparation time (the time it takes to make the life-rafts and slides ready) was set to 4 min (240 s), i.e., for $t \leq 4\,\text{min}$ the embarkation stations are blocked and therefore the persons have to wait in front of them. This value was measured during the exercise.

Another important parameter is the time for the embarkation of one person. In this case this time is usually not directly measured, but the times for, e.g., 50 persons are specified by the manufacturer of the life rafts (e.g., 2.5 minutes). Therefore, the time per person was set $t_{\text{embark}} = 3\,\text{s/P}$ in this case[12]. The agreement between the outcome of the trial and the simulation results is again close (686 s vs. 675 s for the mean value of the simulated times). The results are summarized in table 5.7.

[12] Only integer values can be used, since Δt is 1 s.

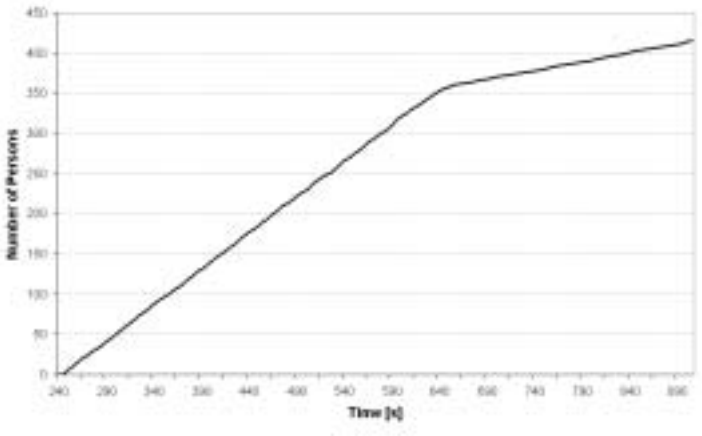

Fig. 5.11. Simulated evacuation curves for the High Speed Craft "Polarstern". The preparation time was 4 min and the individual embarkation time 4 s. The curve shows the case with the maximum time.

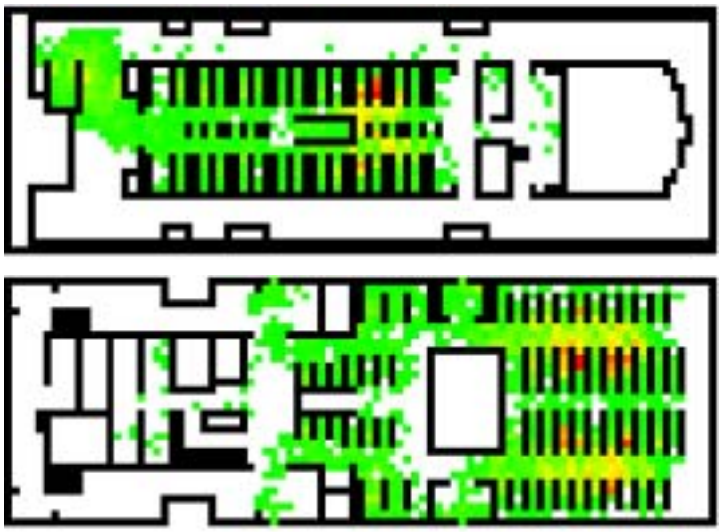

Fig. 5.12. Density Plots for the High Speed Craft "Polarstern". These density plots can be used to identify congestion. There are altogether four embarkation stations on the lower deck. This plot is for $t_{\text{embark}} = T_{\text{prepare}} = 0$ (i.e., embarkation stations are like 'exit doors'). Therefore, there occurs no congestion at the embarkation stations. The overall egress time was 150 s (single run). (cf. fig. 4.13)

Table 5.7. Data for the evacuation of the High Speed Craft "Polarstern" with standard parameters ($v_{\max} = 2 \ldots 5$, $t_{\text{response}} = 0 \ldots 10\,\text{s}$, $p_{\text{dec}} = 0 \ldots 0.3$, $p_{\text{sway}} = 0 \ldots 0.02$) and $t_{\text{prepare}} = 4\,\text{min}$, $t_{\text{embark}} = 3\,\text{s/P}$) and comparison to the outcome of a trial (left part). The right part shows the simulation results for different values of the parameters, i.e., only the one respective parameter is changed, all the others remain the same.

	Exercise	Simulation	Case	Mean	Min	Max
Persons	408	408	Standard parameters	675 s	643 s	758 s
Runs	1	500	$p_{\text{dec}} = 0 \ldots 0.6$	744 s	681 s	830 s
Time	686 s	675 s	$t_{\text{response}} = 0 \ldots 45\,\text{s}$	688 s	639 s	763 s
Min		643 s	$t_{\text{embark}} = 4\,\text{s/P}$	824 s	763 s	904 s
Max		758 s	$t_{\text{embark}} = 2\,\text{s/P}$	571 s	532 s	613 s

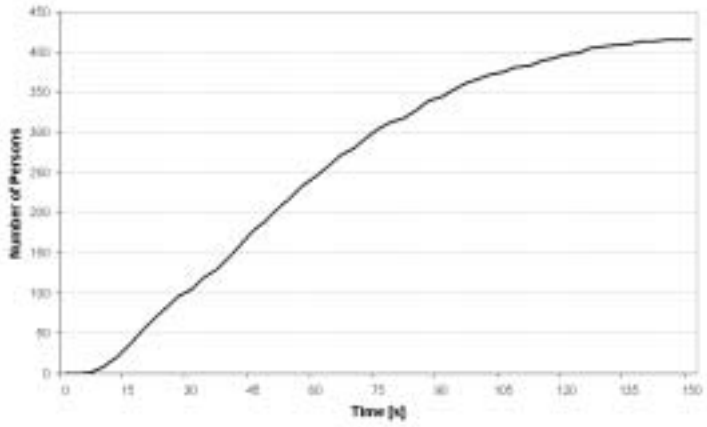

Fig. 5.13. Evacuation curve for the High Speed Craft "Polarstern". There was no preparation time and no embarkation time assumed ($T_{\text{prepare}} = t_{\text{embark}} = 0$).

For an increased response time $t_{\text{response}} = 0 \ldots 45\,\text{s}$, the overall time was 688 s, for an increased $p_{\text{dec}} = 0 \ldots 0.6$ it was 744 s (mean values). Decreasing the embarkation time ($t_{\text{embark}} = 2\,\text{s/P}$) leads to $T = 571\,\text{s}$, increasing it ($t_{\text{embark}} = 4\,\text{s/P}$) to $T = 824\,\text{s}$. This shows that the major influence on the overall egress time is again the embarkation phase, which is a typical (and comprehensible) result for HSC. This statement is also supported by comparing the results for different t_{embark}. The increase by 1 s leads to an increase of the overall time by 149 s, i.e., it is mainly due to the increased t_{embark}. Since there were altogether 4 embarkation stations and different numbers of persons used each embarkation station (see the discussion of the evacuation curve below) the increase in the total time must be larger than $102 \cdot \Delta t_{\text{embark}} = 102\,\text{s}$.

The case with the longer preparation and embarkation times does lead to queues in front of the embarkation stations persisting for a longer time and an evacuation process determined by the embarkation phase. This leads to an evacuation curve with a constant slope $\frac{\partial}{\partial t} n(t) = j(t) \sim t_{\text{embark}} \cdot N$ (cf. fig. 5.11). There is an interesting feature, however, which is the kink at $t \approx 640\,\text{s}$. This means that the flow jumps to a lower value. This is caused by the aft embarkation stations being 'empty' while persons are still embarking at the fore ones.

This interpretation is supported by fig. 5.12 which shows the densities defined in

eq. 4.2 integrated over time. The darker the color, the higher is the cumulative density q_r for cell r. As expected, there are no significant queues on the hallways or the stairs. The bottleneck for the evacuation of HSC are the embarkation stations.

Therefore, in fig. 5.13, the evacuation curve is shown for the preparation and embarkation time set to 0. To identify bottlenecks, it might be preferable, to do a simulation with $t_{\text{prepare}} = t_{\text{embark}} = 0$. The embarkation starts nearly immediately and the egress rate (flow) is nearly constant in the beginning. However, at higher times, the flow (which is given by the slope of the evacuation curve) decreases. This shows that the slower persons determine the overall time if there is no delay in embarkation. However, for the case of $t_{\text{embark}} = 3\,\text{s/P}$ and $t_{\text{prepare}} = 4\,\text{min}$, this influence vanishes.

5.5.2 Evacuation of Ro-Ro passenger ships and large passenger ships

Ro-Ro passenger ferries carry cars and trucks as well as passengers. Their layout is therefore more complex than for HSC and the procedure is separated into an assembly and embarkation phase. The life vests are stored at the assembly stations. The embarkation is mostly into life-boats and t_{embark} as well as T_{prepare} are harder to quantify since data from full scale trials is scarce. Furthermore, there is an overall time limit of 60 minutes, which reflects the more complex evacuation procedure. However, the time for embarkation and launching can be assumed to be 30 minutes according to the relevant regulations. Therefore, the following example is restricted to the assembly process.

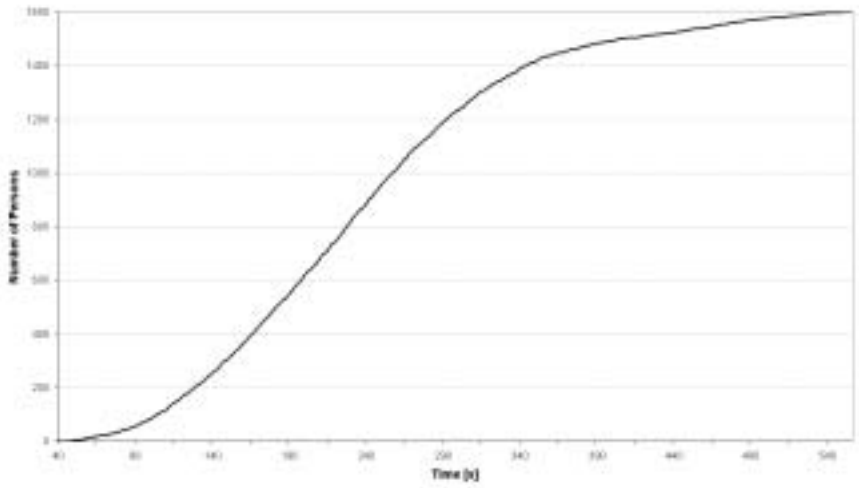

Fig. 5.14. Simulation of the Assembly Process on a Ro-Ro passenger vessel: Evacuation Curve.

The layout of the vessel is shown in fig. 5.15. Four of the eight decks are Ro-Ro decks. The assembly stations are located on deck 5 and 7 (the decks are numbered from bottom up). The example is intented to show typical results for an evacuation simulation of Ro-Ro passenger ships. Since the performance of an evacuation analysis becomes rather lengthy for such types of ships and the outcome of the evacuation depends on the geometrical details, this case does not allow to draw many conclusions regarding the model characteristics.

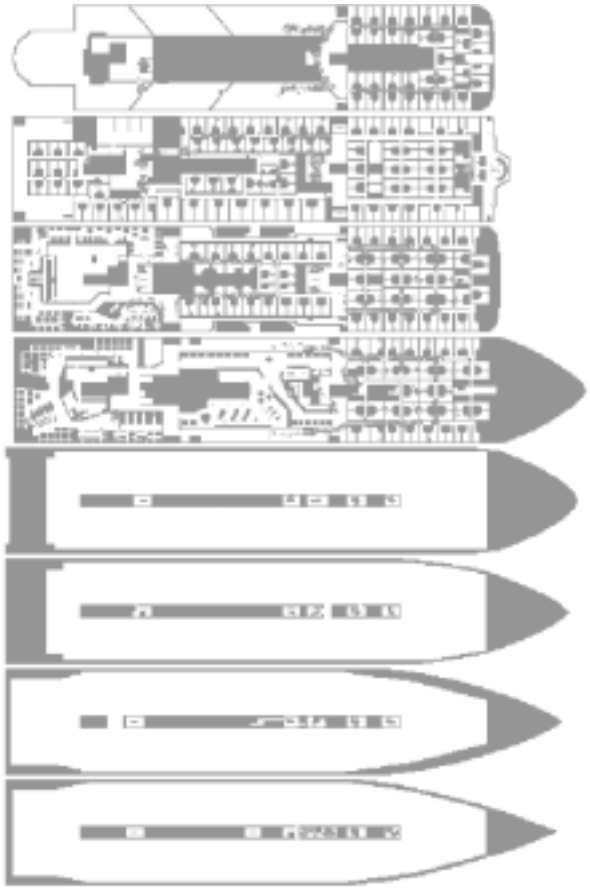

Fig. 5.15. Layout of the Ro-Ro passenger vessel. The evacuation curve is shown in fig. 5.14. Four of the eight decks are Ro-Ro decks. It can be seen that it is possible to do a rather complex layout with the CA approach in a straightforward manner. There are no extra assumptions or features necessary when scaling up from a simple geometry.

The total number of persons on-board is 1600. The vessel has not yet been built and the plans stem from the design stage. The parameters used are the standards ones also used in the previous section (cf. section 5.5.1.2). There is no preparation or embarkation time, since only the assembly phase is simulated. The reaction times $t_{\text{response}} \in [0, 10]\,\text{s}$ are based on the assumption that all persons process the information (alarm) immediately. These values were chosen since a comparison with the alternative hydraulic (macroscopic) calculation method was intented and an awareness time of 10 minutes is used in this method. To compare the results this awareness time has to be used in the simulation, too, which therefore requires a small reaction time.[13]

The evacuation curve is shown in fig. 5.14. The overall evacuation time obtained by the simulation was $554\,\text{s}=9'' 14'^{14}$. It takes the first person about 40 s to reach the

[13]The assumption in the simplified analysis is that people start evacuating immediately after the alarm has been triggered. The awareness time is the time for detection of the hazard.

[14]A single apostrophe denotes seconds and a double one minutes.

assembly point. The assembly process then proceeds rather smooth at a constant rate. It is typical for a complex layout that the flow decreases at the end of the assembly and that it takes about half of the time for the last 25% of the occupants to reach the assembly station.

Improvements of the layout can not be accessed systematically at this point. First of all, it requires additional knowledge concerning the construction of ships. However, if used by an expert, such simulations can provide information on the influences of changes in the layout. At the design stage, this could for example be the change of door or stair widths.

Chapter 6

Summary and Conclusion

> Wir stehen selbst enttäuscht und sehn betroffen den Vorhang zu und alle Fragen offen.
>
> Bertolt Brecht

6.1 Summary

In this thesis several model approaches for crowd movement were described (chapter 2). A specific type of model, namely a cellular automaton, was investigated in detail in chapter 3. The model presented has been successfully validated by comparison to empirical data and experiments from the literature and performed within this work (chapters 4 and 5). The cellular automaton model presented is therefore sufficient for simulating the movement dynamics in egress situations. Furthermore, all known empirical phenomena can be described by cellular automata when taking into account two concepts in addition to the simple hard core exclusion: On the one hand, long range interaction between the pedestrians via a dynamical floor field [Burstedde et al., 2001] which leads to lane formation. The concept of friction [Kirchner et al., 2002], on the other hand, which determines the behavior in conflicts, is able to distinguish competitive from cooperative behavior when combined with increased assertiveness (section 3.7 and [Kirchner et al., 2002]). In egress situations, both of those influences might be neglected as long as there is no strong counterflow (movement against the main flow to the exits) and the scenario under consideration is that of an ordered evacuation, i.e., there are no life threatening hazards. Of course, this is a limitation and an extended version of the model should include some sort of 'social' interaction (like the dynamic floor field) and friction.

There are two arguments for choosing the simple scenario of an ordered evacuation: When considering hazards like fire and smoke, then their dynamics and physiological influences must also be taken into account (fire spread, fluid dynamics calculations, effective doses, incapacitation due to heat and toxic gases, as briefly addressed in section 3.1.1). Secondly, an orderly evacuation is a good starting point for further investigations and assessment of the layout as shown in chapters 4 and 5. There is data available and the assumptions made can be clearly stated and tested. Going to more complicated scenarios requires to weigh the different influences more carefully [Canter, 1990, Smith and Dickie, 1993, Stollard and Johnson, 1994]. Of course, the movement dynamics then still remains important. However, it might become a minor factor concerning the overall performance (time). Therefore, the results are most reliable, if the psychological factors

can to a large extent be included primarily via their influence on the walking speed and orientation as done in chapter 4. In this case, however, evacuation simulations can replace full scale evacuation tests in predicting the overall egress time as has been successfully done for buildings in section 4.3 and for ships in section 5.5. And one can take into account parameter variations which is not possible in trials due to the limited number of repetitions and other practical and ethical constraints.

The following list summarizes the findings. Since the simulations are based on the model, results concerning the model characteristics also apply for the simulations.

Model characteristics

- A model based mainly on hard-core exclusion does not reproduce lane formation. This requires the dynamical variation of the potential (dynamic floor field [Burstedde et al., 2001]). The implementation into a large scale simulation for complex geometries has not yet been done. However, it should require no new concepts.

- A friction parameter μ [Kirchner et al., 2002] which gives the probability for all parties loosing a conflict (i.e., having to stop) can – together with increased coupling to the orientation potential (decreased fluctuations in the walking speed and direction) be used to reproduce empirical findings on competitive behavior (see section 3.7.2).

- The quantitative data on route choice (apart from frequencies for route-choice failure) is sparse. This influence is hard to quantify. The question remains what the probabilities are for choosing alternative routes and which routes are chosen.

- Orientation can be covered by a discrete vector field or a discrete potential if route-choice is pre-determined. Artefacts resulting from this potential are reduced by using an improved metric (compared to the simple Manhattan metric) based on the Moore neighborhood and 'smoothing'. This point has been discussed in section 3.4.

- The distinction between parallel and sequential update is closely related to the occupation numbers o_r of the cells (see section 3.6). If the occupation numbers of all cells are changed at the same time and at most once during a time-step, then the update is parallel. A sequential update might be better to reproduce platooning. This can be seen from the fact that for the parallel update in 1D, the maximum flow occurs at $\rho = \frac{1}{1+v_{\max}}$ and a sequential update against the direction of movement leads to a linear fundamental diagram ($j(\rho) \sim \rho$). This disagrees with the empirical observations presented in section 2.5.1, however.

- A maximal velocity of $v_{\max} = 1$ in the CA model leads to a nearly symmetric (with respect to $\rho = 1/2$) fundamental diagram. A slight deviation is due to the 'lane changing' which breaks particle–hole symmetry. The empirical fundamental diagrams do not show this symmetry.

- A finer discretization of the layout (smaller cells) does not lead to considerable changes in the flow as long as the walking speed is kept constant (i.e., $a' = \frac{a}{2} \rightarrow v' = 2 \cdot v$). The details were described in section 3.3.

Simulation results

- For evacuation scenarios, the restriction to a set of assumptions that basically represent an orderly evacuation (stated in sections 3.1.1 and 4.1.1), allow to perform full scale simulations for the evacuation of all types of passenger vessels and buildings.
- The approach is general in the sense that differences in the scenario do not require modifications of the model but can be covered by adapting the parameters. In this sense, the model is universal.
- All the relevant influences on building evacuation (section 4.1) and ship evacuation (section 5.1) can be taken into account. However, for some of them, like ship motion or familiarity with the layout this can at the moment only be done indirectly via reduction factors (see section 5.4). Since this information was not available for the simulations we performed, these influences were not considered.
- The agreement between simulation results and evacuation trials is sufficient when adapting the parameters to represent the population characteristics correctly (section 4.3). This holds especially for the case of High Speed Craft (section 5.5.1) where full scale tests could be replaced by simulations for determining the overall evacuation time.
- The experience gained concerning the methodology and the implementation of egress and evacuation simulations has been used to promote 'advanced' regulations for the evacuation analysis of passenger ships [IMO, 2002a] (see section 5.3).
- The simulations are scalable in the sense that they can straightforwardly be applied to large (high number of persons and complex layouts) evacuation problems.
- Deviations between simulations and evacuation trials are mainly due to subtleties in the behavior and most prominent on a microscopic level (cf. sections 4.3.2 and 4.3.3). On the macroscopic level they often extinguish each other and add up to only small differences (e.g., the overall evacuation time in section 4.3.2).

6.2 Open Questions

It has already been pointed out in the previous chapter that a comprehensive evacuation simulation requires to take into account many influences that can be neglected for the purpose of simulating egress. Some of those influences have been outlined in chapters 4 and 5, where the procedures have been discussed in detail (especially for ships). Many of the questions are related to realism, i.e., to the question how the details of the rules relevant for the movement in reality can be represented in the simulation. Functions connecting these factors to, e.g., a reduction in walking speed or other quantities that can be represented directly in the simulation have been stated in section 3.7, 4.1 and 5.1 to 5.4. Especially, a further sub-model for the physiological effects of heat and gases is necessary when developing a comprehensive evacuation simulation. However, this is beyond the scope of this thesis.

The open questions formulated in the following therefore concentrate on the crowd dynamics and egress processes and especially their connection to the model properties:

Model characteristics

Characteristic quantities How can decisive quantitative measures for characterization of pedestrian motion be defined? This concerns, e.g., the formation of lanes, time and spatial correlation of walking speed, or the separation of different phases of motion. A first approach is the band index defined in section 3.7.1 for the quantification of lane formation. This has not yet been compared to simulations. Further quantities similar to the congestion index q_r (cf. eq. 4.2) could be introduced and investigated. For quantities like the local flow, the congestion index, and others, the investigation of the temporal and spatial correlations could allow to distinguish different types of movement. Furthermore, they would provide additional insights into the development of congestion.

Synchronization How can effects like platooning be reproduced. These and similar phenomena can be observed in densely packed crowds, e.g., downstairs from the platform into a railway station. Is it necessary to use a sequential update? What is the proper sequence in which the persons are updated? Does it depend on the circumstances? Can smaller cells (i.e., a finer discretization) provide the same effect with a parallel update? Empirical fundamental diagrams usually show a peak at densities below $\rho = 1/2\,\rho_{\max}$. For parallel update, the distance kept for nonzero flow is at least one cell, which has a strong influence on the flow density relation (see the discussion in section 3.6 for further details). It might be worthwhile to introduce a parameter that allows to switch or smoothly interpolate between parallel and sequential update (where the trajectory is not blocked).

Finer discretization Using smaller cell sizes and at the same time allowing velocities of 1 cell/time-step leads to a redefinition of the time scale Δt. In the limit $a \to 0$ the average velocity for $\rho = 1$ will be $\langle v' \rangle = \frac{a'}{\Delta t'} = \frac{a}{\Delta t} = 1$, i.e., the fundamental diagram will be the one for the sequential update. Does such a transition make sense?

Discrete vs. continuous Are there characteristic differences between discrete and continuous models? At the moment it seems that it is rather a matter of taste, whether to take a continuous or discrete approach, since there are no phenomena exclusively present in one of both.

Simulation of Egress and Evacuation

Non regular lattices A cellular automaton is based on a regular lattice (e.g., square grid). Lattices with different coordination numbers for different sites require the explicit representation of the vortices. This increases of course the complexity of the simulations. On the other hand, it allows to represent walls by missing edges instead of black cells. In order to decide, whether such an approach is advantageous it should be simulated and compared to the CA.

Route choice Route choice is reduced to orientation by introducing the discrete potential and coupling the movement of the pedestrians to it. Genuine route choice decisions probably require a graphical representation of the layout on a macroscopic level (cf. section 3.7). A starting point is the investigation of the connection to other graph theoretical problems (like the traveling salesman).

Movement patterns When rounding corners or in front of a staircase certain patterns (e.g., clusters) emerge for high densities. The shape of these patterns has not

yet been investigated in detail. Furthermore, it is connected to the orientation of persons in reality and in the simulation (cf. section 3.4). One of the fundamental questions is: When do people deviate from the shortest path and how can this be implemented in the simulation?

Embarkation and launching The quantification of the embarkation phase could be improved by allowing non-integer values for the individual embarkation time t_{embark}. For the case of HSC, the times obtained in the tests seem to be slightly below 1 s.

Data on familiarity and orientation Even though there are formulas for transforming the familiarity with layout and procedure into a speed reduction, the basic data about this familiarity is usually not available.

Values for ship motion For ship motion the same holds as for the previous topic. What are the values to put into the formulas in section 5.4? And the question remains if the reduction factor really covers all the effects that are caused by the motion of the ship on the pedestrians.

Directional sound The directional sound system (section 5.4.2) is not based on visible exit signs. Therefore, the concept of orientation used in the simulation will probably have to be adapted when such a system is used. How can this be done? How does the definition of the orientation potential, resp. the underlying distance metric have to be changed? It is expected that there will soon be additional experimental results available on orientation based on directional sound.

Measurement points The definition of certain lines (i.e., a chain of cells) where the (specific) flow vs. time is measured would allow to obtain the 'evacuation' curves ($n(t)$) for different spots. This would support an even better assessment of the evacuation performance by comparing different escape route elements.

The influence of the different model characteristics varies according to the circumstances. For example, for egress from a room through a narrow door, the overall egress time is mainly determined by the flow through the exit and the dynamics of the motion might be less important. However, for a large structure, where there are rather long travel distances, quite the opposite might be true. A systematic quantification of those influences would be helpful. This could be done by developing analytic estimates for travel and egress times by neglecting all influences but one. This would show if the egress time is determined mainly by the exit flow rate or the distance traveled.

6.3 Conclusions

There are four major conclusions from the work presented here:

1. Simulation of large crowds with a microscopic and individualistic model is possible. There is no restriction concerning the complexity of the geometric layout. The model is (relatively) easy to implement and the results are reliable and agree well with empirical findings. One has to keep in mind, however, that route-choice is assumed to be pre-determined. If pedestrians are not able to choose the proper route, then they will not make their way out of the building. This case is explicitly excluded by the previous assumption.

2. The model is robust with respect to the influence of the parameters or changes of fundamental quantities like the cell size. Small changes of the parameter values do cause only small changes of the macroscopic results (like egress times, flow values). The cell size in a discrete model has no major influence on the flow as long as the related rules are not changed (cf. section 3.3). This means that changing the cell size and keeping the velocity constant does not increase the flow. In fact, the flow is slightly decreased. However, the width can only by represented in steps of a, a finer discretization is more realistic concerning geometrical details. This might lead to a slightly increased flow (cf. fig. 3.11). Furthermore, the maximum in the fundamental diagram is shifted to the right. Therefore, the question of a continuum limit $a \to 0$ and at the same time $\Delta t \to 0$ is important. In this case, the mean velocity (and therefore also the flow) would not be decreased by increasing the density. On the one hand, this could explain synchronization. On the other hand, it does not agree with the empirical fundamental diagram.

3. Empirical phenomena like lane formation, oscillation at bottlenecks, and lane formation can be reproduced, in continuous [Helbing et al., 2002, 2000] as well as in discrete models [Burstedde et al., 2001, Schadschneider, 2002a]. In order to include all the known phenomena, friction or a similar concept must be present in the model as well as a dynamical variation of the potential.

4. The metric the orientation (or the transition probabilities) is based on is decisive for the simulation results and especially for the paths the pedestrians take and the shapes of the jams (cf. section 3.3). It even might direct the persons in an unrealistic way.

The influence of psychological factors is not as well quantified as of physiological ones. This holds especially for extreme situations, since data usually stems from observations in normal situations or exercises. This can at the moment be taken into account by adapting the parameters by rules of thumb. Parameter studies could provide further insight. One could also introduce more parameters like age, gender, etc. and calculate walking speeds and reduction factors. However, at the end of the day there will be a distribution of walking speeds again. Nevertheless, if a simulation will be used by persons who did not develop it, these parameters would be easier to understand and handle. On the other hand, increasing the number of parameters might lead to less insight.

The inclusion of fire, smoke, and toxic combustion gases is necessary for an evacuation simulation that wants to cover extreme situations. Therefore, before including such cases where extreme behavior occurs, one should have realistic information about the spread of fire and smoke, and should use the models available for the physiological consequences of inhaling such gases (i.e., the fractional effective dose model [Purser and Bensilium, 2001]) to determine the level of incapacitation.

Concerning evacuation simulations, the results of evacuation trials can usually be predicted within a satisfying range of accuracy. This is especially the case for High Speed Passenger Craft, where those trials are part of the legal requirements concerning operational safety. In general, one has to distinguish two purposes anyway:

- Application as a design tool (restriction to changes in the layout).
- Investigation of extreme situations that do not frequently occur.

For the second purpose, the assumptions that have to be made are less clear, the psychological factors become more prominent, and crowd dynamics becomes less important

compared to, e.g., fire spread and the influence of toxic gases. For the application as a design tool, a simple model is sufficient. It allows to do fast calculations and thus obtain estimates for egress times that can be compared to the times that are assumed to be available for safe egress that have been obtained by other methods.

Finally, specific empirical data on fundamental processes of crowd movement can be helpful. A first step would be to perform experiments for the validation cases contained in [IMO, 2002a]. Additional cases can be found in [IMO, 2002c] which is the document the former is partially based on. They can be directly compared to simulations and are simple enough to investigate fundamental model properties. This holds especially for the case of orientation and the formation of movement patterns (the distance to the wall, formation of arches in front of the doors, etc.) when rounding corner, leaving a room, etc.

Tabellarischer Lebenslauf (Curriculum Vitae)

Persönliche Daten

Geburtstag und -ort	14. Oktober 1974 in Würzburg
Familienstand	ledig
Staatsangehörigkeit	deutsch

Bildungsgang

1985 - 1994	**Johann-Schöner Gymnasium Karlstadt/Main** Abitur mit Leistungskursen in Mathematik und Physik
1994-1995	**Sanitätsschule der Luftwaffe, Giebelstadt** Grundwehrdienst
10/1995	**Universität Würzburg** Erstimmatrikulation im Fach Physik
8/1997	**Universität Würzburg** Diplom-Vorprüfung
8/1998 - 8/1999	**State University of New York at Stony Brook** Studium der Physik mit Abschluss "Master of Arts in Physics"
Seit 9/1999	**Gerhard-Mercator-Universität Duisburg** Wissenschaftlicher Mitarbeiter im Projekt *Bewertung und Analyse von Evakuierungsprozessen auf Passagierschiffen mit Hilfe mikroskopischer Simulationstechniken (BYPASS)* in der Arbeitsgruppe *Physik von Transport und Verkehr*

Danksagung (Acknowledgements)

Ich danke meinen ‘Kollegen’ aus der Arbeitsgruppe für ihre Hilfe und Unterstützung: Robert Barlovic, Roland Chrobok, Sigudur Havstein, Dinyo Haygarov, Torsten Huisinga, Andreas Keßel, Ansgar Kirchner, Florian Mazur, Tim Meyer-König, Andreas Pottmeier, Joachim Wahle, Nathalie Waldau, Matthias Woltering und insbesondere Birgit Dahm-Courths für die Unterstützung beim Kampf mit der Bürokratie. Aber auch die ‘Ehemaligen’ haben Anteil daran, dass ich gerne hier gearbeitet habe: Oliver Kaumann, Andre Stebens, Lutz Neubert, Wolfgang Knospe.

Joachim hat den Weg für diese Arbeit geebnet und ich konnte immer auf seine Erfahrung und seinen Rat zählen. Ohne Tims Hilfe wären viele der hier vorgestellten Ergebnisse nicht zustande gekommen. Ansgar und Andreas haben in zahlreichen Diskussionen Ideen und Anregungen gegeben und mir damit sehr geholfen. Außerdem haben sie die Arbeit Korrektur gelesen und viele Verbesserungen vorgeschlagen. Einen erheblichen Anteil am Gelingen der Arbeit hat auch PD Dr. Andreas Schadschneider, dem ich viele wertvolle Hinweise verdanke. Wenn es trotzdem noch Schwachpunkte gibt, so liegt das sicherlich nicht an ihnen, sondern allein an mir. Besonders dankbar bin ich für ihre Hilfe und Unterstützung über das fachliche hinaus.

Mein besonderer Dank gilt Prof. Dr. Michael Schreckenberg für die Betreuung der Arbeit, seine Großzügigkeit und die dadurch eröffnete Gelegenheit, vielfältige Erfahrungen und Eindrücke während meiner Zeit am Lehrstuhl “Physik von Transport und Verkehr” zu sammeln. Für hilfreiche Informationen aus dem maritimen Bereich danke ich (stellvertretend für all die weiteren) T. Weigend von der Jos. L. Meyer Werft, A. Hellesoy von der Flensburger Schiffbau-Gesellschaft, B. Kolberg von der See-Berufsgenossenschaft, Dr. A. Baumgart vom Germanischen Lloyd und insbesondere Kapitän P. Olsson vom Bundesministerium für Verkehr, Bau und Wohnungswesen.

Der Anteil meiner Eltern und Geschwister am Gelingen meiner Ausbildung (falls sie denn gelungen ist, das weiß man ja immer erst nachher) geht weit über das hinaus, was ich hier erwähnen könnte.

List of Publications

Keßel, A., H. Klüpfel, and M. Schreckenberg (2001). Simulation der Bewegung von Fußgängern, Menschenmengen und Evakuierungsprozessen. In K. Panreck and F. Dörrscheidt (Eds.), *Frontiers in Simulation*, Number 15 in Symposium Simulationstechnik, Paderborn, pp. 343–348. ASIM: Society for Computer Simulation International.

Keßel, A., H. Klüpfel, and M. Schreckenberg (2002). Microscopic simulation of pedestrian crowd motion. In [Schreckenberg and Sharma, 2002], pp. 193–202.

Keßel, A., T. Meyer-König, H. Klüpfel, and M. Schreckenberg (2002). A concept for coupling empirical data and microscopic simulation of pedestrian flows. In *Proceedings of the International conference on Monitoring and Management of visitor flows in recreational and protected areas*, Wien. In print.

Klüpfel, H., T. Meyer-König, and M. Schreckenberg (2001). Microscopic modelling of pedestrian motion – comparison of an evacuation exercise to simulation results in a primary school. In *Proceedings of the International Workshop on Traffic and Granular Flow (TGF) '01*. In print.

Klüpfel, H., T. Meyer-König, J. Wahle, and M. Schreckenberg (2000). Microscopic simulation of evacuation processes on passenger ships. In *Proc. Fourth Int. Conf. on Cellular Automata for Research and Industry*, London, pp. 63–71. Springer.

Meyer-König, T., H. Klüpfel, A. Keßel, and M. Schreckenberg (2001). Simulating mustering and evacuation processes onboard passenger vessels: Model and applications. In *The 2nd International Symposium on Human Factors On Board (ISHFOB)*. In print.

Meyer-König, T., H. Klüpfel, and M. Schreckenberg (2001). A microscopic model for simulating mustering and evacuation processes onboard passenger ships. In *Proceedings of the International Emergency Management Society Conference*.

Meyer-König, T., H. Klüpfel, and M. Schreckenberg (2002). Assessment and analysis of evacuation processes on passenger ships by microscopic simulation. In [Schreckenberg and Sharma, 2002], pp. 297–302.

Meyer-König, T., H. Klüpfel, J. Wahle, and M. Schreckenberg (1999). BYPASS: Evakuierungssimulation für Fahrgastschiffe. *OR News 7*, 5–8.

Schreckenberg, M., R. Barlović, W. Knospe, and H. Klüpfel (2001). Statistical physics of cellular automata models for traffic flow. In K.-H. Hoffmann and M. Schreiber (Eds.), *Computational Statistical Physics – From Billiards to Monte Carlo*, Berlin, pp. 113–126. Springer.

Kirchner, A., H. Klüpfel, K. Nishinari, A. Schadschneider, and M. Schreckenberg (2002). Simulation of competitive egress behaviour. In preparation.

List of Figures

List of Tables

Glossary

Agent A concept from computer science. An agent is an autonomous entity interacting with its environment and other agents. A pedestrian in the simulation is an agent.

ASEP Asymmetric simple exclusion process. A discrete model for transport phenomena, where a particle is allowed to hop to the neighboring lattice sites. The NaSch–model with $v_{\max} = 1$ is equivalent to the (totally) ASEP (cf. section 2.3.2).

Assembly phase The evacuation procedure on passenger ships is divided into two separate phases: assembly phase and embarkation phase. First, the passengers gather at the assembly points and then proceed to the embarkation stations, if the decision to abandon the ship is made.

Assembly stations Areas on-board a ship where the passengers gather in case of an alarm. Every passenger is assigned to a specific assembly station. (See also: *assembly phase*).

Awareness time The time it takes to detect an incident and decide to take action is called awareness time. It is therefore rather a global than an individual variable.

Cellular Automaton A lattice, a finite set of states, the definition of a neighborhood and an update function ($\mathcal{L}$, S, $\mathcal{N}$, f) are called a cellular automaton. For explanations and a less formal definition, see section 3.1.

Crowd A gathering of two or more persons. Crowds are different from groups because they persist only for a short time, are at the same place, and share a common focus. For detailed description of different forms of groups see fig. 1.2.

Crowd Dynamics Crowd motion together with the influencing factors.

Crowd Control Reactive measures (used, e.g., by the police) to enforce the desired behavior of a crowd.

Crowd Management Proactive and precautionary measures (e.g., procedural or concerning the layout of a building) to direct crowd movement and behavior into the desired way. The aim of crowd management is to increase the comfort on the one hand and to avoid the necessity for crowd control on the other hand.

Crowd Motion Movement of a crowd determined by physical, physiological, psychological, and social factors.

Continuous model A model in which time and space are represented by continuous variables, i.e., variables that can take real numbers as values. Macroscopic models are usually continuous, microscopic models might be continuous or discrete.

Directional Sound Directional sound is a system of sound beacons which are understood intuitively and guide person to the exit. Since it is based on sound, it is not obscured by smoke.

Discrete model A model in which space and time are discrete, i.e., the corresponding variables take on integer numbers. Discrete models are usually microscopic.

Egress Leaving a building, vessel, or place by a group or an individual. Opposite to evacuation, egress occurs in normal and emergency situations.

Embarkation Entering the life-boats, resp. the life-rafts via the slides.

Embarkation time In the simulation an individual embarkation time t_{embark} can be specified. It is usually assumed to be the same for everyone. This time represents either the time to enter the life-boat or the raft via a slide. Alternatively an overall embarkation time E can be used that covers the embarkation of all the persons. (See also: *Launching time* below).

Evacuation Egress due to a potential or actual hazard (emergency egress).

Evacuation curve The number of persons evacuated vs. time $n(t)$. This curve allows to assess the evacuation, since it contains the information about the total number of persons, the overall time, and the flow vs. time can be obtained by taking the derivative.

Graph A graph is a set of vertices and edges, where each edge connects two vertices. A (regular) lattice is a certain type of planar graph, where each vortex is connected to the same number of other vertices (coordination umber). Cellular automata are based on regular lattices (usually a square grid).

High Speed Passenger Craft (HSC) High Speed Craft are fast passenger ferries usually covering only short distances. The seating arrangement is similar to aircraft and they are evacuated via slides and life-rafts.

IMO International Maritime Organization, sub-organization of the UNO, London. A brief description of the work of IMO is given in section 5.3.

Implementation Transformation of a model into a set of algorithms formulated in a programming language.

Interpretation Interpretation is understood as the formulation of a model that is consistent with a theory (e.g., a discrete, microscopic model based on the general theory for crowd motion). This is done by formulating the assumptions of the theory in a quantitative way and removing ambiguities without loosing consistency. In the context of interpreting simulation results, there is a second meaning: connecting simulation results to real world phenomena.

Launching time The launching time L is the time it takes to launch the life-boats. In the analysis (cf. eq. 5.1), the sum of embarkation and launching time can be set to 30 minutes, if no data are available.

Low location lighting Band of small arrows at the floor which directs persons crawling to the exit (usually phosphorescent). LLL is required for aircraft and by SOLAS for ships.

Macroscopic model In macroscopic models aggregated quantities like densities and flow are used to calculate evacuation times and similar quantities. They are usually based on a coarse network ('hydraulic system', in analogy to fluid-dynamics) and employ flow-density and speed-density relations.

Manhattan Metric The Manhattan metric measures the distance between two sites of a square lattice in steps. For a cellular automaton this is the distance if hopping is allowed only across edges. An extended Manhattan metric (where steps across edges and corners are possible) is illustrated in fig. 3.12.

Marine Evacuation System (MES) The appliances like slides and inflatable life-raft that are used as an alternative to life-boats that have to be launched. They may enable a faster and more flexible evacuation.

Marine Safety Committee (MSC) The Marine Safety Committee (MSC) is one of the major bodies of IMO. Its sub-committee on fire protection is (among other things) concerned with evacuation analysis.

Method Systematic way to obtain knowledge. For the empirical sciences it comprises data collection, analysis, and interpretation. A method should be objective (checkable by others), reliable (repeatable by others), and valid (e.g., it should actually measure what its supposed to measure).

Methodology Theory about methods. A guide to apply methods correctly.

Microscopic model Microscopic models represent space and population in detail, i.e., the geometry is either continuous or a fine network (graph, lattice) and the population consists of individual persons.

Moore neighborhood The eight next neighbor cells of cell r (coordination number $k = 8$) are called Moore neighborhood. See also: *von Neumann neighborhood*.

Nagel-Schreckenberg model The standard cellular automaton model for road traffic. It is described in section 2.3.2.

Objectivity A result should not depend on the person who obtained it. Therefore, the procedure, repeated by someone else, should lead to the same results. A prerequisite for objectivity is the operational definition of the measurement process.

Orientation Orientation is the choice of the desired path, i.e., in the model the desired destination cell. It is represented by information about the current direction to the exit that is contained in each cell. Orientation is then the determination of the transition probabilities, which is distinct from the actual movement carried out after this step has been performed.

Reaction time Reaction time is the time to react to the alarm, i.e., after an hazard has been detected and the decision about, e.g., to abandon the ship, made. It is therefore an individual variable and part of the response time. See also: *response time* and *awareness time*.

Reliability Repeating a measurement or experiment should lead to the same results. This is sometimes difficult for evacuation exercises, since it is hard to exactly specify and prepare the initial conditions.

Response time Response time is the time between the initial alarm and the start of the movement. It is therefore a combination of the awareness time and the reaction time, where the former is usually a global variable and the latter individually different.

Regular Lattice A graph where each knot has the same coordination number is called a regular lattice. In this case, edges must not be explicitly represented.

Ro-Ro passenger ferries Ro-Pax ferries carry cars and trucks as well as passengers. The name is short for roll on/roll off.

Route choice Route choice in the context of the model and the simulation is understood as the decision which path to take. This would require a knowledge about the layout of the complete building or vessel by the pedestrian. This is not the case in the model presented. Therefore route-choice is not explicitly modeled but assumed to be according to the pre-determined escape paths. Therefore, it is reduced to orientation.

Safety factor A safety factor is used to provide a buffer for unforeseen influences. In the case of evacuation simulation, the product of the simulated evacuation time and the safety factor is compared to the available evacuation time.

Safety margin Instead of a safety factor, a safety margin can be used, which is added to the simulated evacuation time. (See: *Safety factor*).

Significant queues Significant queues are areas of congestion that persist for a certain percentage of the overall assembly or evacuation time. The term is used for the evacuation analysis of passenger ships (cf. section 5.3.2).

Simulation A technical or artifical system which represents a part of reality and its dynamics (change in time). Running an implementation of a model on a computer is a special sort of simulation. The system is then the part of reality which is the subject matter of the corresponding theory.

SOLAS Short for *International Convention for the Safety of Life at Sea*. It is the major document for the maritime safety and contains a requirement making evacuation analysis for Ro-Ro passenger ships build from July 1999 on mandatory.

Time step A time step is the minimal time between any two tactical actions of the same individual, where an action might comprise several consecutive steps (cf. section 3.6). The update step and the time step are equal in a cellular automaton model, if a parallel update is used. For a sequential update, the update step scales with $1/N$, where N is the number of individuals.

Theory A theory consists of two sets of statements. The first set determines the subject matter of the theory; the second set is a subset of the first and is called the set of *acceptable* statements. Acceptable means "true" in the sense of being in accordance with reality in the experimental sciences. In axiomatic theories, which belong to the realm of mathematics, acceptable statements are called *theorems*. A theorem is a provable statement that can be derived by logic alone from initial theorems, called axioms.

Update step An update step is the time in which the system is able to change. For a continuous model (not for its implementation) the update step is infinitesimally small ($\mathrm{d}t$). Several update steps might occur during one time step, but not vice versa. The reaction time might be identified with the length of an update step.

Validity The correspondence between a variable and what it actually measures. For example, the overall egress time is a valid measure for the layout of a building with respect to evacuation safety.

von Neumann neighborhood The four cells next to cell r (coordination number $k = 4$) are called von Neumann neighborhood.

Bibliography

Abe, K. (1986). *The Science of Human Panic*. Tokyo: Brain Publ. Co. (in Japanese).

Abrahams, J. (1994). *Fire escape in difficult circumstances*, Chapter 6. In Stollard and Johnson [Stollard and Johnson, 1994].

AlGadhi, S., H. Mahmassani, and R. Herman (2002). A speed-concentration relation for bi-directional crowd movements with strong interaction. See [Schreckenberg and Sharma, 2002], pp. 3–20.

Ando, K., H. Ota, and T. Oki (1988). Forecasting the flow of people. *Railway Research Review 45*, 8–14. (in Japanese).

Babrauskas, V., D. Drysdale, and C. Franks (Eds.) (1999). *Proceedings of the Interflam '99 Conference*, Greenwich. Interscience Communications.

Bandini, S. and T. Worsch (Eds.) (2000). *Theoretical and Practical Issues on Cellular Automata*, London. Springer.

Biham, O., A. Middleton, and D. Levine (1992). Self-organization and a dynamical transition in traffic-flow models. *Phys. Rev. A 46*, R6124.

Björkman, A. (1999). Some outstanding questions about the Estonia. See [Vassalos, 1999].

Bles, W., S. Nooy, and L. Boer (2001). Influence of ship listing and ship motion on walking speed. Technical Report TM-01-C015, TNO Human Factors, Soesterberg, Netherlands.

Bles, W., S. Nooy, and L. Boer (2002). Influence of ship listing and ship motion on walking speed. See [Schreckenberg and Sharma, 2002], pp. 437–452.

Blue, V. and J. Adler (1999). Bi-directional emergent fundamental pedestrian flows from cellular automata microsimulation. In A. Ceder (Ed.), *Proceedings of ISTTT'99*, Amsterdam, pp. 235–254. Pergamon.

Blue, V. and J. Adler (2000). Modelling four directional pedestrian movements. In *Transportation Research Board, 79th Annual Meeting*.

Boer, L. (2000). Mustering and evacuation of passengers: Scientific basis for design. Technical Report BriteEuram project 97-4229 "MEP Design", TNO Human Factors, Soesterberg, Netherlands.

Brown, R. (1986). *Social Psychology* (2 ed.). New York: The Free Press.

Brumley, A. and L. Koss (1997). The need for statistics on the behavior of passengers during the evacuation of high speed craft. In *Proceedings of FAST '97 High Speed Craft Technology Conference*.

Brumley, A. and L. Koss (1998). The implication of human behavior on the evacuation of ferries and cruise ships. In *Proceedings of AME '98 Australian Maritime Engieneering CRC Annual Post-Graduate Conference*.

Brumley, A. and L. Koss (2000a). The influence of human factors on the motor ability of passengers during the evacuation of ferries and cruise ships. In I. of Naval Architects (Ed.), *Conference on human factors in ship design and operation*.

Brumley, A. and L. Koss (2000b). The motor ability of passengers during the evacuation of ferries and cruise ships. Society of Naval Architects and Marine Engineers.

Bukowski, R. W., P. Richard, D. Peacock, and W. W. Joes (1998). Sensitivity examination of the airEXODUS aircraft evacuation simulation model. In *International Aircraft Fire and Cabin Safety Research Conference*, Atlantic City, pp. 1–14.

Burstedde, C. (2001). Simulation von Fußgängerverhalten mittels zweidimensionaler zellulärer Automaten. Diplomarbeit, Universität zu Köln.

Burstedde, C., K. Klauck, A. Schadschneider, and J. Zittartz (2001). Simulation of pedestrian dynamics using a 2-dimensional cellular automaton. *Physica A 295*, 507–525.

Canter, D. (Ed.) (1990). *Fires and Human Behaviour* (2nd ed.). London: David Fulton Publishers.

Chang, B.-C. (1998). *On the Survivability of Damaged Ro-Ro Vessels Using a Simulation Method*. Dissertation, Technische Universität, Hamburg–Harburg. Arbeitsbereiche Schiffbau, Bericht Nr. 597.

Chowdhury, D., D. Wolf, and M. Schreckenberg (1997). Particle hopping models for two-lane traffic with two kinds of vehicles: Effects of lane-changing rules. *Physica A 235*, 417.

de Vries, J. (1998). Cruise ship evacuation. Master's Thesis, TU Delft, Faculty of Maritime Engineering.

Deutscher Fußballbund (1999). *Richtlinien zur Verbesserung der Sicherheit bei Bundesspielen*. Deutscher Fußballbund.

Diedrich, G., L. Santen, A. Schadschneider, and J. Zittartz (2000). Effects of on- and off-ramps in cellular automata models for traffic flow. *Int. J. Mod. Phys. C 11(2)*, 335–345.

Dijkstra, J., H. Timmermans, and A. Jessurun (2000). A multi-agent cellular automata system for visualising simulated pedestrian activity. See [Bandini and Worsch, 2000], pp. 29–36.

DiNenno, P. (Ed.) (1995). *SFPE Handbook of Fire Protection Engineering* (2nd ed.). National Fire Protection Association.

Drager, K., G. Løvås, J. Wicklund, H. Soma, D. Duong, A. Violas, and V. Lanèrès (1994). EVACSIM: A comprehensive evacuation simulation tool. In K. Drager (Ed.), *Proceedings of the 1992 Emergency Management and Engineering Conference*, pp. 101–108. Society for Computer Simulation.

Evans, M. (1997). Exact steady states of disordered hopping particle models with parallel and ordered sequential dynamics. *JPA 30*, 5669–5685.

Federal Aviation Administration (1990). Emergency evacuation. Regulation CFR Sec. 25.803, Federal Aviation Administration.

Forsyth, D. R. (1999). *Group Dynamics* (3 ed.). Belmont, CA: Wadsworth Publishing.

Frantzich, H. (1996). Study of movement on stairs during evacuation using video analysing techniques. Technical report, Department of Fire Safety Engineering, Lund Institute of Technology, Lund University.

Freud, S. (1924). *Massenpsychologie und Ich-Analyse*. Leipzig: Int. Psychoanalytischer Verlag. [gesammelte Schriften].

Fruin, J. (1971). *Pedestrian Planning and Design*. New York: Metropolitan Association of Urban Designers and Environmental Planners.

Fukui, M. and Y. Ishibashi (1999). Self-organized phase transitions in CA-models for pedestrians. *J. Phys. Soc. Japan 8*, 2861–2863.

Galea, E. (1998). A general approach to validating evacuation models with an application to EXODUS. *Journal of Fire Sciences 16*(6), 414–436.

Galea, E. and J. P. Galparsoro (1994). A computer-based simulation-model for the prediction of evacuation from mass-transport vehicles. *Fire Safety Journal 22*(4), 341–366.

Galea, E., M. Owen, and P. Lawrence (1996). Computer modelling of human behaviour in aircraft fire accidents. *Toxicology 115*, 63–78.

GEO (2001, 5). Laufforschung: Ihr Ziel ist der Weg.

Gershenfeld, N. (1999). *The Nature of Mathematical Modelling*. Cambridge: Cambridge University Press.

Gigerenzer, G., P. Todd, and the ABC research group (1999). *Simple Heuristics that make us Smart*. New York, Oxford: Oxford University Press.

Graat, E., C. Midden, and P. Bockholts (1999). Complex evacuation; effects of motivation level and slope of stairs on emergency egress time in a sports stadium. *Safety Science 31*, 127–141.

Grossi, L. and V. Farinetti (1999). Design for safety of HSC: Future developments. See [Vassalos, 1999].

Gwynne, S., E. Galea, M. Owen, P. Lawrence, and L. Filippidis (1999). A review of the methodologies used in the computer simulation of evacuation from the built environment. *Building and Environment 34*, 741–749.

Haken, H. (1983). *Synergetics*. Berlin: Springer.

Hamacher, H. and S. Tjandra (2002). Mathematical modelling of evacuation problems – a state of the art. See [Schreckenberg and Sharma, 2002], pp. 227–266.

Harbst, J. and F. Madsen (1996). The behaviour of passengers in a critical situation on board a passenger vessel or ferry. Technical report, Danish Investment Foundation, Kopenhagen.

Health and Safety Executive (1996). Managing crowds safely. Technical report, Health and Safety Executive, Sudbury, UK.

Health and Safety Executive (1999). Emergency planning for major accidents. Technical report, Health and Safety Executive, Sudbury, UK.

Helbing, D. (1995). Theoretical foundation of macroscopic traffic models. *Physica A 219*, 375.

Helbing, D. (1997). *Verkehrsdynamik*. Berlin: Springer.

Helbing, D. (2001). Traffic and related self-driven many particle systems. *Rev. Mod. Phys. 73*(4), 1067–1141.

Helbing, D., I. Farkas, P. Molnar, and T. Vicsek (2002). Simulation of pedestrian crowds in normal and evacuation situations. See [Schreckenberg and Sharma, 2002], pp. 21–58.

Helbing, D., I. Farkas, and T. Viscek (2000). Simulating dynamical features of escape panic. *Nature 407*, 487–490.

Helbing, D., H.-J. Hermann, M. Schreckenberg, and D. Wolf (Eds.) (2000). *Traffic and Granular Flow '99*, Berlin. Springer.

Helbing, D. and P. Molnar (1995). A social force model for pedestrian dynamics. *Phys. Rev. E 51*, 4284–4286.

Helbing, D., P. Molnár, I. Farkas, and K. Bolay (2001). Self-organizing pedestrian movement. *Environment and Planning B: Planning and Design 28*, 361–383.

Henderson, L. (1971). The statistics of crowd fluids. *Nature 229*, 381–383.

Henderson, L. (1972). Sexual differences in human crowd motion. *Nature 240*, 353–355.

Hofstätter, P. (1990). *Gruppendynamik : Kritik der Massenpsychologie*. Reinbek bei Hamburg: Rowohlt.

Hoogendoorn, S. (2000). Gas kinetic modelling and simulation of pedestrian flows. In *Proceedings of the Transportation Research Board*, Washington.

Hoogendoorn, S. and P. Bovy (2001). Generic gas-kinetic traffic systems modeling with applications to vehicular traffic flow. *Transportation Research B – Methodological 35*, 317–336.

Hoogendoorn, S., P. Bovy, and W. Daamen (2002). Microscopic pedestrian wayfinding and dynamics modelling. See [Schreckenberg and Sharma, 2002], pp. 123–154.

IMO (1999). *Interim Guidelines for a simplified evacuation analysis on ro-ro passengers ships*. IMO. MSC/Circ. 909 (replaced by MSC/Circ. 1033).

IMO (2000a). *International Code For Fire Safety Systems (FSS Code)*. IMO. Resolution MSC.98(73).

IMO (2000b). *International Code of Safety for High-Speed Craft, 2000 (2000 HSC Code)*. IMO. Resolution MSC.97(73).

IMO (Ed.) (2000c). *Safety of Life at Sea (SOLAS)*. London: Bath Press. consolidated edition.

IMO (2001). *Interim Guidelines for a Simplified Evacuation Analysis Of High-Speed Passenger Craft*. IMO. MSC/Circ. 1001.

IMO (2002a). *Interim Guidelines for Evacuation Analyses for New and Existing Passenger Ships*. IMO. MSC/Circ. 1033.

IMO (2002b, February). *Report to the Maritime Safety Committee*. IMO. Sub-Committee on Fire Protection, FP46/16.

IMO (2002c). *Simulation Tools for Evacuation Analysis*. IMO. FP44/3/3, submitted by Germany and Norway.

ISO (1999). Fire safety engineering. Technical Recommendation TR 13387, International Organization for Standardization.

Janosi, I. (1999). Search for intelligence by motion analysis ;-). See [Helbing et al., 2000], pp. 81–86.

Jungermann, H. and C. Göhlert (2000). Emergency evacuation from double-deck aircraft. In M. Cottam, D. Harvey, R. Pape, and J. Tait (Eds.), *Foresight and Precaution. Proceedings of ESREL 2000, SARS and SRA Europe Annual conference*, Rotterdam, pp. 989–992. A.A. Balkema.

Kaumann, O., K. Froese, R. Chrobok, J. Wahle, L. Neubert, and M. Schreckenberg (2000). On-line simulation of the freeway network of North Rhine-Westphalia. See [Helbing et al., 2000], pp. 351–356.

Keßel, A. (2001). Simulation von Fußgängerbewegung mit zweidimensionalen zellulären Automaten. Diplomarbeit, Gerhard-Mercator-Universität, Duisburg.

Keßel, A., T. Meyer-König, H. Klüpfel, and M. Schreckenberg (2002). A concept for coupling empirical data and microscopic simulation of pedestrian flows. In *Proceedings of the International conference on Monitoring and Management of visitor flows in recreational and protected areas*, Wien. In print.

Kinzel, W. and G. Reents (1999). *Physics by Computer*. Berlin: Springer.

Kirchner, A. (2002). *Modellierung und statistische Physik biologischer und sozialer Systeme*. Dissertation, Universität zu Köln.

Kirchner, A., H. Klüpfel, K. Nishinari, A. Schadschneider, and M. Schreckenberg (2002). Simulation of competitive egress behaviour. In preparation.

Kirchner, A., H. Klüpfel, A. Schadschneider, and M. Schreckenberg (2002). Influence of cell size and discretization on the dynamics of a 2D CA model for crowd motion. *In preparation*.

Kirchner, A., K. Nishinari, and A. Schadschneider (2002). Friction effects and clogging in a cellular automaton model for pedestrian dynamics. *submitted to Phys. Rev. E*. cond-mat/0209383.

Klüpfel, H., T. Meyer-König, and M. Schreckenberg (2001). Microscopic modelling of pedestrian motion – comparison of simulation results with an evacuation exercise in a primary school. In *Proceedings of the International Workshop on Traffic and Granular Flow (TGF) '01*. In print.

Klüpfel, H., T. Meyer-König, J. Wahle, and M. Schreckenberg (2000). Microscopic simulation of evacuation processes on passenger ships. In *Proc. Fourth Int. Conf. on Cellular Automata for Research and Industry*, London, pp. 63–71. Springer.

Knospe, W. (2002). *Synchronized traffic – microscopic modelling and empirical observations*. Dissertation, Gerhard-Mercator-Universität, Duisburg.

Knospe, W., L. Santen, A. Schadschneider, and M. Schreckenberg (2000). Towards a realistic microscopic description of highway traffic. *J. Phys. A 33*, L477–L485.

Knuth, D. (1997). *The Art of Computer Programming*, Volume 2 – Seminumerical Algorithms. Reading: Addison-Wesley.

Kreyszig, E. (1999). *Advanced Engineering Mathematics* (7 ed.). New York: Wiley.

Kugihara, N. (2002). Effects of aggressive behaviour and group size on collective escape in an emergency: A test between a social identity model and deindividuation theory. *British Journal of Social Psychology 40*, 575–598.

Le Bon, G. (1895). *Psychologie der Massen*. Stuttgart [1982]: Kröner. [Paris, 1895].

Marine Safety Agency (1997). Report on Exercise Invicta. Technical report, Marine Safety Agency. Available from MCA, 105 Commercial Road, Southhampton.

Meyer-König, T. (1999). Aufbau einer Methode zur Simulation von Fluchtvorgängen bei der Evakuierung von Passagierschiffen. Institut für Schiffstechnik, Universität Duisburg, Studienarbeit.

Meyer-König, T. (2000). Simulation von Evakuierungsprozessen auf Fahrgastschiffen. Diplomarbeit, Gerhard-Mercator-Universität, Duisburg.

Meyer-König, T., H. Klüpfel, and M. Schreckenberg (2001). A microscopic model for simulating mustering and evacuation processes onboard passenger ships. See [TIEMS, 2001].

Meyer-König, T., H. Klüpfel, and M. Schreckenberg (2002). Assessment and analysis of evacuation processes on passenger ships by microscopic simulation. See [Schreckenberg and Sharma, 2002], pp. 297–302.

Moss, S. (Ed.) (2001). *Multi-agent based simulation: second international workshop*, Volume 1979 of *Lecture notes in computer science: Lecture notes in artificial intelligence*, Berlin. Springer.

Muir, H. (1996). Effects of motivation and cabin configuration on emergency aircraft evacuation behavior and rates of egress. *Intern. J. Aviat. Psych. 6*(1), 57–77.

Müller, K. (1999). Die Evakuierung von Personen aus Gebäuden – nach wie vor ein nationales und internationales Problem. *vfdb-Zeitschrift 3*, 131.

Muramatsu, M., T. Irie, and T. Nagatani (1999). Jamming transition in pedestrian counter flow. *Physica A 267*, 487–498.

Nagatani, T. (1993). Self-organization and phase transition in traffic-flow model of a two-lane roadway. *J. of Phys. A 26*, L781–L787.

Nagel, K. (1996). Particle hopping models and traffic flow theory. *Phys. Rev. E 53*, 4655.

Nagel, K. and M. Schreckenberg (1992). A cellular automaton model for freeway traffic. *J. Physique I 2*, 2221–2229.

Nagel, K., D. Wolf, P. Wagner, and P. Simon (1998). Two-lane traffic rules for cellular automata: A systematic approach. *Phys. Rev. E 58*, 1425–1437.

Narendra, K. S. and M. A. Thathachar (1989). *Learning Automata – An Introduction*. Englewood Cliffs: Prentice Hall.

NZZ Folio (2002, Februar). Total Digital – Die Welt als null und eins. Supplement of *Neue Zürcher Zeitung*.

Owen, M., E. Galea, P. Lawrence, and L. Filippidis (1998). AASK – aircraft accident statistics and knowledge: a database of human experience in evacuation, derived from aviation accident reports. *Aero. J. 102*, 353–363.

Pauls, J. (1995). *Movement of People* (2nd ed.)., Chapter 3-13, pp. 3–263—3–285. In DiNenno [DiNenno, 1995].

Popkov, V., L. Santen, A. Schadschneider, and G. Schütz (2000). Boundary-induced phase transitions in traffic flow. *J. Phys. A 34*, L45–L52.

Pradillon, J.-Y. and M. Ferry (2001). SPECS: A mustering simulation tool for the evacuation of passenger vessels. See [TIEMS, 2001].

Predtetschenski, W. and A. Milinski (1971). *Personenströme in Gebäuden – Berechnungsmethoden für die Modellierung*. Köln-Braunsfeld: Müller.

Press, W. H., S. A. Teukolsky, W. T. Vetterling, and B. P. Flannery (2002). *Numerical Recipes in C++*. Cambridge University Press.

Proulx, G. (1995). Evacuation time and movement in apartment buildings. *Fire Safety Journal 24*, 229–246.

Purser, D. (1995). Toxicity assessment of combustion products. See [DiNenno, 1995].

Purser, D. and M. Bensilium (2001). Quantification of behaviour for engineering design standards and escape time calculations. *Safety Science 38*(2).

Rajewsky, N., L. Santen, A. Schadschneider, and M. Schreckenberg (1998). The asymmetric exclusion process: Comparison of update procedures. *J. Stat. Phys. 92*, 151.

Rapaport, D. (1995). *The Art of Molecular Dynamics Simulation*. Cambridge: Cambridge University Press.

Rickert, M., K. Nagel, M. Schreckenberg, and A. Latour (1996). Two lane traffic simulations using cellular automata. *Physica A 231*, 534–550.

Roth, G. (2002). Gleichtakt im Neuronennetz. *Gehirn und Geist 1*, 38–46.

Schadschneider, A. (2002a). Bionics-inspired cellular automaton model for pedestrian dynamics. In Y. Ishibashi, M. Schreckenberg, Y. Sugiyama, and D. Wolf (Eds.), *TGF 01*, Berlin. Springer. In print.

Schadschneider, A. (2002b). Cellular automaton approach to pedestrian dynamics – theory. See [Schreckenberg and Sharma, 2002], pp. 75–86.

Schirmacher, G. (2001). Einsatz von Detektoren für Fußgänger an Lichtsignalanlagen. *Straßenverkehrstechnik* (1), 19–25.

Schneider, V. and R. Könnecke (2002). Simulating evacuation processes with ASERI. See [Schreckenberg and Sharma, 2002], pp. 303–314.

Schneider, V. and H. Weckman (2000). Rechnerische Simulation des Ablaufs einer Evakuierungsübung. *vfdb-Zeitschrift 49*(4), 140–145.

Schreckenberg, M. and S. Sharma (Eds.) (2002). *Pedestrian and Evacuation Dynamics*, Berlin. Springer.

Sick AG (2000). *Lasermesssysteme*. Reute: Sick AG. `www.sick.de`.

Sime, J. (1990). The concept of panic. See [Canter, 1990], Chapter 5, pp. 63–82.

SleipnerReport (2000). The High-Speed Craft MS Sleipner Disaster 26 November 1999. Official Norwegian Reports 2000:31, Norwegian Ministry of Justice and Police, Oslo.

Smith, R. and J. Dickie (Eds.) (1993). *Engineering for Crowd Safety*. Amsterdam: Elsevier.

Spektrum der Wissenschaft (2001, 5). Berechenbare Panik.

Spiegel (2001, 16). Doppelgänger auf der Flucht.

Stahl, F. (1978). A computer simulation of human behavior in building fires: interim report. Technical Report NBSIR 78-1514, National Bureau of Standards, Washington, D.C. 20234.

Stahl, F. (1982). BFIRES-II: A behaviour based computer simulation of emergency egress during fires. *Fire Technology 19*, 49.

Stebens, A. (2001). *Simulation von Eisenbahnverkehr auf der Basis von Zellularautomaten*. Dissertation, Gerhard-Mercator-Universität, Duisburg.

Stinchcombe, R. (2001). Stochastic non-equilibrium systems. *Advances in Physics 50*(5), 431–496.

Stollard, P. and L. Johnson (Eds.) (1994). *Design against fire: an introduction to fire safety engineering design*. London, New York.

SZ (2001, 24.4.). Der menschliche Faktor – Neue Simulationsmethoden verbessern die Sicherheit auf Schiffen.

Thompson, P. and E. Marchant (1995a). A computer model for the evacuation of large building populations. *Fire Safety Journal 24*, 131–148.

Thompson, P. and E. Marchant (1995b). Testing and application of the computer model 'Simulex'. *Fire Safety Journal 24*, 149–166.

Thompson, P., J. Wu, and E. Marchant (1996). Modelling evacuation in multi-storey buildings with 'Simulex'. *Fire Engineers Journal 56*(185), 6–11.

TIEMS (2001). The International Emergency Management Society – Conference. CD-Rom.

TraffGo GmbH (2002). *PedGo Users' Manual*. Duisburg: TraffGo GmbH. `www.traffgo.de`.

Transportation Research Board (1994). *Highway Capacity Manual*. Washington, D.C.: Transportation Research Board.

Trudeau, R. J. (1993). *Introduction to Graph Theory*. New York: Dover Publications.

Vassalos, D. (Ed.) (1999). *Design for Safety Conference*, Glasgow. University of Strathclyde.

Vassalos, D., G. Christiansen, and H. Kim (2001). Evi – passenger evacuation performance assessment in ship design and operation. See [TIEMS, 2001].

Vassalos, D., H. Kim, G. Christiansen, and J. Majunder (2002). A mesoscopic model for passenger evacuation in a virtual ship-sea environment and performance-based evaluation. See [Schreckenberg and Sharma, 2002], pp. 369–392.

Wahle, J. (2002). *Information in Intelligent Transportation Systems*. Dissertation, Gerhard-Mercator-Universität, Duisburg.

Webber, D., N. Ketchell, N. Hiorns, S. Cole, and P. Stephens (1998). Assessment and simulation of crowd evacuation issues. Technical report, AEA Technologies, London.

Weckman, H., S. Lehtimäki, and S. Männikkö (1999). Evacuation of a theatre: Exercise vs calculations. *Fire and Materials 23*(6), 357–361.

Weidmann, U. (1992). Transporttechnik der Fußgänger. Schriftenreihe des IVT 90, ETH Zürich. (in German).

Weimar, J. R. (1998). *Simulation with Cellular Automata*. Berlin: Logos-Verlag.

Werenskiold, P. (1998). Guidelines to for the application of early design evacuation analyses of passenger ships. Summary Report 601493.00.02, Nordic Maritime Administrations, MARINTEK - Norwegian Marine Technology Research Institute.

Willis, A., R. Kukla, J. Kerridge, and J. Hine (2002). Laying the foundations: The use of vedeo footage to explore pedestrian dynamics in PEDFLOW. See [Schreckenberg and Sharma, 2002], pp. 191–186.

Withington, D. (2002). Life saving applications of directional sound. See [Schreckenberg and Sharma, 2002], pp. 277–298.

Wolf, D. and P. Grassberger (Eds.) (1996). *Friction, Arching, Contact Dynamics*, Singapore. World Scientific.

Wood, A. (1997). *Validating Ferry Evacuation Standards.* Available from MCA, 105 Commercial Road, Southhampton.

Yamori, K. (2001). Going with the flow: Micro-macro dynamics in the macrobehavioral patterns of pedestrian crowds. *Psychological Review 105*(3), 530–557.

Index